Bioenergetic profiling of cold stored and room temperature stored platelets as an indicator of platelet viability and function

C E GEORGE

DClinSci 2024

Bioenergetic profiling of cold stored and room temperature stored platelets as an indicator of platelet viability and function

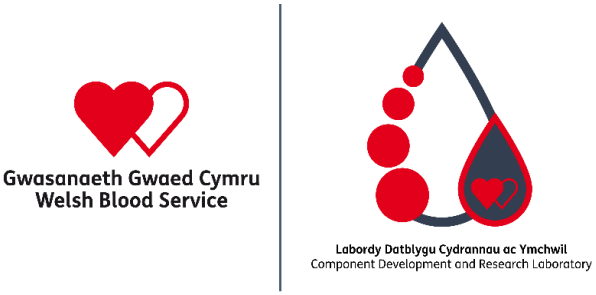

By

Chloë Elizabeth George

A thesis submitted to Manchester Metropolitan University for the degree of Doctor of Clinical Science

May 2024

Declaration

With the exception of any statements to the contrary, all the data presented in this report are the results of my own efforts and have not previously been submitted in candidature for any other degree or diploma. In addition, no parts of this report have been copied from other sources. I understand that any evidence of plagiarism and/or the use of unacknowledged third-party data will be dealt with as a very serious matter.

Signed:

Dated: 22/05/24

Print Name: CHLOË GEORGE

Acknowledgements

When I embarked on my journey to complete a Doctorate in Clinical Science, I had no idea of the highs and lows it would bring with it and the many people I would need to rely on in different ways to be able to complete it, I am very grateful to you all.

Firstly, thank you to my supervisory team at Manchester Metropolitan University, Dr Nina Dempsey-Hibbert and Dr Sarah Jones. You have been encouraging and supportive from inception of this project through to final write up. I thank you for your many insightful comments and suggestions and for sharing your vast knowledge with me. I hope we will work together again in the future.

To the senior managers at the Welsh Blood Service, my employer of the last 20+ years, thank you for providing me with the opportunity to fulfil my lifelong dream of completing a doctorate. With particular thanks to Peter Richardson and Dr Edwin Massey who have both line-managed me during this period and have given me the time and space when I needed it to think and write; I really could not have finished it without this.

A massive thank you to my friend, colleague, mentor and sometimes shoulder to cry on, Dr Christine Saunders. You are an amazing scientist and have helped me with the design of this study, setting up assays and troubleshooting throughout, I feel extremely fortunate to work with you. In addition, this study would not have been possible without the amazing team of scientists in the Component Development & Research Laboratory: Nicola Pearce, Dr Jamie Nash, and Michael Cahillane, who helped me with the testing for this project, due to the large number of assays that had to be performed at each timepoint. Thank you for your time and enabling this to be such an expansive study of cold stored platelets.

I would like to thank Surgeon Commander Tom Scorer for his advice on the clinical use of platelets, enthusiasm for my project and for always being happy to talk about cold platelets with me. I hope that together, we can bring the many potential benefits of cold stored platelets to patients in the UK.

Finally, and most importantly, I would like to express my thanks and gratitude to my family, for going on this journey with me. It has been tough and at times I thought I would never get there. My husband, Gareth, has given me his unwavering support and on many occasions kept our life moving whilst I have taken time to study. To my wonderful children Sebastian and Sienna for their understanding when I could not spend time with them – I hope I have shown you all you can achieve with hard work and determination; and to my mother, my biggest fan, always there to listen and encourage. I love you all.

Related Publications and Presentations

George, C.E., Saunders, C.V., Morrison, A., Scorer, T., Jones, S. and Dempsey, N.C. (2023) '**Cold stored platelets in the management of bleeding: is it about bioenergetics?**', *Platelets*, 34(1), pp.1-9.

Nash, J., Davies, A., Saunders, C.V., George, C.E., Williams, J.O. and James, P.E. (2023) '**Quantitative increases of extracellular vesicles in prolonged cold storage of platelets increases the potential to enhance fibrin clot formation'**, *Transfusion Medicine*, 33(6), pp.467-477.

Nash, J., Saunders, C.V. and George, C.E. (2023) '**pH is unsuitable as a quality control marker in platelet concentrates stored in platelet additive solutions'**, *Vox Sangs*, 118, pp.183-184.

'Cold Stored Platelets'. Presentation at the Closer, Better, Longer: DMS-DSTL Blood Symposium, London, March 2023.

Reilly-Stitt, C., Saunders, C.V., George, C., Scorer, T., Jennings, I., Kitchen, S. and Walker, I. (2023) '**NEQAS blood coagulation launches external quality assessment for light transmission aggregometry (LTA) using cold-stored platelet concentrates'**. BSH23-PO128, *Br J Haematol*, 201 (Suppl. 1):31-118. Poster Presentation at UK NEQAS Blood Coagulation annual meeting, 2023.

Sayle, J., Saunders, C. and George, C.E. (2022) '**Travelling in style - Platelet function and viability following cold storage within a medical transport box and an extended 14 day shelf life**' Poster presentation at the British Blood Transfusion Society annual conference, 2022.

Abbreviations

AA	Antimycin A
ACD	Acid citrate dextrose
Acetyl-CoA	Acetyl coenzyme A
ADP	Adenosine-5'-diphosphate
ATP	Adenosine triphosphate
BSH	British Society of Haematology
CAT	Calibrated automated thrombogram
CCCP	Carbonyl cyanide 3-chlorophenylhydrazone
CoQ	Coenzyme Q
CS	Cold stored
CSP	Cold stored platelets
Cyt c	Cytochrome c
$DIOC_6$	3, 3'-dihexyloxacarboncynanine iodide
DTS	Dense tubular system
dH_2O	Deionised water
ECAR	Extracellular acidification rate
EDTA	Ethylenediaminetetraacetic acid
EDQM	European Directorate for the Quality of Medicines and Healthcare
ELISA	Enzyme linked immunosorbent assay
ESC	Extent of shape change
ETC	Electron transport chain
ETP	Endogenous thrombin potential
EV	Extracellular vesicles
F	Factor
$FADH_2$	Flavine adenine dinucleotide
FC	Flow cytometry
FCCP	Carbonylcyanide-p-trifluoromethoxyphenylhydrazone
FITC	Fluorescein isothiocyanate

FNHTR	Febrile non-haemolytic transfusion reaction
GP	Glycoprotein
HEMS	Helicopter emergency medical service
HLA	Human leucocyte antigen
HRR	High-resolution respirometer
HSR	Hypotonic shock response
JC-1	5,5',6,6'-tetrachloro-1,1',3,3'-tetraethyl-benzimidazolecarbocyanine
JPAC	Joint United Kingdom Blood Transfusion and Tissue Transplantation Services Professional Advisory Committee
LDH	Lactate dehydrogenase
LoQ	Limit of quantification
LTA	Light transmission aggregometry
MB	Marginal band
MHRA	Medicines and Healthcare products Regulatory Agency
MoAb	Monoclonal antibody
MPV	Mean platelet volume
NADH	Nicotinamide adenine dinucleotide
OCR	Oxygen consumption rate
OD	Optical density
OXPHOS	Oxidative phosphorylation
PAS	Platelet additive solution
PBS	Phosphate buffered saline
PC	Platelet concentrates
PDH	Pyruvate dehydrogenase
PER	Proton efflux rate
PPi	Inorganic pyrophosphate
PPP	Platelet poor plasma
PROPPR	Pragmatic, Randomized Optimal Platelet and Plasma Ratios
PRP	Platelet rich plasma
PS	Phosphatidyl serine

PSL	Platelet storage lesion
PSGL-1	P-selectin glycoprotein ligand-1
RT	Room temperature
RTP	Room temperature platelets
sCD62P	Soluble CD62P
SCCS	Surface-connected canalicular system
SRC	Spare respiratory capacity
TBI	Traumatic brain injury
TG	Thrombin generation
TMRE	Tetramethylrhodamine
TMRM	Tetramethylrhodamine methyl ester
T-PAS+	Terumo platelet additive solution
TF	Tissue factor
TRAP-6	Thrombin receptor-activating peptide-6
TSCD	Terumo sterile connecting device
TXA_2	Thromboxane A2
vCJD	Variant Creutzfelt-Jakob disease
VWF	Von Willebrand factor
WBC	White blood cells
WBS	Welsh Blood Service
XF	Extracellular flux
$\Delta\psi_m$	Mitochondrial membrane potential
Δp	Proton motive force

Abstract

Interest in the use of cold stored platelets (CSP) has experienced a resurgence due to changes in clinical practice, driven by a reduction in platelet transfusion for prophylactic reasons and an increase in their use for the treatment of acute bleeding in traumatic haemorrhage resuscitation and surgery, both within hospital and pre-hospital care. CSP demonstrate many benefits over room temperature stored platelets (RTP) including longer shelf life, decreased bacterial risk and easier logistics for transport, as well as making platelet concentrates (PC) accessible in areas where they have not previously been, such as in the pre-hospital environment.

CSP are reported *in vitro* to have superior haemostatic functions, forming stronger, firmer clots. However, clinical trial data on their use is limited and discussion around the maximum potential shelf life continues.

In this study, the *in-vitro* activation and haemostatic function of RTP and CSP were compared, and novel bioenergetic assays were performed to create metabolic profiles of RTP and CSP during prolonged storage.

RTP and CSP were compared for up to 21 days of storage in terms of their morphology, activation state, ability to aggregate and their metabolic function, including glucose production, lactate production and ATP levels. Bioenergetic profiles were deduced by examining the mitochondrial membrane potential and by direct measurement of the oxygen consumption rate and extracellular acidification rate, with the aim of determining an appropriate maximum shelf life for CSP.

This work demonstrates that CSP are 'primed' for use, with higher levels of activation markers and improved functional responses (aggregation response to ADP & collagen and the ability to produce more thrombin and faster) compared to RTP. Bioenergetic profiles showed a move from mitochondrial respiration towards a more glycolytic phenotype by the end of storage for both RTP and CSP, indicating that mitochondria become damaged during prolonged storage. The mitochondrial membrane potential was markedly decreased in CSP by day 21 along with very low glucose levels suggesting that CSP may not be a viable product by 21 days of storage. The findings

indicate that the bioenergetic profile perhaps does not accurately reflect platelet function in CSP. Further, the work has highlighted the extensive potential benefits of CSP for bleeding patients and for the logistics of blood supply chains and has provided some compelling data to help justify initiation of clinical trials involving the use of CSP in the UK.

Table of Contents

List of Figures

List of Tables

Chapter 1: Introduction

1.1 Platelet Structure

Platelets are small, anucleate cytoplasmic fragments that are released by megakaryocytes in the bone marrow and lungs. They are the smallest of the blood cells, with the normal peripheral blood count being in the range of 150 x 10^9/L to 400 x 10^9/L (Ghoshal and Bhattacharyya, 2014). The absence of a nucleus enables the platelet to maintain its small size, permitting morphological flexibility and possibly improving the efficiency of protein expression in response to stress (Melchinger *et al.*, 2019).

In their quiescent state, platelets consist of a lipid bilayer plasma membrane with a thick glycocalyx covering supported by a cytoskeleton of actin and spectrin microfilaments and a single peripheral microtubular ring structure called the marginal bad (MB) (Figure 1-1). The MB is a single polymer of tubulin heterodimers that is wound in 8 to 12 coils in the cytoplasmic periphery and is responsible for resting platelets flat, discoid morphology and the integrity of the plasma membrane as the platelet is exposed to shear and other forces in the circulation (Italiano Jr *et al.*, 2003; Heijnen and Van der Sluijs, 2015; Diagouraga *et al.*, 2014).

The plasma membrane invades the platelet interior producing the unique invaginated surface-connected canalicular system (SCCS) which is closely aligned to the dense tubular system (DTS) (Fritsma, 2015). On the surface of platelets, within the glycocalyx, are various surface receptors, such as glycoproteins (GP). GPIb-IX-V complex, GPVI and integrin αIIbβ3 are considered the most important for the haemostatic functions of platelets (Gremmel, Frelinger and Michelson, 2016).

Platelets contain three major types of secretory organelles: α-granules, dense granules and lysosomes, all of which are transported and discharged by the SCCS upon activation (Heijnen and Van der Sluijs, 2015). There are approximately 3-8 dense granules per platelet which contain very high concentrations of small molecules including calcium, ADP, ATP and epinephrine (Holinstat, 2017) and approximately 50-80 α-granules per platelet, taking up roughly 10% of the platelet

volume, which contain membrane-associated and soluble proteins including coagulants, integral membrane proteins and adhesion glycoproteins.

In addition, platelets contain simple mitochondria, which are important for energy metabolism. In the absence of a nucleus, it is likely that the platelet lifespan of 7-10 days (Leeksma and Cohen, 1956) is largely determined by the health of their mitochondria (Melchinger *et al.*, 2019).

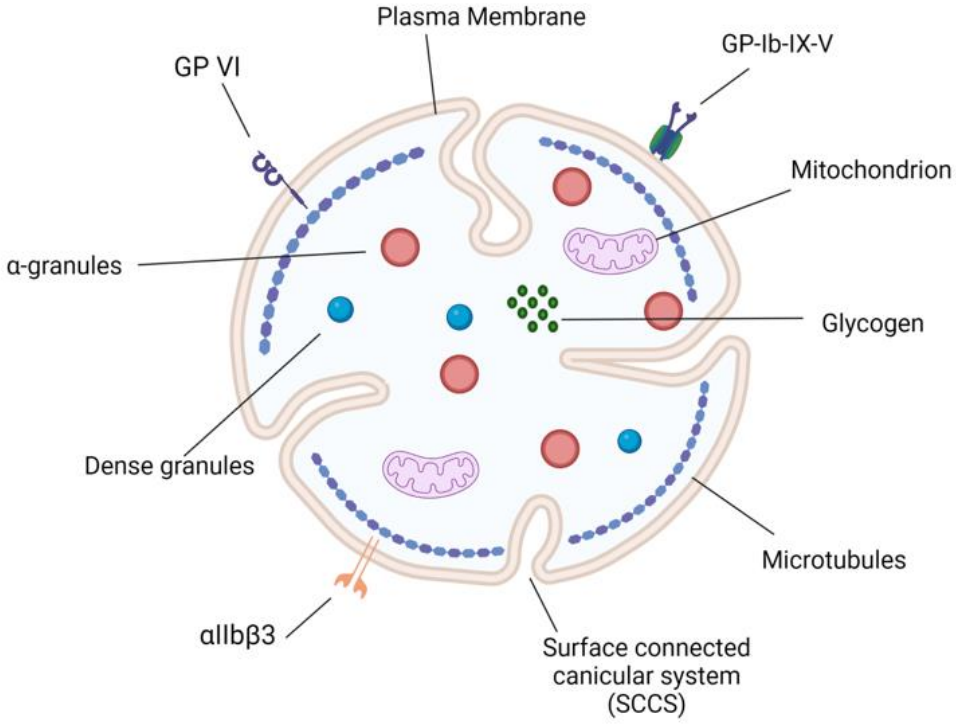

Figure 1-1: Ultrastructure of platelets. demonstrating the three main surface glycoproteins.

1.2 Platelet Function

Platelets circulate in a quiescent state towards the edges of blood vessels where they are ideally placed to respond rapidly to vessel damage (Moore, 2016). Their primary function is to maintain haemostasis by preventing haemorrhage during vascular injury. This is achieved through a dynamic activation process that occurs when platelets are exposed to vessel wall damage. The activation process involves platelets adhering to the cell wall, aggregating and secreting their granule contents, processes

that often occur simultaneously (Fritsma, 2015), resulting in the formation of the platelet haemostatic plug (Holinstat, 2017).

1.2.1 Platelet adhesion

Vessel walls contain a continuous lining of endothelium, serving as a barrier between the circulating platelets and the prothrombotic subendothelial matrix (Dorsam and Kunapuli, 2004). When a vessel wall is injured, subendothelial collagen is exposed and Von Willebrand Factor (VWF), released from endothelial cells, adheres to the injured site (Fritsma, 2015). The VWF is unrolled by the sheer force of the flowing blood and exposes its GPIb-IX-V binding site. This enables VWF to loosely bind to the platelet glycoprotein (GP) Ib-IX-V receptor complex on passing platelets, tethering them to the site of injury (Figure 1-2) (Yun *et al.*, 2016).

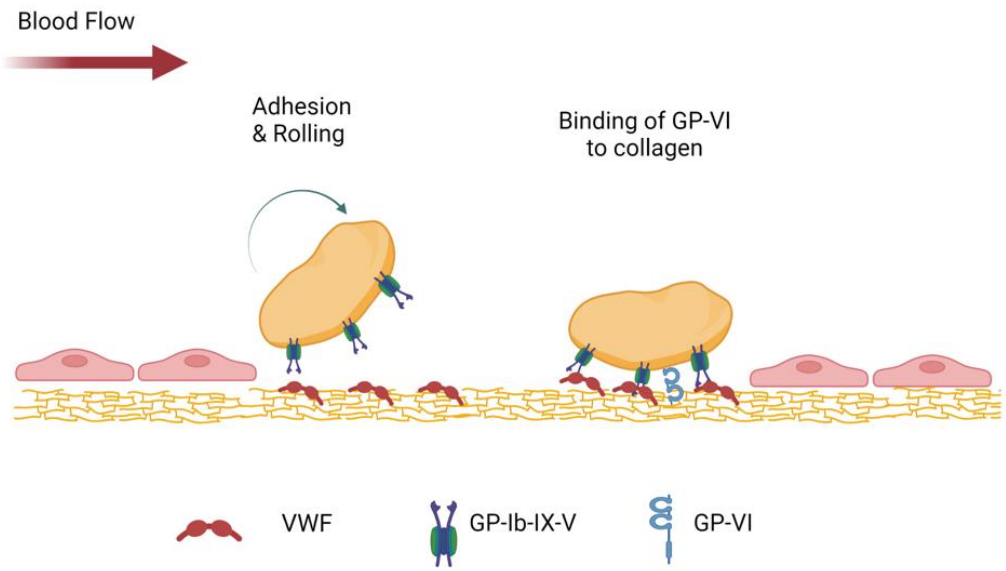

Figure 1-2: Platelet adhesion & rolling. Created with BioRender.com

Once tethered, the platelet rolls over the exposed VWF in the direction of blood flow and forms new VWF-GPIb-IX-V interactions. The platelet continues to roll along the surface making these reversible interactions until the platelet collagen receptors, GPVI mediate a firm adhesion to the damaged surface (Figure 1-2) (Fritsma, 2015).

1.2.2 Platelet shape change

The firm adhesion of GPVI to collagen triggers signal transduction and activation within the platelet, along with numerous other agonists including thrombin generated from blood coagulation and VWF (Davlouros *et al.*, 2016). The signalling from these agonists leads to a rapid increase in cytosolic Ca^{2+} concentration via two main mechanisms: the release of Ca^{2+} from intracellular stores and the entry of Ca^{2+} into the cell from the extracellular compartment (Davlouros *et al.*, 2016).

The increase in cytosolic free [Ca^{2+}] causes the microtubules in the MB to move apart and extend. Due to the limited space in the platelet, the MB coil and fold into the middle of the activated platelet, resulting in a shape change to a spherical 3D morphology. From this spherical shape the platelet protrudes finger-like projects called filapodia which extend from the cell periphery (Figure 1-3).

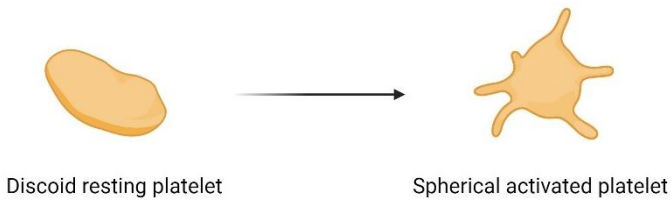

Figure 1-3: Platelet shape change from a flat, discoid morphology to a 3D, sphere-shaped morphology following activation.

The platelet then begins to spread out, driven by the polymerization of actin filaments. These morphological changes result in a dramatic increase in the surface area of the platelet, which is likely to enhance the haemostatic function of platelets at sites of injury (Flaumenhaft *et al.*, 2005). During this process the platelet centralizes the granules and organelles to the centre of the cell (Gremmel, Frelinger and Michelson, 2016).

1.2.3 Platelet granule secretion

The reorganisation of the granules to the centre of the platelet enables them to be closely opposed to the SCCS and plasma membrane for secretion (Gremmel, Frelinger and Michelson, 2016). Following initial activation, the dense granules fuse

with the plasma membrane and secrete their contents into the extracellular vascular space. These small molecules are vasoconstrictors and platelet agonists that amplify primary haemostasis through surface receptors. In particular, ADP and TXA_2 activate neighbouring platelets in the microenvironment as well as triggering internal activation pathways through binding to receptors that raise the affinity of GP Ia-IIa for collagen. This results in the platelet becoming firmly affixed to the damaged surface (Fritsma, 2015).

The α-granules contain a number of larger proteins and are released into the channels of the SCCS and ultimately into either the extracellular space for the soluble proteins or are expressed on the platelet surface. The proteins released provide a cellular milieu that supports coagulation as they include fibrinogen, FV, FVIII and VWF ensuring that coagulation is localized and controlled (Fritsma, 2015). In addition to proteins that support coagulation, the α-granules release the membrane protein CD62P, which is an important laboratory marker of activation. CD62P functions as a tether between platelets and other cells in the vessel and is only expressed on activated (rather than resting) platelets (Holinstat, 2017).

1.2.4 Platelet aggregation

All of these platelet signalling events converge upon the final common pathway of platelet activation, the conversion of αIIbβ3 from its low affinity state, by inside out signalling from GPVI, into a high-affinity receptor for fibrinogen and VWF. Activation of αIIbβ3 results in cross-linking of fibrinogen or vWF between receptors leading to platelet aggregation (Gremmel, Frelinger and Michelson, 2016; Yun *et al.*, 2016). Further platelets are recruited to the site of vascular injury ending with the thrombus formation.

1.2.5 The role of platelets in coagulation

In a resting platelet, phosphatidylserine (PS) and other negatively charged phospholipids are sequestered in the inner leaflet of the platelet membrane. Upon activation, platelets lose the natural asymmetry of their plasma membrane and PS becomes exposed on the outer leaflet of the activated platelet in a process regulated by active transport mechanisms including a 'flip-flop' mechanism (Monroe, Hoffman

and Roberts, 2002). Exposure of PS on the surface of platelets enables platelet procoagulant activity by facilitating the assembly of the intrinsic tenase complex (factor (F)VIIIa, FIXa, FX) and the prothrombinase complex (FVa, FXa, prothrombin) (Reddy and Rand, 2020; Reddy *et al.*, 2018).

The combination of granule secretion to provide the cellular milieu (fibrinogen, VWF, FV, FVIII and Ca^{2+}) required for coagulation and the exposure of PS on the surface on activated platelets results in accelerated thrombin generation (Fritsma, 2015). Thrombin then converts fibrinogen to fibrin to stabilize the platelet plug (Yun *et al.*, 2016). Where the concentration of thrombin is high enough, new platelets are recruited and activated by thrombin binding and cleaving the PAR-1 and PAR-4 receptors on the platelet surface (Brass, 2003; Hemker *et al.*, 2006).

1.3 Platelet clearance from the circulation

To maintain a steady platelet count, the body produces and clears platelets at a rate of 10^{11} platelets per day, which is dependent on a balance between proapoptotic and anti-apoptotic activity (Quach, Chen and Li, 2018). The anti-apoptotic Bcl-2 family proteins inhibit the pro-apoptotic molecules Bak and Bax. When the Bcl-2 family proteins are in turn inhibited, Bak and Bax bring about mitochondrial apoptosis by causing outer mitochondrial membrane permeabilization, resulting in cytochrome c release and caspase activation (Josefsson *et al.*, 2023). The subsequent activation of a caspase-dependent scramblase promotes externalization of PS from the inner to the outer leaflet of the plasma membrane, then serves as a molecular cue for engulfment and clearance by phagocytes (Quach, Chen and Li, 2018). It is important to recognise that PS exposure on platelets in response to activation, creating procoagulant platelets, is a separate and distinct pathway to PS exposure due to apoptotic signals.

1.4 Platelet metabolism

In order to achieve the biomechanical transition of platelets from a quiescent state to an activated state, a highly efficient source of energy is required. Bioenergetics fuels all biological processes, with cellular metabolism being central to biological

function and cell health. In platelets the bioenergetic demand is met through the production (and subsequent hydrolysis) of adenosine triphosphate (ATP) to adenosine diphosphate (ADP) using a metabolic system that combines glycolysis and oxidative phosphorylation (OXPHOS) (Aibibula, Naseem and Sturmey, 2018; Melchinger *et al.*, 2019).

Glucose ($C_6H_{12}O_6$) is broken down in metabolism to CO_2 and H_2O, in the presence of O_2. The first stage of this process, glycolysis, is independent of oxygen and takes place in the cytosol of the cell (Protasoni and Zeviani, 2021). Glycolysis relies on the hydrogen carrier NAD^+ to accept electrons from glucose as it is split into pyruvate ($C_3H_3O_3^{1-}$), NADH and H^+, a process that generates two ATP molecules. The fate of the two pyruvate molecules generated depends on whether O_2 is present. In anaerobic conditions, pyruvate is reduced to lactate anions (La^-) by lactate dehydrogenase (LDH), regenerating NAD+ (Rogatzki *et al.*, 2015):

$$2\ Pyruvate^- + 2\ NADH + 2\ H^+ \leftrightarrow\ \ 2\ Lactate^- + 2\ NAD^+$$

Under aerobic conditions, the glucose-derived pyruvate generated by glycolysis is fully oxidised to CO_2. It is transported across the mitochondrial membrane where it is converted into acetyl coenzyme A (acetyl-CoA). Acetyl-CoA is the starting material for the citric acid cycle which is composed of nine different enzymatic reactions which breakdown the carbon backbone of pyruvate releasing the volatile acid CO_2 (Divakaruni *et al.*, 2014). This process results in the harvesting of energy in the form of the reduced compounds NADH and $FADH_2$, that deposit their electrons into the electron transport chain (ETC) to generate ATP through the oxygen-dependent process of OXPHOS, yielding 30-32 ATP molecules (Judge and Dodd, 2020).

1.4.1 Platelet mitochondria

Mitochondria are cellular organelles that play an essential role in energy production and metabolism in the cell and are the main source of ATP, the energy rich compound that drives fundamental cell functions. Apart from ATP synthesis, mitochondria have numerous other essential functions such as involvement in the generation of reactive oxygen species (ROS), Ca^{2+} homeostasis and apoptosis regulation (Melchinger *et al.*, 2019; Kühlbrandt, 2015). A healthy platelet contains 5 – 6 mitochondria, the majority

of which need to remain healthy in order for the platelet to function properly (Melchinger *et al.*, 2019). As platelets are anuclear and unable to *de novo* synthesise proteins, they have a short lifespan of 7-10 days, which is likely determined by the lifespan of the mitochondria. Mitochondria are required for energy production and as platelets do not contain a nucleus they are unable to replenish nuclear encoded mitochondria proteins, limiting their lifespan and that of the platelet (Diaz and Moraes, 2008; Melchinger *et al.*, 2019).

Mitochondria are surrounded by two phospholipidic membranes – the outer mitochondrial membrane and the inner mitochondrial membrane, which divide the organelle into the matrix and the intermembrane space (Protasoni and Zeviani, 2021) (Figure 1-4). The inner mitochondrial membrane forms highly packed invaginations, called cristae that extend deeply into the matrix and have embedded within them the enzymatic machinery for cellular respiration: the ETC.

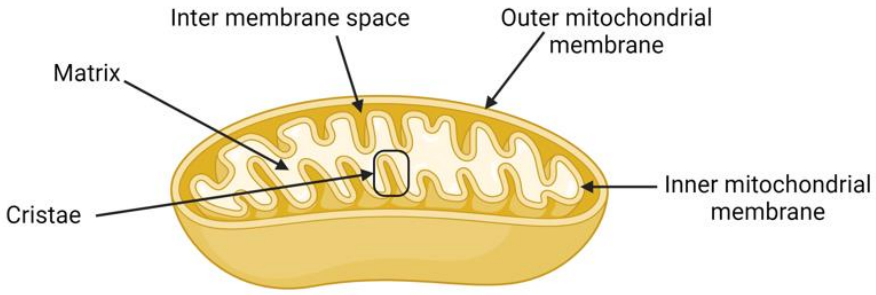

Figure 1-4: Schematic representation of mitochondrial structure.

1.4.2 Electron transport chain

The ETC is composed of four protein complexes embedded in the inner mitochondrial membrane and two mobile electron carriers (coenzyme Q and cytochrome *c*) (Protasoni and Zeviani, 2021). The close proximity of the ETC in the inner mitochondrial membrane to the citric acid cycle in the matrix enables NADH and $FADH_2$ generated from the citric acid cycle to donate electrons to the ETC, either at Complex I or Complex II (Figure 1-5).

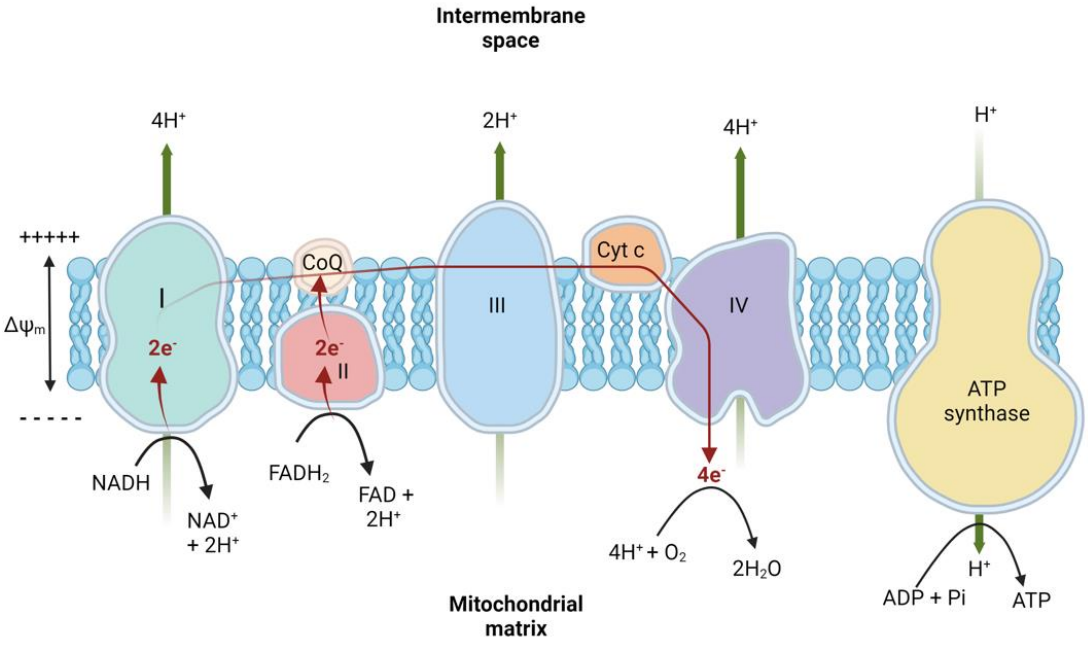

Figure 1-5: Basic schematic of the electron transport chain (ETC), demonstrating electron transfer and proton (H+) production, driving synthesis of ATP from ADP.

The electrons are passed to coenzyme Q (CoQ), which is reduced to ubiquinol, inducing the pumping of protons (H^+) from Complex I into the intermembrane space (Nolfi-Donegan, Braganza and Shiva, 2020). Electrons also enter the ETC through Complex II and are transferred to CoQ where they are further transferred to Complex III and then to cytochrome c (Cyt c). Once Cyt c is reduced, it ferries electrons to Complex IV where this series of exergonic reactions ultimately reduces O_2 to H_2O (Nolfi-Donegan, Braganza and Shiva, 2020). This reductive transfer of electrons through the ETC protein complexes I-IV coupled to the endergonic (uphill) pumping of protons against their concentration gradient from the matrix to the inter membrane space generates a protonmotive force (Δp) across the inner membrane (Divakaruni *et al.*, 2014) (Perry *et al.*, 2011). The Δp has two components, ΔpH (the pH gradient across the inner membrane) and $\Delta\psi_m$ (mitochondrial membrane potential) which is the difference in electrical potential between the cytoplasm and the matrix) (Brand and Nicholls, 2011). This Δp is consumed by ATP synthase, which dissipates Δp to drive the rotary catalysis of the enzyme to produce ATP from ADP (Divakaruni *et al.*, 2014).

1.4.3 Platelet bioenergetics

The production and consumption of energetic substrates is referred to as 'platelet bioenergetics' (George *et al.*, 2018). Platelet bioenergetics is not however a simple dichotomy between the processes of glycolysis and OXPHOS, as platelets demonstrate considerable metabolic plasticity between the two avenues (George *et al.*, 2018). At a basal state, both OXPHOS and glycolysis play a role in energy production in platelets (Kramer *et al.*, 2014). However, there appears to be some discrepancy in the literature around the amount of ATP supplied by glycolysis and the amount suppplied by OXPHOS in a resting state, with Wang and colleagues suggesting approximately 60% from glycolysis & 40% from OXPHOS (Wang *et al.*, 2017), Kilkson and colleagues suggesting 15% : 85% (Kilkson, Holme and Murphy, 1984) and Reddoch-Cardenas suggesting 25% : 75% (Reddoch-Cardenas *et al.*, 2019b).

The transition of platelets to an activated state promotes rapid uptake of exogenous glucose, associated with a shift to energy generation predominately through glycolysis with a minor rise in mitochondrial oxygen consumption (Aibibula, Naseem and Sturmey, 2018). Platelet adhesion is one of the few energy independent biomechanical processes (Misselwitz, Leytin and Repin, 1987), whereas platelet spreading and aggregation have been shown to be primarily fuelled by glycolysis and platelet contraction showing more of a correlation with OXPHOS (George *et al.*, 2018). This metabolic flexibility allows platelets to utilize glycolysis instead of OXPHOS so as to adapt to different situations, such as hypoxia (Melchinger *et al.*, 2019).

1.5 Clinical Use of Platelet Concentrates

The use of platelet component therapy (platelet transfusions) as an alternative to whole blood transfusion was made feasible in the 1960s, through the introduction of plastic containers and revolutionised the treatment of thrombocytopenic patients (Vassallo and Murphy, 2006). Platelet transfusions are generally categorised into prophylactic treatment (to prevent bleeding in thrombocytopenic patients) or therapeutic treatment (to treat and halt bleeding). Prophylactic platelet transfusions

are predominantly used for patients following chemotherapy or bone marrow transplant and ideally have prolonged survival to increase intervals between transfusions and reduce risk of alloimmunization. Conversely, platelet transfusion to treat bleeding and regain haemorrhage control for example, in trauma patients, requires fast initiation of the clot, favouring platelets that are able to activate and function rapidly after transfusion (Pidcoke *et al.*, 2014).

Approximately 67% of platelet transfusions are used for prophylactic management of haematological disorders/conditions with the remainder being used therapeutically (Estcourt *et al.*, 2016). However, there is a shift away from prophylactic platelet transfusion with the introduction of lower transfusion triggers (10×10^9/L instead of 20×10^9/L) being implemented in management of acute leukaemia (Wandt, Ehninger and Gallmeier, 2001). There have been several studies indicating that patients who have undergone autologous stem cell transplants and are haemostatically stable, can be managed safely without prophylactic platelet transfusion (Wandt *et al.*, 1995; Gil-Fernández *et al.*, 1996) reducing use of platelet concentrates (PC) in this cohort. In addition, evidence based guidelines on platelet transfusion are advocating restrictive use of prophylactic platelet transfusions to patients by maintaining lower platelet count triggers for transfusion and employing a one PC dose for routine prophylactic transfusion strategy (Estcourt *et al.*, 2016). In the US, at least the shift has moved to nearly equal amounts of PC being utilised for bleeding as for prophylactic use (Shea *et al.*, 2023; Gottschall *et al.*, 2020)

As well as changes in the clinical practice for platelet prophylaxis, there has been increasing use of PC to treat acute bleeding in traumatic haemorrhage and surgery as well as other causes of bleeding (Cap and Reddoch-Cardenas, 2018). Within the UK, there has been an intense focus on improving trauma care by setting up regional trauma networks which contain major trauma centres (Stanworth *et al.*, 2022). This has led to a more consistent and organised approach to trauma care. The foundation of damage control resuscitation for trauma patients with major haemorrhage is that early correction of coagulopathy limits blood loss and decreases blood product transfusion (Milford and Reade, 2016).

The UK BSH guideline for the haematological management of major haemorrhage (Stanworth *et al.*, 2022) recommends that initially in trauma, there should be empirical use of red cells and plasma, usually given in a ratio of 1:1 and that platelets should be transfused to maintain the platelet count at > 50 $x10^9$/L or at higher thresholds in patients with intracranial bleeding/spinal bleeding or in actively bleeding patients with falling platelet counts (Stanworth *et al.*, 2022). A sub-study of the Pragmatic, Randomized Optimal Platelet and Plasma Ratios (PROPPR) trial (Cardenas *et al.*, 2018) has since demonstrated that early platelet administration in severely injured trauma patients is independently associated with improved haemostasis and reduced mortality, suggesting that a ratio of 1:1:1 (4 red cells units : 4 plasma units : 1 platelet concentrate) should be used in all trauma cases with major bleeding.

Taking these factors into consideration, there is an expectation that there will continue to be a reduction in prophylactic transfusions and an increase in therapeutic platelet transfusions going forward.

1.6 Preparation and Storage of Platelet Concentrates

There are two main types of PC used for transfusion: buffy coat derived pooled PC and apheresis derived PC, with usage of the two components varying greatly between countries. Within the UK, they are generally used interchangeably with around half supplied PC produced by each method.

Apheresis PC are collected using licensed plateletpheresis platforms which remove venous whole blood from the arm of a volunteer donor and automatically separate the platelets from the other blood cells and plasma through centrifugation. The platelets are diverted into a collection pack, along with a portion of plasma, whilst the remainder of the blood is returned to the donor (Tynngård, 2009). Apheresis platelets can either be collected into 100% plasma or into a mixture of plasma and a platelet additive solution (PAS). It has been demonstrated in previous studies that plateletpheresis collection can induce various degrees of platelet activation (Holme *et al.*, 1997; Krailadsiri and Seghatchian, 2000).

PC produced from the buffy coat method requires the pooling of platelets from four whole blood donors to obtain a single platelet dose (as opposed to one donor for plateletpheresis). Whole blood donations are centrifuged to separate out the red cells, buffy coat (containing platelets and white cells) and the plasma, before being pooled together with a platelet additive solution (PAS). The pool is further centrifuged to separate the platelet rich supernatant from the residual red cells which are leucocyte depleted and transferred to the final PC storage container as a PC suspended in approximately 35%: 65% plasma to PAS (Figure 1-6).

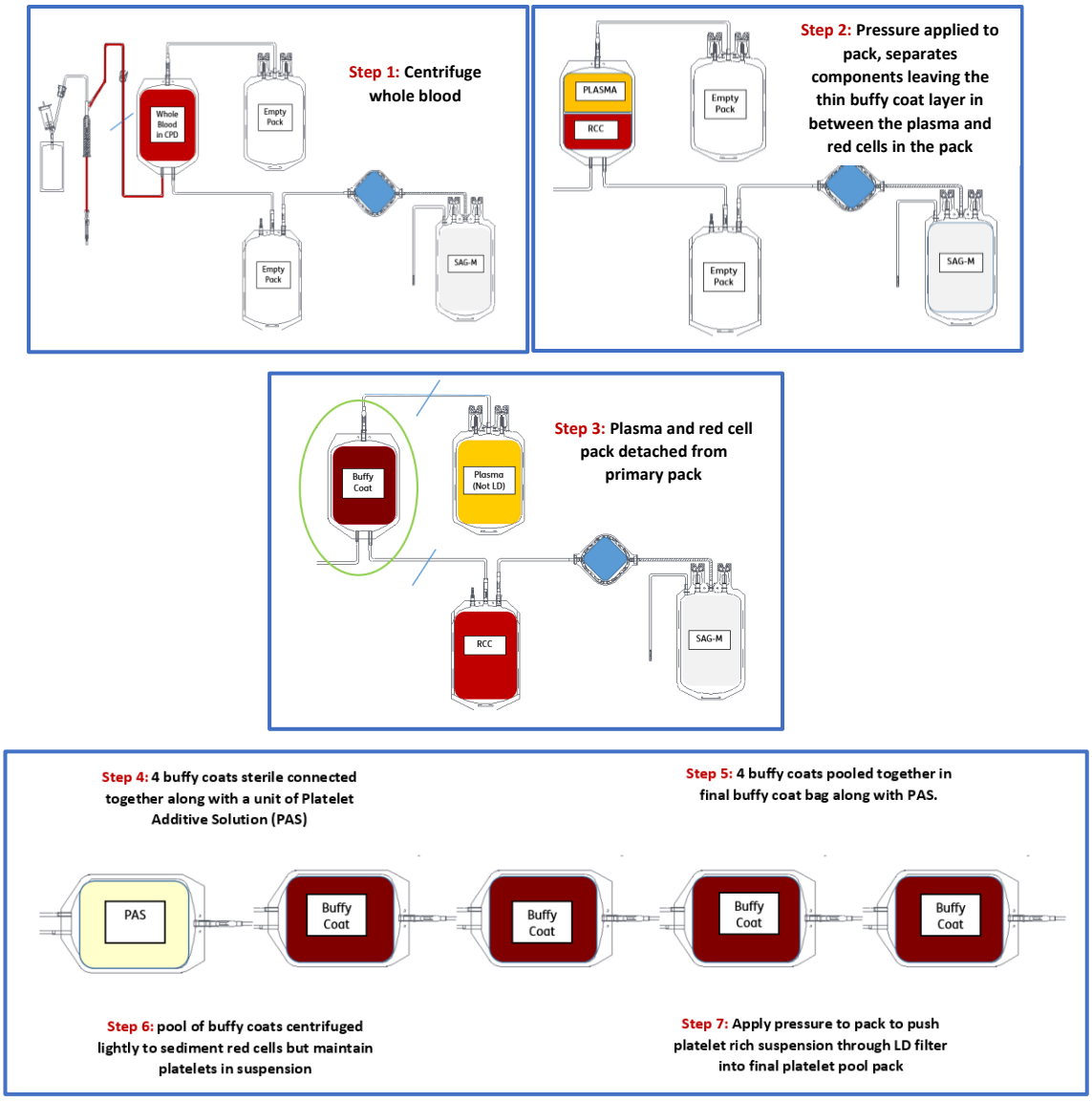

Figure 1-6: Pooled platelet manufacture from four buffy coats and one platelet additive solution (PAS). LD = leucocyte depletion.

Pooled and apheresis PC are prepared into specially designed platelet storage packs that allow gaseous exchange with the environment and can generally be used interchangeably for transfusion purposes, with no evidence of difference in clinical efficacy between the two for room temperature storage (Vassallo and Murphy, 2006). The exceptions to this in the UK are for neonatal transfusion, where apheresis PC are used to reduce donor exposure, and thus the risk of a transfusion transmitted infection, and when donor and recipient need to be matched for HLA antigens.

1.6.1 Platelet additive solution

PAS was developed in the 1980's to improve PC storage conditions and to decrease the risk of adverse transfusion reactions (Vit, Klüter and Wuchter, 2020), particularly allergic and febrile non-haemolytic transfusion reactions, where a reduction in reactions has been demonstrated (Tobian *et al.*, 2014; Cohn *et al.*, 2014). There are several PAS's on the market which are composed of compounds that regulate platelet metabolism and activation as well as providing additional buffering capability to prevent the fall of pH (Reddoch-Cardenas *et al.*, 2019b). Although the composition of each PAS differs, they all rely on a combination of nutrients and electrolytes for example Na^+, K^+, Mg^{2+} Cl^- as well as some residual plasma, to preserve the platelets (Reddoch-Cardenas *et al.*, 2019a).

When PC are suspended in PAS, a residual amount of plasma is always maintained (in the UK this would usually be 35% plasma : 65% PAS). The main limitation to further reduction of the plasma content below this level is the requirement for a minimum amount of glucose to sustain metabolism, which is provided by the plasma (Saunders, 2012). Although PAS's containing glucose (PAS-G) have been studied (Hirayama *et al.*, 2012; Wagner *et al.*, 2008), there is currently no commercially available PAS-G on the market.

1.6.2 Platelet storage

PC are logistically more challenging to store than other blood components as they require continuous gentle agitation at 22^{o}C ± 2^{o}C (room temperature (RT)) in specialised incubators and agitators (Scorer *et al.*, 2019a). They are stored in specially designed packs that are gas permeable, allowing influx of O_2 and efflux of CO_2 to

support the metabolic activity of the platelets. This assumes that under high oxygen tensions, glucose metabolism will proceed through the citric acid cycle, generating larger quantities of ATP through OXPHOS and preventing lactate build up and the accompanying pH drop, associated with glycolysis (Farrugia, 1994). The continuous gentle agitation prevents platelet aggregation and ensures that sufficient gaseous exchange occurs for metabolism (Michelson, 2019). When room temperature platelets (RTP) are not agitated, pH drops below 6.3 have been demonstrated (Snyder *et al.*, 1983).

The temperature and method of storage provides ideal conditions for bacterial proliferation with bacterial contamination of PC ranging from 1:1000 to 1:2500 (Levy, Neal and Herman, 2018). The risk of bacterial contamination is a major factor in the shelf life of PC being limited to three to five days. In some countries, such as the UK, these risks are mitigated by bacterial culturing of all PC, allowing their shelf life to be extended to seven days (JPAC, 2021). However bacterial culturing systems have their short-comings, and bacterial contamination can be missed (Wilson-Nieuwenhuis *et al.*, 2021), with potentially fatal consequences. The short shelf life, even when extended to seven days makes stock management of PC challenging and can result in considerable component wastage due to time expiry.

1.7 The Platelet Storage Lesion

In addition to the risk of bacterial growth, the second reason for the short shelf life of PC is that they begin to show evidence of a significant loss of platelet function *in vitro* during storage, that may affect the efficacy of platelets once transfused into patients (Devine and Serrano, 2010). This decline in function throughout storage is referred to as the 'platelet storage lesion' (PSL).

The PSL is a complex biological event, involving a series of biochemical, structural and functional changes that occur within platelets as a result of blood collection, mechanical manipulation during manufacture and storage conditions (Ng, Tung and Fraser, 2018; Árnason and Sigurjónsson, 2017). It is important to understand these changes as they are associated with reduced *in vivo* platelet survival (Quach, Chen

and Li, 2018) and if they can be reduced, the shelf life and availability of PCs may be improved.

The manufacture of PC exposes them to stresses, such as centrifugation, manipulation, continuous movement, suspension in chemical storage medium and exposure to foreign surfaces such as the plastic of storage packs (Berzuini, Spreafico and Prati, 2017), as well as the loss of protection that is conferred by the endothelium when in the circulation. All of these stressors can cause physiological responses that resemble platelet activation (Ng, Tung and Fraser, 2018; Devine and Serrano, 2010), hence many of the assays used to study the PSL are functional assays similar to those used to study platelet activation for diagnostic purposes in patients. PC are currently stored in a medium that enables them to be metabolically active, at 20-24^{o}C with constant agitation, in a pack that enables gaseous exchange. During storage at this temperature, glycolysis is enhanced and mitochondrial function reduces leading to glucose depletion, increased lactate production and a resulting acidification of the PC (Ng, Tung and Fraser, 2018). For this reason, assessment of PC during storage often includes and benefits from measures of metabolism and mitochondrial health.

The PSL has been the focus of intense research. Despite earlier hopes of finding a simple assay that could reliably predict the function and survival of stored platelets post-transfusion, the complex nature of the PSL means there is no single assay which can accurately predict the efficacy of a platelet transfusion (Rinder and Snyder, 1992).

Table 1-1 outlines the commonly used assays to study the PSL and the effect that the PSL has on the assay results for RTP.

Table 1-1: List of commonly utilised assays to measure the PSL in RTP

Type	Assay	Purpose	Effect of PSL on RTP
Morphological	Visual inspection of swirling	Measures disk to sphere shape change in platelets. Discoid platelets when rocked gently against a light source scatter light in different directions, causing the phenomenon known as 'swirling'.	Lack of swirling (Devine and Serrano, 2010; Bertolini *et al.*, 2000)
	Platelet morphology score	Visual assessment of platelet morphology using phase contrast microscopy. Quantified using scoring systems such as the Kunicki morphology score	Platelets lose their discoid shape. (Reddoch-Cardenas *et al.*, 2019b; Maurer-Spurej and Chipperfield, 2007; Kunicki *et al.*, 1975)
Functional	Platelet aggregation in response to agonists	Measures platelets responsiveness to different agonists for e.g., thrombin, collagen, epinephrine & ADP	Ability to respond to agonists declines (Scott, Harris and Bolton, 1983; Owens *et al.*, 1992)
	Hypotonic shock response	Measures the ability of the platelet to return to its normal shape after hypotonic challenge.	Declines (Chacko *et al.*, 2013; Ravi *et al.*, 2015a)

Type	Assay	Purpose	Effect of PSL on RTP
Functional	Extent of shape change	Measures the amount of shape change that the platelet undergoes in response to a pre-set dose of ADP	Declines (Devine and Serrano, 2010; Kim and Baldini, 1974)
	CD62P / P-selectin surface expression	Monitor's platelet degranulation. Flow cytometric assay for platelet activation markers released from alpha granules and subsequently expressed on the surface of the platelet	Enhanced exposure (Sweeney *et al.*, 2000; Metcalfe *et al.*, 1997)
	Annexin V binding	Flow cytometric assay using Annexin V to monitor exposure of anionic phospholipids, measures phosphatidyl serine exposure on the platelet membrane	Enhanced exposure (also an indicator of apoptosis) (Metcalfe *et al.*, 1997; Li *et al.*, 2000)
	Soluble CD62P	Measures levels of CD62P shed from the platelet membrane by an ELISA technique	Increases during storage. (Devine and Serrano, 2010; Ng, Tung and Fraser, 2018)
	Thrombin generation (CAT)	Measures kinetics of thrombin generation in response to tissue factor stimulus. Measured by a calibrated automated thrombogram	Thrombin generation indicators suggest platelets become more procoagulant. (Johansson *et al.*, 2008)

Type	Assay	Purpose	Effect of PSL on RTP
Metabolic	Lactate	Measures metabolism of platelets. Lactate is generated by glycolysis	Increases during storage while glucose is available. (Ng, Tung and Fraser, 2018; Sweeney *et al.*, 2000; Paglia *et al.*, 2014)
	Glucose	Measures metabolism of platelets. Glucose is broken down to pyruvate and lactate by glycolysis	Depletes during storage. (Paglia *et al.*, 2014; Sweeney *et al.*, 2000)
	pH	pH meter - measures level of acidity in PC	Decreases (increased acidification secondary to glycolysis) (Devine and Serrano, 2010)
	pO_2 & pCO_2	Measured to ensure that sufficient gas exchange is occurring during storage	While platelets are metabolically active, O_2 declines, CO_2 increases. (Hogge, Thompson and Schiffer, 1986)
	Mitochondrial membrane potential	Flow cytometric assay. Key indicator of cell health - results are relatable to cells capacity to generate ATP by oxidative phosphorylation	Depolarises and thus decreases as mitochondrial function is impaired. (Verhoeven *et al.*, 2005)
	Extracellular ATP	Measures ATP-dependent oxidation of luciferin	Decreases during storage, suggestive of a deficiency in glycolysis &/or OXPHOS. (Holme, 1998)

The PSL is characterized by platelet activation during storage: α-granule contents are released into the media (soluble CD62P), expression of CD62P and phosphatidylserine (PS) on the platelet membrane is increased and platelet shape change including an increase in the mean platelet volume (MPV) and a lack of the 'swirling' phenomenon are observed (Albanyan, Harrison and Murphy, 2009).

The ability of PC to aggregate is assessed using platelet aggregometry in response to agonists. Platelet aggregometry has been reported to correlate well with clinically relevant outcomes like bleeding and thromboembolic events in clinical settings (van Hout *et al.*, 2017). During the PSL, the ability of platelets to respond to agonists and aggregate significantly decreases, suggesting a likely decrease in *in vivo* function post-transfusion although there is evidence to suggest that decreased function may be reversed in the days following transfusion (Bikker *et al.*, 2016).

As PC are metabolically active due to their storage temperature and gas permeable bag, many studies of the PSL examine measures of metabolic function. During storage, PC accumulate lactate as a result of glycolysis. As such, measuring lactate and glucose can give an indication of the amount of metabolism occurring in the cells, but is not a direct measure. Lactate generation results in hydrogen ions being produced which acidifies the PC (reducing the pH) causing the platelets to swell and lose their discoid shape. Once pH falls to below 6.1, the return to the original shape is not possible (Bertolini, Murphy and Transfusion, 1996).

Metabolomics analysis (Paglia *et al.*, 2014) has demonstrated that glucose is exclusively converted to lactate via glycolysis with decreased mitochondrial function during the first three days of storage but that towards the end of shelf life, OXPHOS increases to generate ATP (Paglia *et al.*, 2014; Ng, Tung and Fraser, 2018). It is plausible that if metabolism (and the active glycolytic pathway) can be reduced during storage of PC, that the effects of the PSL could also be reduced, leading to a better quality product with a prolonged shelf life. One potential way of reducing metabolism in PC is to store them at refrigerated temperatures.

1.8 History of Cold Stored Platelets

Prior to 1969, PCs were stored at 4°C with a very limited shelf life due to the prevailing view that platelets should be transfused within a few hours of being isolated from the donor (Filip and Aster, 1978). However, platelets became increasingly important as a therapy for treatment of malignant disorders requiring intensive chemotherapy and there was increasing pressure to produce them in adequate quantities to meet demand (Filip and Aster, 1978). This in turn drove research into alternative methods of storage which could prolong shelf life and improve supply.

A watershed came in the late 1960s / 1970s with the publication of several critical studies comparing cold-stored platelets (CSP) with RTP (Murphy and Gardner, 1969; Valeri, 1974; Filip and Aster, 1978). Micro doses of CSP and RTP were labelled with radioactive chromium (^{15}Cr), transfused to healthy volunteers and the platelet yield and life-span in the circulation measured (Murphy and Gardner, 1969) (Figure 1-7). This study showed that RTP had enhanced post-transfusion recovery and survival compared to CSP.

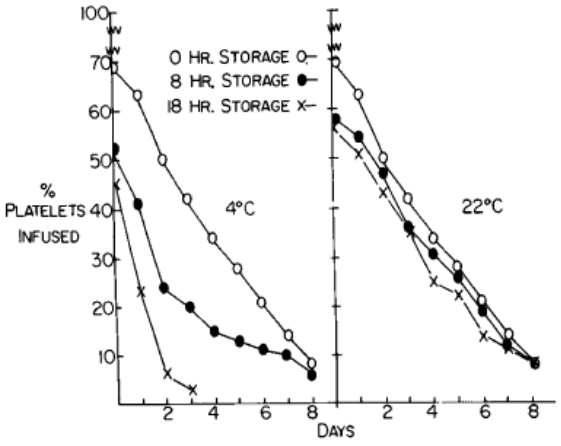

Figure 1-7: ^{15}Cr-labeled platelet lifespan after platelet rich plasma storage at 4°C and 22°C. Taken from (Murphy and Gardner, 1969)

The mechanism of reduced survival of CSP in the circulation has since been shown to be caused by clustering of GPIbα receptors on the surface of platelets and desialylation exposing β-N-acetylglucosamine (β-GlcNAc) moieties on CSP (Hoffmeister *et al.*, 2003; Zhao and Devine, 2022). The exposed β-GlcNAc is

recognised by Ashwell-Morell receptors on hepatic macrophages, resulting in CSP being rapidly phagocytosed and removed from the circulation (Hoffmeister *et al.*, 2003; Hoffmeister, 2011).

Despite survival of RTP being shown to be better than CSP, functionality, as measured by the ability to aggregate in response to agonists, was better preserved in CSP. It was also demonstrated that the haemostatic effectiveness of RTP was impaired, for at least 24 hours, after transfusion (Handin and Valeri, 1971; Valeri, 1974; Becker *et al.*, 1973), with clinical studies showing that CSP were more effective than RTP at correcting bleeding time and bleeding scores in thrombocytopenic patients, immediately upon being transfused (Becker *et al.*, 1973; Valeri, 1974).

Although suggestions had been made that a dual inventory should be kept by blood banks – RTP for prophylaxis and CSP for acute haemorrhage (Valeri, 1974; Kattlove and Alexander, 1971), CSP had all but been abandoned by the end of the 1970s, driven by the logistical challenges of managing dual inventories and due to hypoproliferative thrombocytopenia outnumbering other indications for platelet transfusion (Pidcoke *et al.*, 2014). Another contributing factor may have been the platelet clumping that is seen in CSP stored in 100% plasma which is ameliorated when stored in 70% plasma to 30% platelet additive solution (Getz *et al.*, 2016).

1.9 The Case for Cold Platelet Storage

Over the past decade, interest in CSP has experienced a revival due to the changes in clinical practice already discussed, with a shift away from prophylactic platelet transfusions and new evidence to support the use of platelet transfusions during major haemorrhage (Cardenas *et al.*, 2018).

Along with these changes in practice, the conflicts in Iraq and Afghanistan, where there was limited access to PC due to their short shelf life and storage challenges, placed a greater emphasis on the importance of being able to supply PC ,with the studies performed by Pidcoke and Perkins (Pidcoke *et al.*, 2012) demonstrating benefit of early platelet transfusion in military casualties requiring massive

transfusion. As a result of these studies, a renewed interest in CSP emerged (Reddoch-Cardenas *et al.*, 2019a). CSP may have greater haemostatic properties due to their partially activated or 'primed' state as well as the potential for a longer shelf life than RTP. Table 1-2 summarises the main benefits and constraints of CSP vs RTP.

Table 1-2: Comparison of benefits and disadvantages of CSP vs RTP.

Cold Stored Platelets (CSP)	Room Temperature Platelets (RTP)
Not conductive to most bacterial growth due to low temperature (Ketter *et al.*, 2019), therefore reduced risk of transfusion-associated bacterial infection/ transfusion-associated sepsis. Bacterial monitoring methods not required.	Ideal environment for bacterial growth, leading to increased risk of bacterial contamination and sepsis (Brecher *et al.*, 2013). Costly bacterial monitoring/pathogen inactivation strategies required.
Reduced circulation time – half-life of around 1.3 days* (Murphy and Gardner, 1969) therefore unlikely to be suitable for prophylactic transfusions	Increased circulation time (half-life of 3.9 days), reduces transfusion frequency for prophylaxis and thus risk of alloimmunization (Pidcoke *et al.*, 2014)
Dual inventory would be required – CSP for therapeutic transfusions and RTP for prophylactic transfusions, increasing complexity of supply chain	Single inventory for both therapeutic and prophylactic transfusions
Cheaper and easier to store - can be stored with red cell concentrates without agitation, no requirement for separate agitators and incubators	Logistics of storage difficult - requires constant agitation to maintain gas exchange and aerobic respiration (Milford and Reade, 2016). Using bulky & expensive agitators at a regulated temperature of 22 ± 2°C.

Cold Stored Platelets (CSP)	Room Temperature Platelets (RTP)
Can be transported in isothermal transport boxes with red cells and other medications to be used in pre-hospital treatment of trauma (Pidcoke *et al.*, 2014)	Requires separate transport boxes to other components. Logistics make it difficult to use in pre-hospital settings
Licensed in US and Norway for use up to 14 days in specified clinical situations (FDA, 2023) (Strandenes *et al.*, 2020)	Shelf life 5-7 days (depending on bacterial screening protocol) due to platelet storage lesion and bacterial contamination risk.
PC in 100% plasma (current UK apheresis product) known to produce aggregates on cold storage	Minimal aggregate formation in RTP in 100% plasma
Significantly reduced accumulation of some pyrogenic cytokines whose presence correlates with the frequency and severity of febrile non haemolytic transfusion reactions (FNHTR) (Ferrer *et al.*, 2001)	Higher levels of pro-inflammatory cytokines such as sCD40L and thus increased risk of FNHTRs (Reddoch *et al.*, 2014)
Superior haemostatic function * (Becker *et al.*, 1973)	Haemostatic function rapidly deteriorates throughout storage * (Becker *et al.*, 1973)
Rapid clearance from the blood could reduce risk of thrombosis (Scorer *et al.*, 2019b)	Develop a functional defect during storage which is not corrected until 24 hours post-transfusion * (Becker *et al.*, 1973)
Preliminary data suggesting that CSP are superior to RTP in reversal of anti-platelet agents (Scorer *et al.*, 2018; Stolla *et al.*, 2018)	

**The evidence in these points was generated prior to the introduction of platelet storage packs that allowed gaseous exchange.*

Attempts have been made to prevent the rapid clearance of CSP in the circulation by galactosylation of the β-GlcNAc moieties on platelets. This has been successful in murine studies but ineffective with human platelets (Wandall *et al.*, 2008).

CSP derived from apheresis platforms are currently licensed in the US by the Food and Drug Administration (FDA) for up to 14 days at 1 to 6^{o}C for treatment of active bleeding when conventional platelets (RTP) are not available or their use is not practical (FDA, 2023). In addition, CSP are licensed in Norway, by the Norwegian Directorate of Health, as a response to the Covid-19 pandemic to mitigate the risk of blood shortages, for storage up to 14 days, with the caveat that they are used only when there is an insufficient supply of platelets (Braathen *et al.*, 2022). It is feasible that the shelf life of CSP could be extended further and there are many studies examining CSP function up to 21 days. As of yet however, there is no consensus on what the optimal maximum shelf life should be.

Outside of haematology-oncology there is only two completed clinical trials of CSP versus RTP. The first was a pilot trial in complex cardiac surgery, which aimed to provide preliminary data on safety and feasibility for further evaluation of the haemostatic potential of CSP (Strandenes *et al.*, 2020). The study showed reduced chest drain output (as a means of measuring blood loss) in CSP compared to RTP and supported the feasibility of a 14-day shelf life (Strandenes *et al.*, 2020). The second is a recently published randomised clinical trial comparing the early use of CSP in patients with haemorrhagic shock compared to the standard care (RTP) (Sperry *et al.*, 2024). This outcome of this trial was that early use of CSP was not associated with significant outcome differences compared to RTP, was feasible, safe and did not result in a significant lower rate of 24-hour mortality (Sperry *et al.*, 2024)

There are now a series of clinical trials ongoing on the use of CSP (NIH, 2024), the majority of which are based in the US with one registered trial in Norway and one in Canada (Table 1-3).

Table 1-3: Current registered clinical trials of CSP (NIH, 2024)

Study Name	Acronym	Patient Cohort	Country
Chilled Platelet Study	CHIPS	Complex cardiac surgery	US
Cold-stored platelet early intervention in TBI	CriSP-TBI	Traumatic brain injury (TBI)	US
Extended cold stored apheresis platelets in cardiac surgery	CHASE	Cardiac surgery	US
Reversal of aspirin antiplatelet therapy with cold stored platelets	RASP	Reversal of aspirin	US
Cold stored platelets in haemorrhagic shock	CriSP-HS	Haemorrhagic shock	US
Transfusion of cold stored platelet concentrates	4CPLT	Post operative thoracic surgery	Norway
Cold apheresis platelets in PAS	CAPP	Survival study of CSP	US
Delayed cold stored platelets	PLTS-1	Cardiac surgery	Canada
Reversal of dual antiplatelet therapy with cold stored platelets	R-DAPT	Patients on dual anti-platelet therapy	US
Assessment of whole blood cold stored platelets	Brrr	Healthy donors	US

1.10 *In Vitro* characteristics of CSP

Platelets rapidly change shape after refrigeration from smooth discs into an activated spherical morphology that is defined by a loss of 'swirling' and an increase in the MPV (Wood *et al.*, 2016). Platelets are less able to maintain their energy-dependent low cytosolic calcium levels when stored in the cold, resulting in an increase in free cytosolic calcium. The rise in calcium causes actin filament fragmentation which alongside microtubule depolymerization, results in shape change (White and Krivit, 1967), which has been shown to be maintained throughout 21 days of storage (Johnson *et al.*, 2016).

CSP exhibit an increased activation status, as demonstrated by an upregulation of the markers of activation such as CD62P, Annexin V and phosphatidylserine (PS) (Reddoch *et al.*, 2014). This does not appear directly related to the activation associated with the release of α-granule contents, however, since levels of cytokines such as RANTES are significantly lower with storage in CSP compared to RTP (Sandgren, Shanwell and Gulliksson, 2006). Instead CSP are described more as being 'primed' for use (Hoffmeister *et al.*, 2003). Despite their increased activation marker levels, CSP have been shown to be responsive to endothelial inhibitors (nitric oxide and prostacyclin) and thus retain the ability to deliver haemostasis to the site of injury without causing thrombosis (Reddoch *et al.*, 2016).

CSP demonstrate a superior ability to aggregate when exposed to agonists such as ADP, collagen and thrombin receptor activated peptide-6 (TRAP-6) as compared to RTP (Becker *et al.*, 1973; Choi and Pai, 2003). In addition, they have been shown by Nair and colleagues (Nair *et al.*, 2017) to produce clots that are denser, thinner, straighter and with more branch points than RTP. All of these factors suggest that CSP are likely to have superior *in vivo* function compared to RTP.

1.11 Metabolic Activity of CSP

Cold storage of platelets significantly lowers metabolic activity, resulting in a reduction in the metabolic rate of glucose consumption and lactate production

through glycolysis (Getz *et al.*, 2016). The platelet count, pH ,pO_2, pCO_2, bicarbonate and ATP concentrations are also better maintained in CSP compared to RTP (Sandgren, Shanwell and Gulliksson, 2006). Overall, this diminution of metabolic activity means that glucose remains present in CSP up to 21 days of storage, supporting the extension of PC shelf life (Johnson *et al.*, 2016).

1.12 Bioenergetic Profiles of Platelet Concentrates

The ability to assess mitochondrial function enables advanced understanding of platelet metabolism's key role in platelet physiology, which is not covered by the established platelet metabolic assays that focus on measuring the substrates or by products of metabolism such as glucose and lactate. The development of fluorescence based oxygen sensors, however, has opened up new avenues for measuring bioenergetic profiles of intact cells, including platelets (Divakaruni *et al.*, 2014).

Recent advances in extracellular flux (XF) analysers in particular, have enhanced the ability to measure the bioenergetic profiles of intact cells *ex vivo*, by measuring the oxygen consumption rate (OCR) and the extracellular acidification rate (ECAR) or proton excretion of the cells (Kramer *et al.*, 2014). This reflects the function of mitochondrial respiration (OXPHOS) and glycolysis respectively and unlike endpoint assays such as lactate, enables detection of metabolic function in real time, as well as avoiding isolation of mitochondria from the platelets which may lead to damage of the organelle (Ravi *et al.*, 2015a). The total ATP production rate can be measured, distinguishing between the fractions of ATP that are produced from OXPHOS and glycolysis, in addition to measuring key parameters of mitochondrial function through the use of modulators to isolate different parts of the ETC.

The ETC 's role, as previously discussed, is to transfer electrons through complexes I-IV in the inner mitochondria membrane (Figure 1-5) to the final electron acceptor, oxygen (Judge and Dodd, 2020). As the electrons travel through the ETC they undergo a series of reductions. This provides the energy to drive protons against their concentration gradient into the intermembrane space, creating an electrochemical gradient comprised of the increased concentration of H^+ and positive charge

distribution collectively referred to as the proton motive force (Δp). The H^+ then flow back into the mitochondria through ATP synthase resulting in the production of ATP (Perry *et al.*, 2011).

The use of modulators of the ETC in extracellular flux analysers have the potential to provide a more precise understanding of platelet concentrate metabolism during storage, by the isolation and measurement of individual parts of the ETC (Figure 1-8).

The use of the modulator oligomycin, inhibits proton translocation through ATP synthase, resulting in an increase in membrane potential which decreases electron transport through complexes I-IV (Braganza, Annarapu and Shiva, 2020). Any residual OCR not affected by oligomycin treatment is due to 'proton leak' and is independent of ATP production. If the OCR due to proton leak is deducted from the basal respiration OCR, then the ATP production coupled respiration can be calculated.

The maximal respiratory capacity of platelets and the reserve capacity can be measured through the administration of the uncoupling agent, FCCP. FCCP abolishes the inner mitochondrial potential by transporting protons across the mitochondrial inner membrane, uncoupling electron transport through complexes I-IV with ATP synthesis (Braganza, Annarapu and Shiva, 2020) and allowing protons to bypass ATP synthase and consume oxygen at the maximum potential rate. By subtracting the basal OCR from this maximal rate it is possible to quantify the ability of the cells to respond to a stressor with increased ATP production (Nolfi-Donegan, Braganza and Shiva, 2020), for example, during platelet activation.

To measure the portion of OCR that is non-mitochondrial, the inhibitors rotenone (a complex I inhibitor) and antimycin A (a complex III inhibitor) are utilised which completely inhibit the ETC and therefore prevents oxygen consumption due to mitochondrial respiration (OXPHOS) (Braganza, Annarapu and Shiva, 2020). The use of these inhibitors along with the simultaneous measurement of the extracellular acidification rate (ECAR), enables the calculation of glycolysis-driven ATP production (Romero *et al.*, 2018).

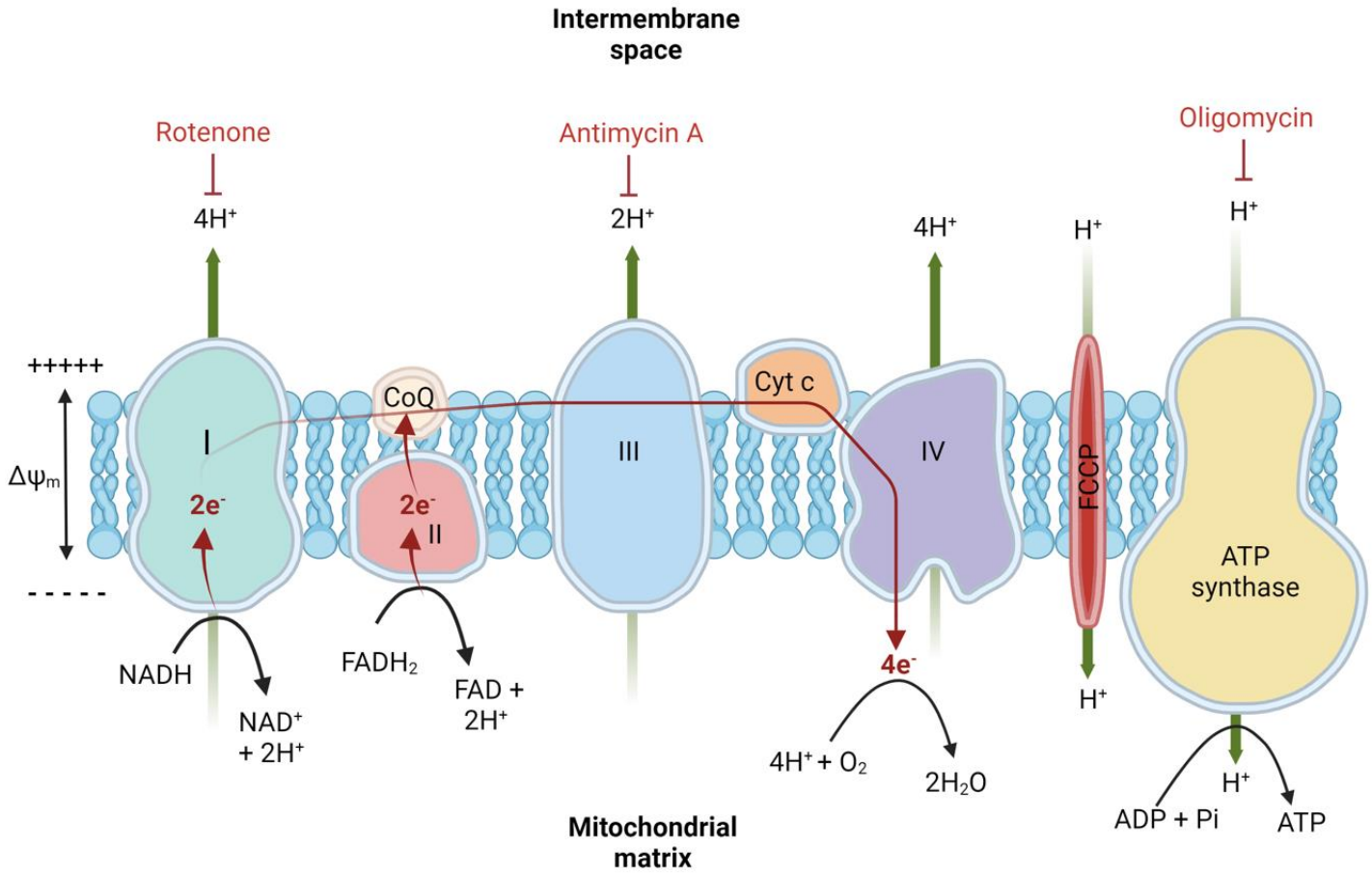

Figure 1-8: Electron transport chain (ETC) demonstrating the action of modulators of respiration utilised in XF analysers.. Rotenone acts on complex I, antimycin A on complex III and oligomycin on ATP synthase. The cylinder 'FCCP' represents the action of protonophoric uncoupling agents such as FCCP and CCCP that collapse the $\Delta\psi_m$.

XF analysers have been used to examine the bioenergetic profiles of platelets as biomarkers for the deterioration of mitochondria in different clinical settings, including cardiopulmonary bypass (Mazzeffi *et al.*, 2016), asthma (Xu *et al.*, 2015) and Alzheimer's Disease (Prestia *et al.*, 2019), but has had very limited use in examining bioenergetic profiles of PC for transfusion (Ravi *et al.*, 2015a).

Where bioenergetic profiles of platelets have been examined using XF analysers, they have been shown to have a metabolic plasticity that enables them to switch freely between glycolysis and OXPHOS (Aibibula, Naseem and Sturmey, 2018) (Ravi *et al.*, 2015b) and to shift to a predominantly glycolytic phenotype when they transition from a quiescent to an activated state (Aibibula, Naseem and Sturmey, 2018). The only published study using an XF analyser to study PC, compared mitochondrial and glycolytic function of PC stored at 22^{o}C on day 6-9 of shelf life with freshly isolated platelets from healthy donors (Ravi *et al.*, 2015a). This study showed that storage of platelets causes a modest decrease in OXPHOS driven by an increase in mitochondrial proton leak (Ravi *et al.*, 2015a).

This ability to assess mitochondrial function and examine bioenergetic profiles of PC, could provide an advanced understanding of the key role of platelet metabolism and mitochondrial health in the PSL, which is not easily discernible by the established platelet metabolic assays discussed previously (for example, glucose consumption and lactate production). This understanding can then be further applied to compare the different metabolic profiles of CSP and RTP, determining if metabolism is reduced in CSP and the impact it has on the functional ability of the platelets.

1.13 Thesis hypothesis and aims

1.13.1 Hypothesis

Storage of PC in the cold (at 2 - 6 ^{o}C) preserves mitochondrial function and reduces metabolism, resulting in a reserve of energy in the platelets that results in superior response to functional assays.

1.13.2 Aims of the study

- Characterise the bioenergetic profiles of PC stored at 2-6 ^{o}C and 20-24 ^{o}C as a measure of the rate of metabolism and mitochondrial function.
- Determine whether the bioenergetic profiles of the PC represents an accurate marker of PC function.
- Based on these assessments determine a potential shelf life for CSP and if they are likely to be more efficacious when transfused than RTP.

Chapter 2: Methods

2.1 Collection and sampling of platelet concentrates

2.1.1 Donor consent

The PC collected were donated by volunteer donors on the Welsh Blood Service (WBS) apheresis donor panel who had provided informed consent (APPENDIX I) for their donations to be used for research purposes, as approved by the WBS Research, Development and Innovation committee. The project was also approved by the Manchester Metropolitan University Ethics Committee (EthOS number: 63053). No further research/ethical approvals were required.

2.1.2 Collection of platelet concentrates

Twelve double PC (i.e. two adult therapeutic doses) single donor apheresis PC were collected with concurrent plasma units by the Trima Accel apheresis platform (Terumo, Colorado, USA, software version 7.0.1) into Trima Accel® LRS® Platelet + Auto PAS plasma set (Figure 2-1). Alongside the donation, acid citrate dextrose (ACD) solution (Terumo, Colorado, USA) was added as an anticoagulant. At the end of collection, once the donor was disconnected from the apheresis machine, the PAS-E Terumo platelet additive solution (T-PAS+) (Terumo, Colorado, USA), which has a pH of 7.2, was added to the PC to give a final ratio of approximately 65% PAS : 35% plasma (chemical composition of T-PAS+ is shown in Table 2-1). The double PC was roughly split into the two storage packs and allowed to rest.

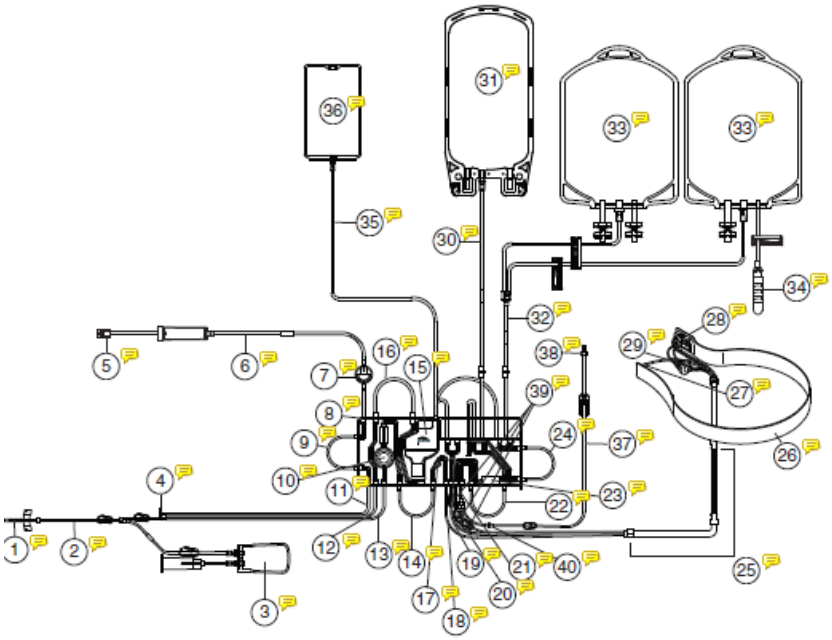

1 Needle
2 Donor line
3 Sample bag
4 Anticoagulant (AC)/draw/return manifold
5 AC luer
6 AC line
7 Sterile barrier filter
8 Cassette
9 AC pump header
10 Draw/return pressure diaphragm
11 AC line
12 Return line
13 Draw line
14 Inlet pump header
15 Return reservoir
16 Return pump header
17 Centrifuge pressure sensor
18 Inlet line to centrifuge
19 RBC line from centrifuge
20 Platelet line from centrifuge
21 Plasma line from centrifuge
22 Plasma pump header
23 Cassette label
24 Platelet pump header
25 Centrifuge loop
26 Channel
27 Inlet port
28 Collection chamber
29 LRS chamber
30 Plasma collect line
31 Plasma bag
32 Platelet collect line
33 Platelet bag
34 Platelet product sampler
35 Vent bag line
36 Vent bag
37 Auto PAS line
38 Auto PAS luer
39 Channel line clamps
40 Auto PAS one-way valve

Figure 2-1: Configuration of the Trima Accel® LRS® Platelet + Auto PAS, plasma set . The PC is collected into one of the two platelet storage bags (33) and concurrent plasma is collected into the plasma bag (31).

Table 2-1: Chemical composition of T-PAS+

Chemical substance	Quantity in 1000 mL of solution
Sodium citrate dihydrate	3.18g
Sodium acetate trihydrate	4.42 g
Sodium dihydrogen phosphate	1.05 g
Disodium hydrogen phosphate	7.69 g
Potassium chloride	0.37 g
Magnesium chloride hexahydrate	0.30 g
Sodium Chloride	4.05 g
Water for injection	-

After 1 hour of rest at ambient temperature, the double apheresis PC were pooled into one pack, sampled (see point 2.1.3) and equally split by weight into two separate packs via the pool and split method (Figure 2-2). One pack was stored at 22°C ± 2°C with continuous horizontal agitation (RTP) and the other was stored at 4°C ± 2°C (CSP) without agitation.

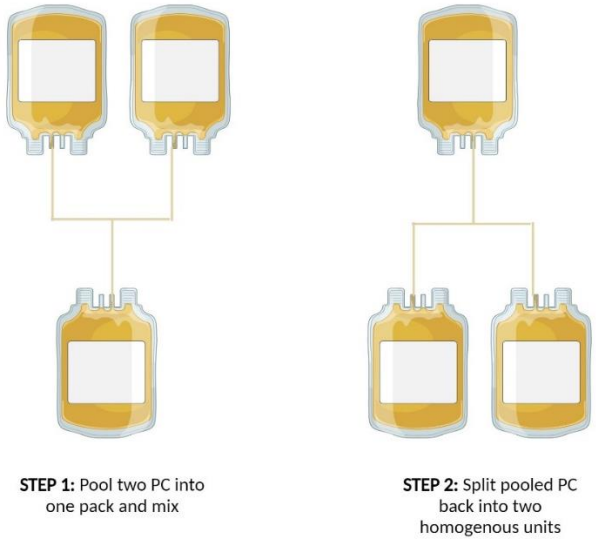

Figure 2-2: Pool and split method to obtain two homogenous packs of PC.

2.1.3 Sampling of PCs

Samples were collected from each PC on day 0 (prior to splitting into two units), day 2, day 8, Day 14 and Day 21 (cold stored platelet (CSP) only). On day 0, the apheresis donation was pooled into one of the two platelet packs and a sampling pouch (Macopharma Mouveaux, France) was sterile connected to the platelet pack using a sterile tubing welder (Terumo, TSCD®-II, Colorado, USA). The unit was gently agitated to ensure a homogenous sample and 14 mL was allowed to flow into the docked-on pouch (measured using a weighing scales). The line of the pouch was heat sealed to provide a sterile seal and the pouch removed from the pack. The sample was then decanted into two polypropylene universal tubes, one containing 4 mL and the other 10 mL. The further aliquoting of samples for individual assays is shown in Figure 2-3 and Figure 2-4. This process was repeated for sampling of the RTP on Days 2, 8 and 14.

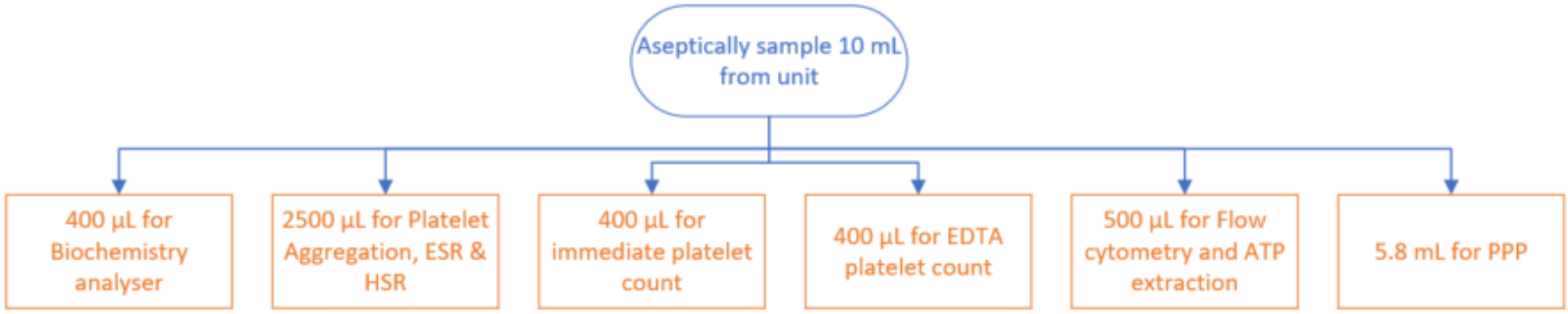

Figure 2-3: Aliquoting of samples for individual assays from the 10 mL universal.

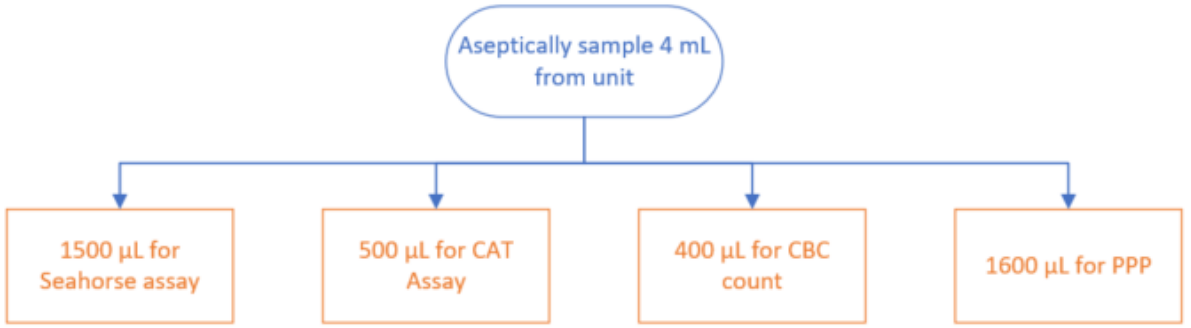

Figure 2-4: Aliquoting of PC samples for individual assays from the 4 mL universal.

Due to differences in timing of the assays for the flow cytometer, the calibrated automated thrombinoscope (CAT) and Seahorse analyser, the CSP were sampled at two different times on day 2, 8, 14 and 21. The first was a small 4 mL sample for the assays shown in Figure 2-3. Due to the small volume, it was difficult to accurately measure the volume in a docked-on pouch. Therefore, on day 2, a sample site coupler (Fresenius, Bad Homburg, Germany) was inserted into the pack in a class II laminar flow cabinet (Airstream AC2-351, ESCO Lifesciences, Singapore). After cleaning the port with a sterile alcohol swab and allowing to air dry, a 17-gauge needle attached to a 10 mL syringe was inserted into the sample site coupler. The pack was gently agitated to ensure a homogenous sample and a 4 mL sample withdrawn into the syringe and placed into a universal tube. On days 8, 14 and 21 samples were taken aseptically from the same sample site coupler. The second samples from the CSP of 10 mL were taken by docking on a pouch as described above.

2.1.4 Platelet poor plasma (PPP) from concurrent plasma

The concurrent plasma (Figure 2-1) was separated from the apheresis platelet packs using a heat sealer on the day bled and the plasma was dispensed into 25 mL polypropylene universal tubes within a class II safety cabinet prior to being centrifuged (Hettich Rotina 420R, Tuttlingen, Germany) at 2000 *g* for 10 minutes at 22^{o}C. Once centrifuged, the plasma from each universal was decanted into a fresh universal tube using a Pasteur pipette, within a class II safety cabinet. This process was repeated a further time to generate PPP (approximately 20-25 mL). One universal of PPP was used on Day 0 for testing and all remaining universals of PPP were frozen at -40^{o}C for subsequent testing days.

2.1.5 Platelet poor plasma (PPP) from PC platelet rich plasma samples

Aliquots of platelet rich plasma (PRP) from the PC were centrifuged at 2000 *g* in a 12 x 75 mm polypropylene tube for 10 minutes at 22^{o}C and the supernatant was decanted into a second 12 x 75 mm tube. This was centrifuged again at 2000 *g* for 10 minutes and decanted into another 12 x 75 mm tube as the final PPP.

2.2 Indicators of component quality

2.2.1 Background

There is no single test that is sufficient to assess PC quality, therefore a panel of tests are employed as part of the quality control of PC. The Joint United Kingdom Blood Transfusion and Tissue Transplantation Services Professional Advisory Committee (JPAC) describes the specifications that must be met for all clinical blood components. For apheresis derived PC, this includes volume within 150–380 mL, platelet count of ≥240 x 10^9/unit (units tested and found to have <160 x 10^9/unit should not be used), pH at end of shelf life of ≥6.4 and a leucocyte count of <1 x 10^6/unit (JPAC, 2021). In addition, visual assessment of units for the swirling phenomenon, clumping/aggregates and excessive red cell contamination is recommended prior to issue to a patient.

2.2.2 Visual assessment of platelet concentrates

Prior to each sampling event the PC were scored for the 'swirling' phenomenon. The PC were held up to a light source and gently rotated. Normal discoid platelets scatter the incident light in different directions producing a swirling effect in the plasma. Once platelets have undergone shape change from disc to sphere, they all scatter light in the same direction, resulting in a dull unchanging appearance to the sample. Therefore, observation of the 'swirling' phenomenon can be used to decipher whether platelets are discoid or activated and spherical.

Swirling was scored as shown in Table 2-2.

Table 2-2: Scoring method for platelet swirling , as described by Fratantoni et al [1].

Score	Swirling Description
0	No swirling, sample appears homogenously turbid (same before rotating as afterwards)
1	Some inhomogeneity, but contrast poor and only observed in a few places
2	Swirling inhomogeneity throughout the bag with good contrast
3	Swirling inhomogeneity throughout the bag with contrast observable as fine detail

In addition to scoring for the swirling phenomenon, the platelets were examined for macro-aggregates, visible with the naked eye, which were scored as shown in Table 2-3. Clumping/aggregation can be a sign of platelet activation or bacterial contamination and units with a score >1 would not be issued for clinical use.

Table 2-3: Scoring method for platelet aggregates.

Score	Aggregate Description
0	No aggregates
1	Minor aggregates (a few small aggregates)
2	Moderate (>10 obvious aggregates)
3	Extensive aggregates (large clumps)

2.2.3 Unit volume

Prior to sampling on day 0, 2, 8, 14 and 21 the unit volume was calculated using the following formula:

$$Volume = \frac{weight\ of\ unit - weight\ of\ empty\ pack\ (40g)}{specific\ gravity\ of\ platelets\ in\ 65\ \%\ SSP+\ and\ 35\%\ plasma\ (1.02)}$$

2.2.4 Platelet count, mean platelet volume and platelet yield

PC samples were placed in dry ethylenediaminetetraacetic acid (EDTA) tubes and mixed for a minimum of 30 minutes prior to testing on an ABX Pentra XL80 analyser (Horiba, Kyoto, Japan) which uses impedance to obtain the platelet concentration ($x10^9$/L) and the MPV. The platelet yield ($x10^9$/unit) was calculated by multiplying the platelet concentration by the unit volume in litres.

2.2.5 Residual white cell counting

Leucocyte reduction of all blood components (with the exception of granulocytes) was introduced in the UK as a variant Creutzfelt-Jakob disease (vCJD) risk reduction measure in 1999. Residual white cell counting was performed via a flow cytometric assay used routinely for quality monitoring of leucodepletion of blood components at the WBS.

The assay utilises the Leukosure Enumeration kit (Beckman Coulter, CA, USA) which uses propidium iodide solution as a nuclear stain. The samples were run alongside fluorospheres of a known concentration on a DX Flex flow cytometer (Beckman

Coulter, CA, USA) which enables absolute counting of residual white cells. Samples were acquired for three minutes at high flow rate. Any WBC results outside of these specifications will be removed from the study as high numbers of WBC can have a detrimental effect on platelet storage conditions, increasing glucose consumption and lactate production (Vit, Klüter and Wuchter, 2020).

2.2.6 End of storage sterility

At the end of the storage period, each PC was tested for bacterial contamination. Any units found to be contaminated with bacteria will be removed from the study, as similar to white cells, bacteria have a detrimental effect on platelet storage conditions, particularly for platelets stored at room temperature (Ketter *et al.*, 2019). The units were gently agitated to ensure a homogenous sample and 20 mL removed via an aseptically attached pouch. The sample was divided into an aerobic and an anaerobic culture bottle (Biomerieux, Marcy L'Etoile, France) in a class II biological safety cabinet and cultured for seven days in a bacterial monitoring system (BacT Alert 3D system Biomerieux, Marcy L'Etoile, France) at 36^{o}C before recording the bacteriology status of the unit.

2.2.7 Assessment of platelet count of unit pre and post infusion

The transfusion sets (Infusomat ® Space Line, Braun, Melsungen, Germany) used to transfuse blood products contains a 200 µm filter. To assess the potential loss of platelets in the giving set filter due to micro-aggregates, the CSP units were run through a giving set at the end of the study. A pre and post platelet count was performed on the unit as described in 2.2.4.

2.3 Functional analysis

2.3.1 Background

Light transmission aggregometry (LTA) assesses the ability of platelets in PRP to aggregate in response to agonists for different platelet activation pathways. ADP is a mild platelet agonist which binds to $P2Y_1$ and $P2Y_{12}$ and induces aggregation and stabilization of platelet aggregates. Collagen binds to the platelet receptors GPIa/IIa,

which contributes to platelet adhesion and GPVI which is responsible for platelet signalling and activation leading to TxA_2 formation. Thrombin receptor-activating peptide-6 (TRAP-6) is a synthetic peptide that mimics the effect of thrombin - the most potent physiologic agonist of platelets, which activates protease-receptors 1 (PAR1) and 4, resulting in subsequent signal propagation (Zhou and Schmaier, 2005).

The principle of the hypotonic shock response (HSR) assay is that the addition of water to a cuvette containing a set concentration of platelets, results in an influx of water into the platelets, causing them to swell. This swelling has a dilutionary effect on the cytoplasmic contents resulting in a decrease in the platelet refractive index and an increase in transmitted light (Murphy *et al.*, 1994). Where the platelets have normal membrane integrity and metabolism, they are able to extrude the water to regain normal volume which is accompanied by an increase in the refractive index and a decrease in transmitted light. The measurement of the transmitted light enables the % of platelets that recover their original shape to be measured (Holme, Moroff and Murphy, 1998).

The extent of shape change (ESC) assay measures the change in shape of platelets from discoid to spherical, in response to ADP. EDTA is added to a set concentration of platelets in a cuvette (to prevent aggregation) before addition of ADP to activate the platelets. Discoid platelets undergo a rapid disc-to-sphere transformation that is associated with a decrease in transmitted light (Holme, Moroff and Murphy, 1998). The extent of decrease in transmitted light has been shown to be directly related to the percentage of discoid platelets in the PRP (Holme, Moroff and Murphy, 1998).

2.3.2 Light transmission aggregometry

The PC ability to aggregate in response to physiological agonists was determined using LTA performed on a PAP-4 aggregometer (Bio Data Corporation, PA, USA). PC PRP samples were normalised to 300 x 10^9/L by diluting with PPP generated from the concurrent plasma unit (point 2.1.4) in a total volume of 2 mL prior to testing.

2.3.2.1 Reagent preparation

Lyophilised adenosine-5'-diphosphate (ADP) (Bio Data Corporation, PA, USA), collagen (Hyphen Biomed, Neuville sur Oise, France) and TRAP-6 (Diagnostica Stago,

Asniéres sur Seine, France) were removed from refrigerated storage and allowed to reach room temperature. ADP was reconstituted with 500 µL of deionised water (dH_2O) to provide a working concentration of 200 µM. Collagen was reconstituted with 500 µL of dH_2O, mixed and allowed to stabilise at room temperature for 30 minutes. The collagen was then diluted to a ratio of 1:10 of reconstituted collagen to kit diluent (Hyphen Biomed, Neuville sur Oise, France) to give a working concentration of 100 µg/mL. TRAP-6 was reconstituted with 1 mL of dH_2O to give a neat concentration of 500 µM. A further 1:2 dilution of TRAP-6 was made from the neat solution by diluting with 0.9 % saline to give a concentration of 250 µM. The saline (0.9 %, w:v) was made by dissolving 0.09 g of sodium chloride in 10 mL of dH_2O.

2.3.2.2 Measurement

Glass, siliconized cuvettes (Bio Data Corporation, PA, USA) containing a stir bar (Bio Data Corporation, PA, USA) were pre-warmed prior to the addition of 450 µL of PRP. Once PRP was added, the cuvette was incubated for 2 minutes at 37°C in the PAP-4. The test channels were calibrated with a cuvette containing 500 µL of PPP to represent 100% light transmittance and the PRP cuvette to represent 0% transmittance. To run the test samples, 50 µL of agonist was added to the PRP cuvette and the increase in light transmittance recorded via a paper graph trace on the aggregometer for a minimum of 5 minutes. The final concentrations of agonists used were 10 µg/mL of collagen; 20 µM ADP; 50 µM TRAP-6 and 25 µM TRAP-6.

2.3.3 Extent of shape change

The ESC was determined using the SPA-2000 aggregometer (Chrono-log Corp, PA, USA).

2.3.3.1 Reagent preparation

Phosphate buffered saline (PBS) was prepared by dissolving one tablet (Sigma-Aldrich, Dorset, UK) in 200 mL of dH_2O to give a pH of 7.4. HEPES buffer was prepared to a concentration of 1 mol/L by dissolving 2.383 g of HEPES (VWR International Ltd, Lutterworth, UK) in 10 mL of dH_2O. ADP (1 mmol/L) was prepared by dissolving 0.0043 g ADP (Sigma-Aldrich, Dorset, UK) in 10 mL of PBS. EDTA disodium salt was

prepared by dissolving 0.3722g of EDTA (VWR International Ltd, Lutterworth, UK) in 10 mL of dH_2O to give a concentration of 0.1 mol/L.

2.3.3.2 Sample preparation

PPP buffered with HEPES (prepared by adding 150 µL of HEPES buffer to 10 mL of autologous PPP to give a final concentration of 15 mmol/L of HEPES) was used to adjust the platelet count of the PRP to 300 x 10^9/L for testing.

2.3.3.3 Measurement

HEPES-buffered PPP (500 µL) was pipetted into a microcuvette (Chrono-log Corp, PA, USA) containing a siliconized stir bar (Chrono-log Corp, PA, USA) and placed into the SPA-2000 aggregometer in the 'PPP' well at 37°C. The pre-warmed (37°C) PRP (500 µL) was added to two separate cuvettes containing stir bars and placed in the 37°C incubation wells on the SPA-2000 aggregometer. The first PRP cuvette was placed in the test well and was firmly injected with 10 µL of EDTA followed by 10 µL of ADP. The instrument automatically calculates the % ESC and with a chart recorder (Chrono-log Corp, PA, USA) and prints a graphical representation of the reaction.

This was repeated with the second PRP sample to obtain a duplicate result – where the results were not within 5% of each other the assay was repeated.

2.3.4 Hypotonic shock response

The Hypotonic Shock Response (HSR) assay was performed using the SPA-2000 aggregometer (Chrono-log corp, PA, USA). PPP buffered with HEPES (prepared by adding 150 µL of HEPES buffer to 10 mL of autologous PPP to give a final concentration of 15 mmol/L of HEPES) was used to adjust the platelet count of the PRP to 300 x 10^9/L for testing.

2.3.4.1 Reagent preparation

Reagents were prepared as described in point 2.3.3.1. PBS and dH_2O were pre-warmed at 37°C prior to use.

2.3.4.2 Measurement

HEPES-buffered PPP (500 µL) was pipetted into a microcuvette containing a siliconized stir bar and placed into the SPA-2000 aggregometer in the 'PPP' well at

37°C. Pre-warmed (37°C) PRP (500 µL) was added to four separate cuvettes containing stir bars and placed in the 37°C incubation wells on the SPA-2000 aggregometer. The first PRP cuvette was placed in the test well and was firmly injected with 250 µL of PBS to assess the effect of dilution on the reading. A second tube with PRP was then added to the test well and was firmly injected with 250 µL of dH_2O. The instrument automatically calculated the % recovery from HSR and a graphical representation of the reaction was printed from a chart recorder (Chrono-log Corp, PA, USA).

This was repeated with the third and fourth PRP samples to obtain duplicate results – where the results were not within 10% of each other the assay was repeated.

2.3.5 Thrombin generation

Thrombin generation was measured in PC PRP samples adjusted to 150 x 10^9/L with autologous plasma, using a Calibrated Automated Thrombogram® (CAT) method (Hemker thrombinoscope, Diagnostica Stago, Asniéres sur Seine, France).

2.3.5.1 Background

Thrombin generation is essential for intact coagulation by activating platelets and amplifying the coagulation rate at the phospholipid surface, as well converting fibrinogen to fibrin (Johansson *et al.*, 2008). The CAT is a broad function test of the haemostatic-thrombotic mechanism of blood (as there are no pathways that bypass thrombin) and can be used to assess the ability of PC to aid in thrombin generation and stable clot formation.

The CAT assay utilises a slow-reacting fluorogenic substrate that enables continuous measurement of thrombin generation (Hemker *et al.*, 2003). A sample of PRP is split into two parts with the fluorogenic substrate added to both (Figure 2-5). In the first PRP sample (Figure 2-5A) coagulation is triggered by the addition of calcium and a set concentration of tissue factor (TF). In the second sample a thrombin calibrator is added along with Ca^{2+} (Figure 2-5B).

As the fluorescent signal is not linearly dependent upon the concentration of fluorescent product and the colour of the plasma can influence the fluorescence intensity, each plasma needs to be compared to its own calibration measurement,

which is why the stable concentration of thrombin in the calibrator is measured in parallel with the PRP sample (Figure 2-5) (Hemker *et al.*, 2002). The calibrator consumes the substrate, increasing the fluorescence level and thus the Kc can be measured over a range of fluorescence levels (Hemker *et al.*, 2002).

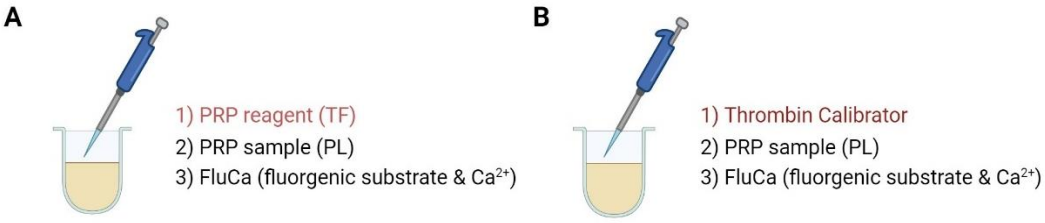

Figure 2-5: Constituents of the CAT test . A: Thrombin generation well (test sample); B: Thrombin Calibrator well. TF = tissue factor, PL = phospholipids. PL are supplied by the surface of the platelets in the PRP sample.

2.3.5.2 Reagent preparation

Thrombin Calibrator and PRP-Reagent (contains re-lipidated TF at a final assay concentration of 1 pmol/L) at final assay concentrations of 4 µmol/L and 1 µmol/L, respectively, were removed from 4°C storage and reconstituted with 1 mL of dH_2O. Vials were gently mixed and left at room temperature for 10 minutes prior to use.

FluCa solution was prepared by diluting the Fluo-Substrate, which contains a fluorogenic substrate (Z-GGR-AMC), 1:40 with Fluo-Buffer containing calcium chloride. All reagents were from Diagnostica Stago, Asniéres sur Seine, France.

2.3.5.3 Microplate preparation

Each experiment required two sets of readings – one from the thrombin generating wells and the second from wells in which calibrator has been added. The calibrator wells were used to calculate the thrombin generation in nM. Each assay was prepared in triplicate.

To a 96 well round-bottomed microplate, 20 µL of PRP reagent was added to the thrombin generating wells and 20 µL of thrombin calibrator to the calibrator wells. After addition of reagents, 80 µL of sample was added to the relevant wells (Figure 2-6).

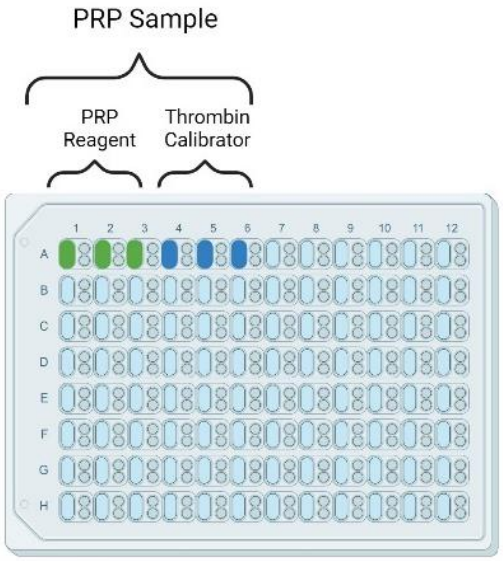

Figure 2-6: Microplate set up for the calibrated automated thrombogram (CAT) , each test performed in triplicate.

2.3.5.4 Measurement

Thrombin generation in the microplate was detected using a fluorometer equipped with a 390/460 filter set (excitation/emission) and a dispenser. Microplates were incubated for 10 minutes at 37°C. The dispenser was flushed with warm (37°C) dH_2O and then primed and filled with warm FluCa reagent. To start the experiment 20 µL of FluCa was automatically dispensed by the fluorometer into each of the wells to be measured. Microplates were shaken for 10 seconds and readings of the fluorogenic substrate taken every 15 seconds for 90 minutes.

The Thrombinoscope™ software (version 5.0, Stago, Asniéres, France) calculates the thrombin concentration by continuous comparison of the signal from the thrombin generating test wells to the calibrator wells which have a constant thrombin-like activity (Wolberg, 2007). The results are displayed as thrombin activity versus time. The possible parameters derived from the thrombin generation curve are illustrated in Figure 2-7.

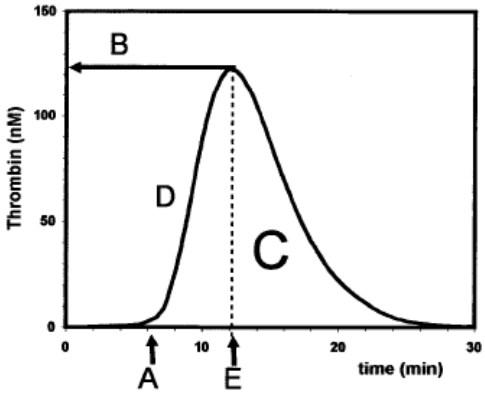

Figure 2-7: Thrombin generation curve . A = Lag time (min); B = peak height (nM); C = Endogenous thrombin potential (ETP) (nM x min); D = maximal rising slope (nM/min); E = time to peak (min); Velocity index (VI) = peak height/(time to peak – lag time). Figure taken from Hemker et al (2006)(Hemker et al., 2006).

For this study we chose to report the lag time for thrombin generation to occur, the peak amount of thrombin generated and the endogenous thrombin potential (ETP).

2.4 Platelet activation assays

2.4.1 Background

CD62P (also known as P-selectin) is an integral membrane protein of α-granules in platelets. Upon activation of platelets, α-granules fuse with the external platelet membrane, leading to exposure of CD62P on the platelet cell surface (Curvers *et al.*, 2008). Once exposed on the membrane, CD62P mediates physical interactions between platelets, leukocytes and endothelial cells via P-selectin glycoprotein ligand-1 (PSGL-1). The presence of CD62P on the platelet surface can be quantified via flow cytometry (FC) using a CD62P specific monoclonal antibody (MoAb) conjugated to a fluorescent dye and provides an indication of the activation status of the platelets. A soluble and potentially functional form of CD62P has been shown to be secreted from platelets and present in the serum of healthy individuals (Dunlop *et al.*, 1992) which can also be used as a marker of platelet activation.

In resting platelets anionic phospholipids, such as phosphatidyl serine (PS), are distributed predominantly on the inner leaflet of the plasma membrane. Once activated, PS is translocated to the external membrane leaflet transforming it to a negatively charged surface, where it facilitates the assembly of the intrinsic tenase

complex (FVIIIa, FIXa and FX) and the prothrombinase complex (FVa, FXa, prothrombin), contributing to the rapid generation of thrombin (Reddy and Rand, 2020). PS also acts as an apoptotic 'eat me' signal on platelets for phagocytic cells to remove them from the circulation (Segawa and Nagata, 2015).

Levels of PS on the platelet surface can be measured by flow cytometry either using a fluorescently labelled Annexin V, which binds PS with a high affinity in a Ca^{2+} dependent manner or using lactadherin that does not require Ca^{2+} (Reddy and Rand, 2020) and has been shown to be more sensitive than Annexin V (Hou *et al.*, 2011).

2.4.2 Flow cytometric measurement of CD62P and phosphatidyl serine using Annexin V stain

2.4.2.1 Reagent preparation

The PS assay using Annexin V was performed using the Annexin A5 – FITC Kit (Beckman Coulter, CA, USA). Annexin V buffer was prepared by diluting one part of the buffer concentrate with nine parts of dH_2O.

2.4.2.2 Sample preparation & staining

For the CD61, IgG negative control and CD62P tests, PRP was diluted to 1 x 10^{12}/L in PBS (Sussex Biologicals, East Sussex, UK). For the Annexin V assay PRP was diluted in Annexin V buffer to create a solution containing 5 x 10^{10} platelets per litre.

2.4.2.3 CD61 – verifier sample

Five µL of the 1 x 10^{12}/L PRP sample was further diluted with 20 µL PBS (2 x 10^{11}/L) before removing 5 µL of the dilution into a separate tube and adding 10 µL CD61-PC7 (Beckman Coulter, CA, USA). The sample was incubated in the dark for 15 minutes at room temperature before being made up to a volume of 1000 µL in PBS.

2.4.2.4 IgG mab negative (isotype) controls

To 5 µL of the 1 x 10^{12}/L PRP sample, 10 µL IgG1 PC7, 20 µL IgG1 FITC and 20 µL IgG1 PE was added, incubated in the dark for 15 minutes at room temperature before being made up to a volume of 100 µL in PBSS. A 20 µL aliquot of this sample was removed into another tube and 980 µL of PBS added.

2.4.2.5 CD62P test sample

To 5 µL of the 1 x 10^{12}/L PRP sample, 20 µL of CD62P PE was added, incubated in the dark for 15 minutes at room temperature before being made up to a volume of 100 µL in PBS. An aliquot of 20 µL of this sample was removed into another tube and 980 µL of PBS added.

2.4.2.6 Annexin V test sample

The PRP containing 5 x 10^{10} platelets/L was further diluted in Annexin V buffer to give a concentration of 5 x 10^{5} in 100 µL prior to adding 1 µL AV-FITC and incubating in the dark at ambient temperature for 15 minutes. Post incubation, 400 µL of Annexin V buffer was added to the sample.

2.4.2.7 Measurement & gating strategy

Fluorescence analysis of the samples was performed using a Cytoflex S flow cytometer (Beckman Coulter, CA, USA). Platelets were distinguished from other blood cells /debris in the sample on the basis of their forward and 90^{o} light scatter profile using logarithmic mode and a gate drawn around the platelet population (Figure 2-8 (A)). The negative (isotype) control was used to delineate the positively stained platelet population. The limit above which platelets were considered positive was determined by setting a gate on the fluorescence histogram so that approximately 1% of platelets stained with the isotype reagents showed fluorescence above this level (Figure 2-8 (B-D)). A total of 20,000 platelet events were collected. When measuring the CD62P and Annexin V samples the data was expressed as the percentage fluorescent positive platelets and the median fluorescence intensity (MFI), which provides an approximation of how many markers there are per individual cell. The data was exported and analysed via the Kaluza software (Beckman Coulter, CA, USA).

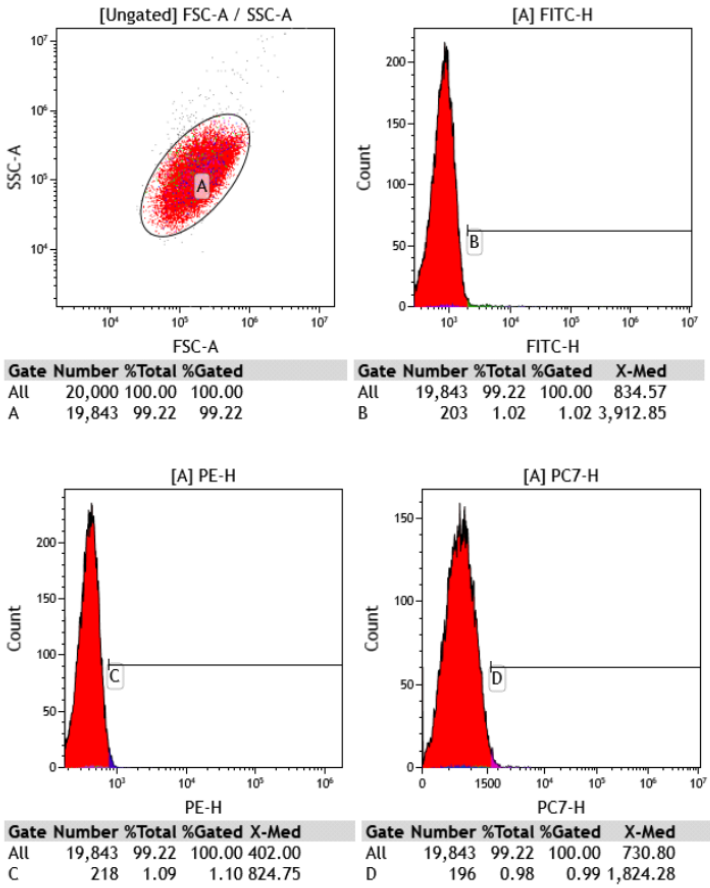

Figure 2-8: Gating strategy for PS using Annexin V stain Representative example of histograms for flow cytometry controls. A = Platelet population identified by scatter. B = Isotype control for Annexin V binding. C = Isotype control for CD62P. D = Isotype control for CD61 (used to confirm events identified in histogram A).

2.4.3 Soluble CD62P

Soluble CD62P (sCD62P) levels in frozen aliquots of PC-derived PPP from each timepoint were measured using the Quantikine® solid phase ELISA kit (Bio Techne, Abingdon, UK).

2.4.3.1 Reagent preparation

An aliquot of 10 mL of wash buffer concentrate was diluted in 240 mL of dH_2O. The kit standard was reconstituted with 1 mL dH_2O to produce a stock solution of 250 ng/mL. The stock solution was further diluted to 50 ng/mL with sample diluent before creating doubling dilutions of 25 ng/mL, 12.5 ng/mL, 6.25 ng/mL, 3.13 ng/mL, 1.56 ng/mL, 0.781 ng/mL and a 0 ng/mL containing only sample diluent.

The sCD62P control was reconstituted with 500 µL of dH2O and diluted 1:20 in sample diluent. A 250 µL volume of conjugate concentrate was dispensed into the vial of conjugate diluent. The PPP samples were defrosted prior to being diluted 1:20 with sample diluent. The substrate was prepared by mixing equal volumes of Colour Reagent A with Colour Reagent B.

2.4.3.2 Measurement

The required number of microplate strips pre-coated with a monoclonal antibody specific for human CD62P were removed from the kit and 100 µL of sample diluent (blank), the seven standard dilutions, the sCD62P control and the diluted test samples were added to individual wells in duplicate. Conjugate (100 µL) was added to each well before gently mixing by tapping and the plate incubated for 1 hour at ambient temperature.

The wells were washed three times to remove any unbound conjugated antibody by aspirating the liquid in the well, adding 300 µL of wash buffer and re-aspirating the wash buffer solution. This was repeated twice before inverting and blotting the plate dry. Substrate (200 µL) was added to each well, the plate covered with a plate sealer and incubated in the dark at ambient temperature for 15 minutes. To halt colour development, 50 µL of stop solution was added to the wells which changed the colour in the wells from blue to yellow.

The optical density (OD) of the plate was read on an Infinite F50 microplate reader (Tecan, *Männedorf, Switzerland,*) set to 450 nm with a reference filter of 570 nm. The Magellan Tracker software (Tecan, *Männedorf, Switzerland, V*ersion 7.0) was used to average the duplicate readings for each standard, control and sample, with the average OD of the blank subtracted from the results. The software generates a four-parameter standard curve which was used to calculate the sCD62P concentration of each sample.

2.4.4 Flow cytometric measurement of phosphatidyl serine using lactadherin stain

2.4.4.1 Reagent preparation

Modified Tyrode's buffer was prepared in 200 µL of dH_2O using the quantity of reagents shown in Table 2-4. It was then adjusted to a pH of 7.4 with 1 mmol/L of

sodium hydroxide before being filtered through a 0.2 µm syringe filter and stored at 2-8°C. On each testing day, an aliquot of 10 mL was paced into a universal tube and 0.035g of Bovine Serum Albumin (0.35% w:v) was added.

Table 2-4: Modified Tyrode's buffer constituents

Reagent	Molarity (mmol/L)	Weight (g)
Sodium chloride	137	1.6013
Potassium chloride	2.8	0.0417
Magnesium chloride	1	0.0407
Sodium hydrogen carbonate	12	0.2016
Disodium hydrogen phosphate	0.4	0.0114
HEPES	10	0.4766
Glucose	5.5	0.1982

2.4.4.2 Sample preparation & staining

PRP was diluted to 100 x 10^9/L in Tyrode's buffer (Table 2-4).

2.4.4.3 Staining test sample with lactadherin

Lactadherin-FITC (Haematologic Technologies, VT, USA) (3.13 µL) was added to 5 µL of the 100 x 10^9/L PRP sample before making the sample up to a volume of 50 µL in Modified Tyrode's buffer. The sample was then incubated for 10 minutes at room temperature in the dark before adding 950 µL of Modified Tyrode's buffer.

2.4.4.4 Lactadherin negative control

Modified Tyrode's buffer (45 µL) was added to 5 µL of the 100 x 10^9/L PRP sample to give a final volume of 50 µL. The sample was then incubated in the dark for 10 minutes at room temperature before adding 950 µL of Modified Tyrode's buffer.

2.4.4.5 Measurement

Fluorescence analysis of the samples was performed using a Cytoflex S flow cytometer. The negative control was used to set a gate on approximately 1% of events (Figure 2-9 A). This same gate was transferred to the test sample (Figure 2-9 B) and the % positive population reported.

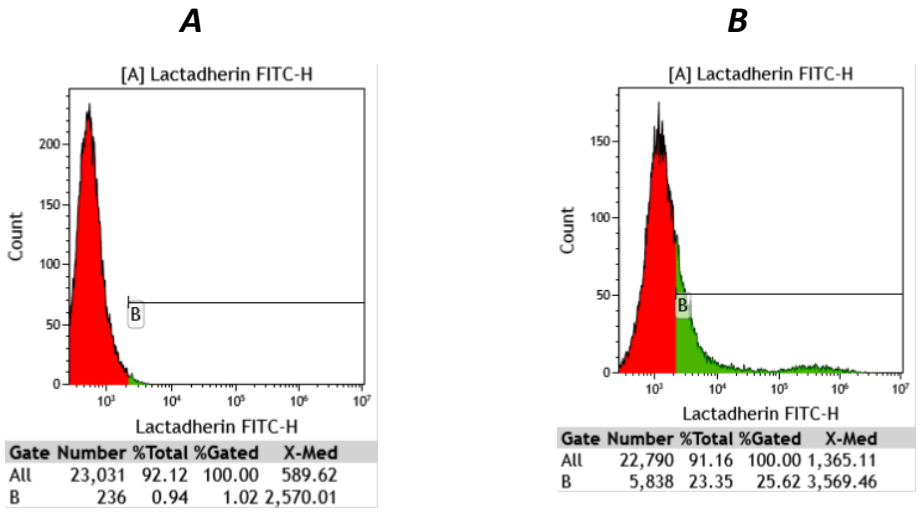

*Figure 2-9: Gating strategy for PS using Lactadherin stain . Representative flow plots showing the negative unstained control (A) that was used to set up the gate for the test result in (B). The '% Gated' figure for gate B is the result reported as % cells positive for PS.*A total of 20,000 platelet events were collected and the data was exported and analysed via the Kaluza software.

2.5 Metabolic analysis

2.5.1 Glucose, lactate, pO_2, pCO_2 and pH

2.5.1.1 Background

Blood gas analysers are used to understand the respiratory function and the acid-base balance of blood samples and consist of electrodes that measure pH (H^+), pCO_2, pO_2, glucose and lactate amongst other electrolytes. These measurements can also be used within transfusion medicine to assess metabolism and blood gas exchange of platelets within PC. When PC are assessed on blood gas analysers, the glucose level reflects how metabolically active the cells are (glucose is the main substrate for metabolism in PC), lactate levels indicate how much anaerobic metabolism is occurring, the pH measures the acidification rate (how much H^+ is being generated through metabolism) and the pCO_2 and pO_2 are indirect measures of aerobic metabolism, although the storage packs of PC are gas permeable meaning that O_2 and CO_2 can cross in and out and be influenced by atmospheric partial pressure. Note that in this study, pH levels are reported at 37°C. Due to a thermal coefficient for

blood of approximately -0.016 pH units/°C, a temperature-corrected pH at 22°C would be some 0.24 pH units higher.

2.5.1.2 Method

Immediately after sample collection, the metabolites glucose, lactate, pO_2 pCO_2 and pH were measured using a blood gas analyser (ABL800, Radiometer, Copenhagen, Denmark). All measurements were performed at 37°C.

2.5.2 Calculation of Bicarbonate Levels

2.5.2.1 Background

Formation of CO_2 in an aqueous environment causes its reversible hydration and dissociation into bicarbonate (HCO_3^-) and a proton (H^+) (Divakaruni *et al.*, 2014). Bicarbonate is an analyte that is used to assess the acid-base status of samples and makes up ~95% of the total carbon dioxide in plasma (Nasir *et al.*, 2010). Bicarbonate acts as a buffer within PC by binding with generated H^+ to create carbonic acid (H_2CO_3), which in turn is changed into CO_2 (extruded through the gas permeable pack) and H_2O (Nash, Saunders and George, 2023).

$$H^+ + HCO_3^- \longleftrightarrow H_2CO_3 \longleftrightarrow CO_2 + H_2O$$

2.5.2.2 Calculation

Bicarbonate levels were calculated based on the pCO_2 and pH results using the Henderson-Hasselbalch equation, which is based on the following relationship between pH, $[CO_2]$ and $[HCO_3^-]$:

$$pH = pK + \log \frac{[HCO_3^-]}{[CO_2]}$$

Where pK is the first dissociation constant for carbonic acid (equal to 6.1 for blood at 37°C) (Nasir *et al.*, 2010). A value for the Henry constant of 0.034 was used to relate the concentration of CO_2 to its measured partial pressure (Saunders, 2012). The concentration of bicarbonate was thus calculated as:

$$[HCO_3^-] = pCO_2 \times 10^{(pH-6.1)} \times 0.034$$

2.5.3 Total ATP

2.5.3.1 Background

ATP is the main energy source of platelets and contains large amounts of energy in its phosphate bonds. The amount of ATP in the PC was measured using the ATP Kit SL (BioTherma Luminescent Assays, Handen, Sweden).

The principle behind the assay is the ATP-dependent oxidation of D-luciferin in the following reaction:

$$\text{ATP + D-luciferin + } O_2 \xrightarrow{\text{Luciferase}} \text{AMP + PPi + oxyluciferin+ } CO_2 \text{ + photons}$$

This firefly luciferase catalysed reaction generates photons (light) in the visible range (540-600nm), the intensity of which can be related to the concentration of ATP by means of a standard line.

2.5.3.2 Extraction of ATP

PRP was diluted to approximately physiological levels of 300 x 10^9/L in PPP and the dilution factor noted. EDTA (50 µL, 0.1M) and 10% Triton X-100 (50 µL) were added to 500 µL of 300 x 10^9/L PRP in a cryovial and vigorously vortexed before addition of 500 µL of absolute ethanol. The cryovial was allowed to stand for 15-30 minutes at 2-8°C before freezing below -70°C.

2.5.3.3 Reagent & sample preparation

Samples were thawed in a water bath at 37°C before centrifuging at 2000 *g* for 15 minutes at 4°C. The supernatant was decanted into a new cryovial and the lysed platelet membranes in the first tube discarded. The supernatant from each sample was diluted in Tris-EDTA Buffer to provide a 1:500 dilution for testing.

The ATP Reagent SL was reconstituted by adding the contents of the Diluent C vial (10 mL) and mixing gently. The ATP Standard (10^{-5} mmol/L) was serially diluted 1/10 in Tris-EDTA Buffer to provide ATP standards of 10^{-6} mmol/L - 10^{-10} mmol/L.

2.5.3.4 Measurement

Chromalux HB high binding, high reflectivity white polystyrene microplates suitable for luminescence applications were used (Perkin Elmer, Waltham, MA, USA). To the microplate, 225 µL of sample or diluted standard was added in duplicate to two wells followed by 25 µL of ATP Reagent SL (containing D-luciferin, luciferase, magnesium ions and stabilizers). In addition, two 'blank' wells were set up containing 225 µL of Tris-EDTA Buffer and 25 µL of ATP Reagent SL. The plate was inserted into the Tristar2 LB942 multimode reader (Berthold Technologies, Wildbad, Germany) and luminescence detected.

2.5.3.5 Analysis

The raw data, measured as Relative Light Units (RLU), was entered into GraphPad Prism (version 9.3.0, GraphPad Software Inc., San Diego, CA) for analysis. A standard curve was generated from the diluted standard and used to interpolate the log of the results for the test samples. The interpolated values were then transformed (x = 10^X) to provide the concentration of ATP in the sample well (mol/L). The calculated result for the blank was subtracted from the sample results to remove background noise. Finally, to factor in the dilution of the sample (1:500) and express the ATP concentration as µmol/10^{11} platelets:

ATP concentration (mol/L)	=	ATP Concentration (mol/L) in sample well x Dilution factor (500)
ATP concentration (µmol/10^{11} platelets)	=	ATP concentration (mol/L)/Platelet concentration (x10^{11}) x 10^{6}

2.5.4 Mitochondrial membrane potential ($\Delta\psi_m$)

2.5.4.1 Background

The mitochondrial inner membrane potential ($\Delta\psi_m$) is the charge or electrical gradient across the inner mitochondrial membrane which along with the mitochondrial pH gradient (ΔpH_m, an H^+ chemical or concentration gradient) provides the total force for driving protons into the mitochondria (Perry *et al.*, 2011). The $\Delta\psi_m$

relates to the platelets' capacity to generate ATP by oxidative phosphorylation and can be used as a key indicator of PC cell health or injury.

Fluorescent cationic dyes can be used to measure $\Delta\psi_m$ in individual platelets, due to their essential attributes of membrane permeability and low membrane binding. These positively charged lipophilic dyes are attracted to the negative potential across the inner mitochondrial membrane and preferentially accumulate in the mitochondria matrix (Cottet-Rousselle *et al.*, 2011). Hyperpolarized mitochondria (where the interior is more negative) will accumulate more cationic dye and depolarized mitochondria (where the interior is less negative) accumulate less cationic dye (Perry *et al.*, 2011).

Two complementary dyes were used to confirm the results for the $\Delta\psi_m$ - Tetramethylrhodamine methyl ester (TMRM) and 5,5',6,6'-tetrachloro-1,1',3,3'-tetraethyl-benzimidazolecarbocyanine (JC-1). TMRM accumulates in healthy mitochondria because of its positive charge and is released if the $\Delta\psi_m$ decreases. JC-1 also accumulates in the healthy mitochondrial matrix due to its positive charge and shows a shift in fluorescence from green (monomeric form) to a red aggregate form if there is sufficient concentration within the mitochondrial matrix (Amorini *et al.*, 2013). If the concentration of JC-1 dye in the mitochondrial matrix is not sufficient to cause aggregation (due to a decrease in the $\Delta\psi_m$) then the fluorescence remains green.

A $\Delta\psi_m$ challenge control can be employed to further confirm dye behaviour using the protonophore carbonyl cyanide m-chlorophenylhydrazone (CCCP), which depolarises the mitochondria by increasing their permeability to protons.

2.5.4.2 Measurement of $\Delta\psi_m$ using TMRM dye

2.5.4.2.1 Sample preparation & staining

PRP was diluted to provide a platelet concentration of 1 x 10^{10}/L in Tyrode's buffer (Table 2-4: Modified Tyrode's buffer constituents).

2.5.4.2.2 Staining test sample with TMRM

To 1 µL tetramethylrhodamine methyl ester (TMRM) (Mitoprobe TMRM Kit, Life Technologies, Paisley, UK) stock solution (20 µmol/L) add 1 µL of modified Tyrode's

buffer followed by 1 mL of 1 x 10^{10}/L test sample. Incubate for 20 minutes in the dark at 37°C.

2.5.4.2.3 Mitochondrial challenge sample (negative control)

To dissipate $\Delta\psi_m$ and create a negative control, cells were treated with CCCP. To 1 µL of TMRM stock solution 1 µL of 50 mmol/L CCCP (Merck Life Sciences UK Ltd, Gillingham, UK) in DMSO (50 mM) was added followed by 1 mL of 1 x 10^{10}/L test sample. This was then incubated for 20 minutes in the dark at 37°C.

2.5.4.2.4 Measurement & gating strategy

The intensity of TMRM fluorescence was measured via flow cytometry with each sample measured to 25,000 events. Forward scatter and side scatter were used to gate the platelets by size and complexity with a gate drawn around the platelet population (Figure 2-10 A). A hinged gate was set on the histogram of TMRM stained cells vs SS (Figure 2-10 B) so that that the two populations of cells (positive for TMRM & negative for TMRM) are separated to enable counting of % positive. The gating strategy from the first sample on Day 0 for each individual PC was then applied to all subsequent samples for that PC. The results were reported as % TMRM positive cells.

TMRM fluorescence was excited with a yellow 561-nm laser and detected by a PE detector with 585/42 bandwidth filter.

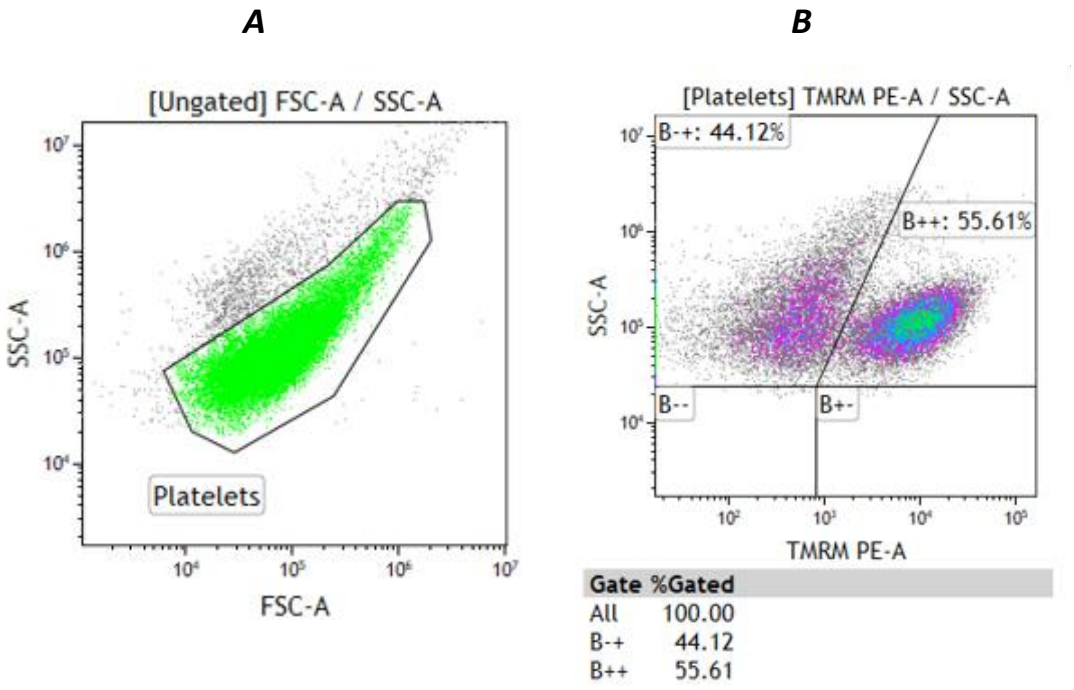

Figure 2-10: Gating strategy for TMRM results where (A) is the gating of the platelet population and (B) is the result histogram showing the hinged gating used to separate negative and positive populations of cells. The B++ value was used to record the % positive result.

2.5.4.3 Measurement of $\Delta\psi_m$ using JC-1 dye

2.5.4.3.1 Sample preparation & staining

PRP was diluted to 3 x 10^{10}/L in Tyrode's buffer (Table 2-4).

2.5.4.3.2 Staining test sample with JC-1

To 2.5 µL of 5,5',6,6'-tetrachloro-1,1',3,3'-tetraethyl-benzimidazolecarbocyanine (JC-1) (Life Technologies, Paisley, UK) stock solution (200 µmol/L) 1 µL of modified Tyrode's buffer was added, followed by 1 mL of 3 x 10^{10}/L test sample. This was then incubated for 30 minutes in the dark at 37°C.

2.5.4.3.3 CCCP challenge sample

To 2.5 µL of JC-1 stock solution 1 µL of 20 mmol/L CCCP was added, followed by 1 mL of 3 x 10^{10}/L test sample. This was incubated for 30 minutes in the dark at 37°C.

2.5.4.3.4 Measurement & gating strategy

The intensity of JC-1 fluorescence was measured via flow cytometry with each sample measured to 25,000 events. Forward scatter and side scatter were used to gate the platelets by size and complexity with a gate drawn around the platelet

population (Figure 2-11 A). A quadrant gate was set on the histogram of JC-1 stained cells vs SS (Figure 2-11 B) so that that the two populations of cells (positive for JC-1 & negative for JC-1) were separated to enable counting of % positive. The gating strategy from the first sample on Day 0 for each individual PC was then applied to all subsequent samples for that PC. The results were reported as % JC-1 positive cells.

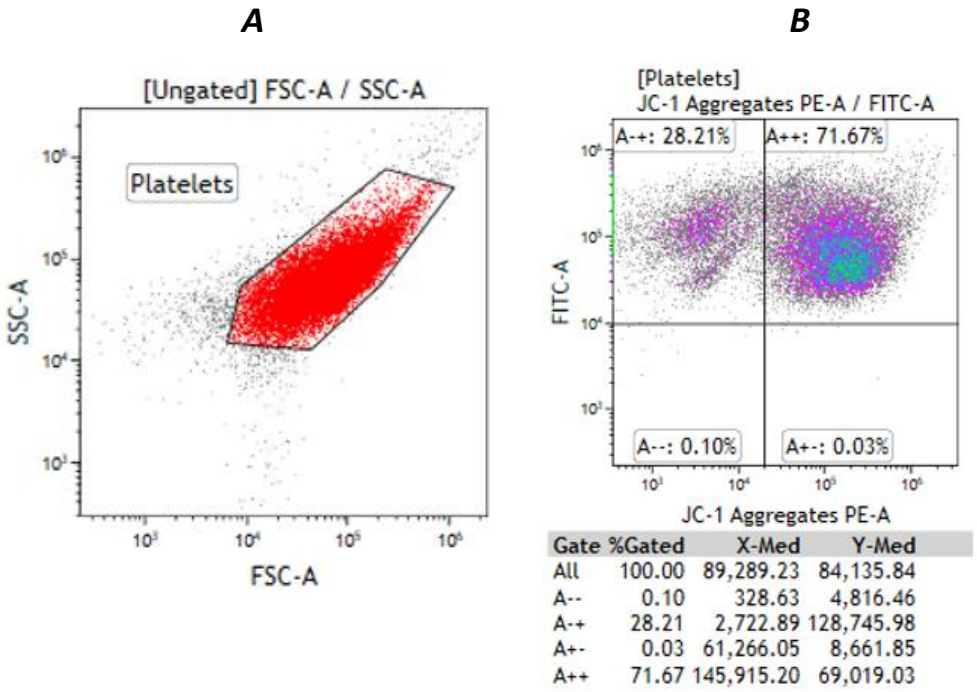

Figure 2-11: Gating strategy for JC-1 where (A) is the gating of the platelet population and (B) shows the quadrat gating used to separate cells containing no JC-1 aggregates from those containing JC-1 aggregates. The A++ value was used to record the % positive result.

2.5.5 Bioenergetic profiling

2.5.5.1 Background

Measurement of cellular respiration can be used to assess the bioenergetics of platelets within PC utilising the oxygen consumption rate (OCR) and the extracellular acidification rate (ECAR). O_2 consumption during OXPHOS is coupled to ATP synthesis, as the terminal reaction in the ETC and is therefore both a measurement for the flux of electrons through the respiratory chain ('supply' of the protonmotive force (Δp)) as well as an indirect measure of the processes that consume Δp ('demand').

The Agilent Seahorse XF HS Mini Analyser (Agilent Technologies, CA, USA) enables high throughput assessment of the bioenergetics of small numbers of intact platelets from PC. The platelets are seeded to the bottom of a microplate and suspended in a medium containing glucose, pyruvate and L-glutamine (Figure 2-12). A sensor cartridge containing two fluorophores is inserted into the chamber, one which measures O_2 (OCR) and the other that measures H^+ (ECAR). The fluorophores measure O_2 and H^+ production in real time and generate a bioenergetic profile for the cells.

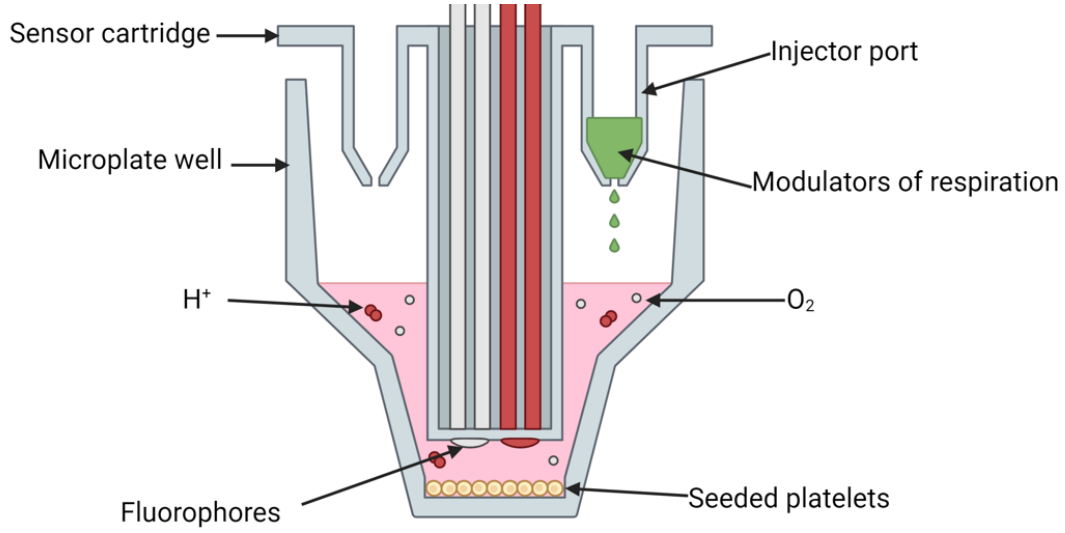

Figure 2-12: Agilent Seahorse microplate with sensor cartridge. The sensor cartridge contains two fluorophores that measure H^+ and O_2 is inserted into the microplate well and measures the amount of H^+ and O_2 produced by the platelets.

The XFp Cell Mito stress test (Agilent Technologies, Texas, USA) measures the OCR and how it is affected by sequential addition of the modulators of respiration oligomycin, FCCP and rotenone/antimycin A. Once the basal respiration rate is established, the ATP synthase inhibitor, oligomycin, is injected into the medium which prevents ATP synthase from generating ATP – this allows the rate of ATP-linked respiration to be estimated. The next modulator to be added is the protonophore/uncoupler FCCP which shuttles protons across the inner membrane and dissipates the Δp, resulting in the maximum activity of the ETC. Finally, the inhibitors of complex I (rotenone) and Complex III (antimycin A) are added to halt

electron transfer through the ETC to correct for O_2 consumption from non-mitochondrial oxidases. The effect of these modulators is depicted in Figure 2-13.

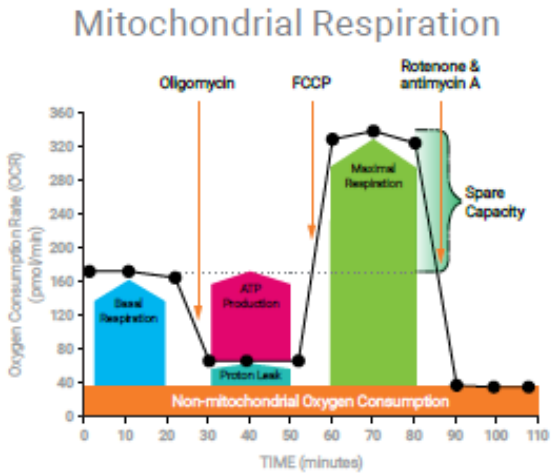

Figure 2-13: Seahorse XFp cell mito stress test profile , showing the key parameters of mitochondrial function. Figure courtesy of Agilent Technologies.

The XFp real-time ATP rate assay (Agilent Technologies, Texas, USA) measures the cellular rate of ATP production through the flux of both H^+ production (ECAR) and O_2 consumption (OCR) and is able to distinguish between the fractions of ATP that are produced from mitochondrial OXPHOS and glycolysis. Basal OCR and ECAR are measured first before injecting oligomycin to inhibit ATP synthesis (Figure 2-14). This results in a decrease in OCR enabling the 'mitoATP' production rate to be quantified. The ECAR data (combined with the buffer factor of the assay medium) allows calculation of the total proton efflux rate (PER). Finally, rotenone and antimycin A are injected to completely inhibit mitochondrial respiration. This accounts for mitochondrial associated acidification and when combined with PER data allows calculation of the 'glycoATP' production rate.

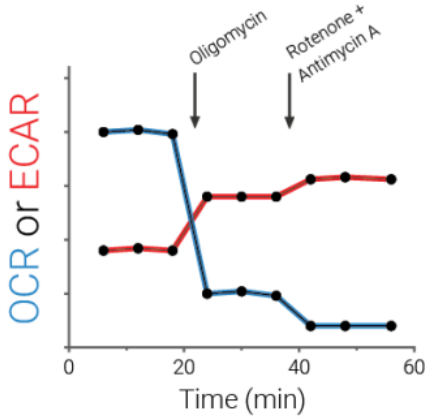

Figure 2-14: Kinetic profile of OCR and ECAR measurements in the Agilent Seahorse XFp Real-Time ATP Rate-Assay. Figure courtesy of Agilent Technologies.

2.5.5.2 Assay preparation

Extracellular flux sensor cartridges (Figure 2-15) were incubated overnight at 37°C with the sensors submerged in 200 µL of XF Calibrant. In addition, 400 µL of XF Calibrant was added to each moat outside of the sensor wells.

Figure 2-15: Seahorse sensor cartridges. A: sensor cartridge being lifted from utility plate. B: Utility plate next to sensor cartridge

Cell-Tak coated plates were prepared by adding 25 µL of Cell-Tak adhesive made up to a concentration of 22.4 µg/mL in $NaHCO_3$ to each well in the cell culture mini plates. The plates were incubated for 20 minutes at room temperature before being washed twice using sterile water and left to air dry for 15 minutes.

2.5.5.3 Reagent Preparation

XF assay medium was prepared in a laminar flow cabinet by adding the volumes shown in Table 2-5 to a universal tube. The XF assay medium was stored in a water bath at 37°C until use.

Table 2-5: Constituents of XF assay medium

Reagent	Quantity for 1 plate	Quantity for 2 plates
Seahorse XF RPMI Medium, pH 7.4	9.7 mL	19.4 mL
Seahorse XF Glucose (1.0 M solution)	100 µL	200 µL
Seahorse XF Pyruvate (100 mM solution)	100 µL	200 µL
Seahorse XF L-Glutamine (200 mM solution)	100 µL	200 µL

A 1 mmol/L solution of prostaglandin E1 (PGE_1) was prepared by adding 2.66 µL of PGE_1 stock solution (Sigma, MA, USA) to 7.34 µL of ethanol in an Eppendorf tube.

2.5.5.4 Sample preparation

To 1500 µL of PRP in a polypropylene tube, 1.5 µL of 1 mmol/L PGE_1 working solution was added. The tube was gently inverted to mix prior to centrifuging for 10 minutes at 600 *g* to pellet the cells out of the plasma. The supernatant was removed and discarded and 1.2 mL of XF assay media was added to the platelet pellet which was gently re-suspended in solution using a Pasteur pipette. An aliquot of 400 µL of this sample was removed into a separate tube and used to perform a platelet count on the sample (see point 2.2.4). The remaining sample was used to create a 0.2 x 10^6/ µL suspension of platelets in a 1000 µL volume, based on the platelet count. This standard concentration of platelets was used across all samples to ensure normalisation of the results.

2.5.5.5 Seeding of microplates

To the prepared Cell-Tak plates, 50 µL of 0.2 x 10^6/ µL cell suspension was added to each test well (tested in triplicate). Wells A and H were not seeded and acted as background wells. The plate was centrifuged for 5 minutes at 500 *g* to form a monolayer in the well, excess fluid was removed and 180 µL of XF Assay Medium

added along the side of each well, taking care not to disturb the cells in addition to 380 µL being added to the moats alongside the wells. The plates were incubated for (15-25 minutes at 37°C) and used within 1 hour of centrifuging.

2.5.5.6 Real time ATP rate assay – reagent preparation

Stock solutions of oligomycin and rotenone + antimycin A (Rot/AA) were produced as described in Table 2-6.

Table 2-6: Stock solutions for ATP rate assay

Compound	Volume of Assay Medium	Resulting Stock Concentration
Oligomycin	168 µL	75 µM
Rotenone + Antimycin A	216 µL	25 µM

The stock solutions were used to prepare 300 µL of working solution for injection into the ports (Table 2-7).

Table 2-7: Compound preparation for real-time ATP rate assay

Compound	Stock Volume	Medium Volume	Final well
Port A Oligomycin	60 µL	240 µL	1.5 µM
Port B Rot/AA	60 µL	240 µL	0.5 µM

2.5.5.7 Mito stress test kit – reagent preparation

Stock solutions of oligomycin and rotenone + antimycin A (Rot/AA) were produced as described in Table 2-8.

Table 2-8: Stock solutions for mito stress test

Compound	Volume of Assay Medium	Resulting Stock Concentration
Oligomycin	280 µL	45 µM
FCCP	288 µL	50 µM
Rot/AA	216 µL	23 µM

The stock solutions were used to prepare 300 µL of working solution for injection into the ports (Table 2-9).

Table 2-9: Compound preparation for mito stress test

Compound	Stock Volume	Medium Volume	Final Well
Port A oligomycin	100 µL	200 µL	20 µM
Port B FCCP	30 µL	270 µL	22 µM
Port C Rot/AA	60 µL	240 µL	25 µM

2.5.5.8 Measurement

Volumes of oligomycin and Rot/AA for the real-time ATP rate assay were dispensed into wells A and B, respectively (Figure 2-16), as shown in Table 2-10.

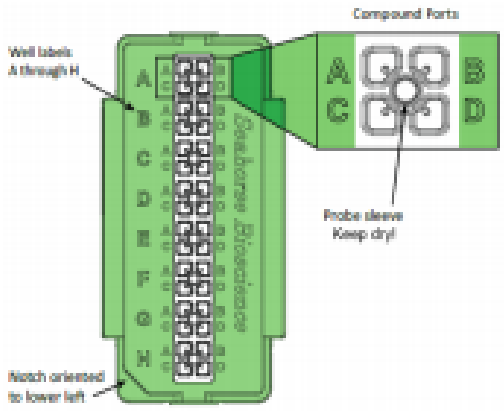

Figure 2-16: Orientation of Seahorse XFp assay cartridge.

Table 2-10: Volume of respiratory modulators added to Real-Time ATP Assay

Real-Time ATP Rate Assay		
A	Oligomycin	20 µL
B	Rot/AA	22 µL

For the mito stress test Assay, volumes of oligomycin, FCCP and Rot/AA were dispensed into the ports as shown in Table 2-11.

Table 2-11: Volume of respiratory modulators added to Cell Mito stress test Assay.

Cell mito stress test		
A	Oligomycin	20 µL
B	FCCP	22 µL
C	Rot/AA	25 µL

The real-time ATP rate assay and the mito stress test were run on the Seahorse XF HS Mini with each stage of the measurement being performed in triplicate. For the ATP rate assay, the platelets were consecutively treated with oligomycin A followed by rotenone + antimycin A. For the mito stress test assay, the platelets were consecutively treated with oligomycin, FCCP and rotenone + antimycin A.

2.5.5.9 Analysis

Analysis of the results was performed using the Seahorse Analytics software.

2.6 Data handling & statistical analysis

All statistical analyses were performed using statistical software (GraphPad Prism software, version 9.3.0, GraphPad Software Inc., San Diego, CA). Comparisons over time between groups were made using two-way repeated measures ANOVA with a p value <0.05 regarded as statistically significant. Where there were missing values in the dataset, the data was analysed by fitting the Šídák's multiple comparisons mixed model rather than by repeated measures ANOVA. Normality was not met by some of the data groups (using the D'Agostino & Pearson test for normality) and where the data could not be transformed, the non-parametric Friedman test was performed. The sample size used for the study follows the recommended number of replicates for an initial evaluation of a novel blood component as set out in JPAC Guidelines (JPAC, 2021). Comparisons between each test sample and the baseline result were made using a one-way ANOVA.

Chapter 3: Impact of prolonged cold storage on platelet *in vitro* function

3.1 Introduction

In order for platelets to fulfil their primary function of preventing haemorrhage during vascular injury, they must be able to undergo dynamic activation processes when exposed to vessel wall damage. This involves responding to chemical signals in the blood stream, adhering to the damaged vessel wall surface through specific receptors, aggregating together and releasing the contents of their granules.

It is important when manufacturing PC for transfusion, that the platelets within the units are able to function when transfused to a patient, either for prophylactic use to prevent bleeding or to halt bleeding. In most countries, PC can be stored for 5-7 days at 22^{o}C ± 2^{o}C with gentle agitation. During storage the platelets within PC deteriorate, a phenomenon termed the platelet storage lesion (PSL) (Ng, Tung and Fraser, 2018; Árnason and Sigurjónsson, 2017). The PSL results in a decrease in the quality of the platelets and is defined by a significant loss of platelet function *in vitro* which may render the platelets less efficacious for clinical use (Árnason and Sigurjónsson, 2017). For this reason, it is vital that extensive functional analysis of PC is performed before introducing changes to the way in which they are manufactured or stored. This provides assurance, through the interpretation of *in vitro* assays, that the platelets within the PC will function once transfused.

The JPAC describes the specifications that must be met for all clinical blood components in the UK, including PC (JPAC, 2021), ensuring that the platelets remain functional for the duration of their shelf life (7 days for RTP). In addition, JPAC recommends an assessment format for evaluation of novel blood components, listing the *in vitro* assays of platelet function which should be performed prior to a novel blood component being used for clinical use (JPAC, 2021).

The standard measure of PC quality performed on all PC prior to transfusion is visual assessment for the 'swirling' phenomenon and aggregate formation. Swirling in PC results from discoid shaped platelets scattering light in different directions, whereas

when platelets undergo a morphological shape change to spherical they scatter light in a single direction and the swirling appearance is lost (Maurer-Spurej and Chipperfield, 2007). Loss of swirling can be an indicator of bacterial contamination of the PC, as can aggregate formation (Vit, Klüter and Wuchter, 2020) and RTP that lack swirling are removed from the supply chain and not transfused.

The unit volume and platelet concentration are also important factors in PC quality, ensuring there is a relatively standard dose of platelets for the patient, but also to ensure that there is sufficient plasma/platelet additive solution to support the platelets with metabolites during storage. A decline in platelet concentration throughout storage can be an indicator of platelet apoptosis or microaggregate formation.

Platelets in PC can become activated during storage either by physiological agonists or by shear stress from the manufacturing process (Metcalfe *et al.*, 1997). Activation of platelets results in intracellular granule release (α, dense and lysosomes) into the nearby microenvironment, as well as translocation of receptors to the platelet surface (Fritsma, 2015). An important marker for platelet activation in PC is CD62-P. CD62-P is released from α-granules upon platelet activation and is translocated to the platelet surface, where it is required for platelet adhesion to other cells (Cardigan and Williamson, 2003). Due to its surface expression, measurement of CD62P on the surface of stored platelets using flow cytometry has frequently been utilised as an *in vitro* indicator of platelet activation (Metcalfe *et al.*, 1997; Holme *et al.*, 1997; Reddoch-Cardenas *et al.*, 2019b; Badlou *et al.*, 2005).

Another marker of activation is the measurement of expression of PS on the platelet surface by flow cytometry. PS and other negatively charged phospholipids are sequestered on the inner leaflet of the resting platelet membrane (Monroe, Hoffman and Roberts, 2002). Once activated, platelets 'flip' PS onto the surface of the membrane where it facilitates the assembly of the tenase and prothrombinase complexes and generates large quantities of thrombin (Reddy and Rand, 2020). The procoagulant profile of PC during storage time and under different temperatures can be determined by measuring the level of PS on the cells and their ability to generate thrombin.

Platelets ability to respond to physiological stimuli such as ADP, thrombin and collagen, is critical for adhering to damaged endothelium and aggregating, key functions in the prevention and cessation of bleeding (Cardigan and Williamson, 2003). Light transmission aggregometry (LTA) is often deemed the 'gold standard' assay for platelet function and assesses the ability of platelets to respond to agonists and aggregate (Duncan *et al.*, 2009). Other functional assays measure platelets' ability to change shape in response to the agonist ADP (extent of shape change assay) and the ability of platelets to extrude water (hypotonic shock response) (Holme, Moroff and Murphy, 1998).

3.2 Aims

The aim of this chapter was to study the functional profiles of PC following cold storage (4 ± 2 ^{o}C) compared to PC stored under standard room temperature conditions (22 ± 2 ^{o}C) to enable assessment of the effect of cold storage on platelet function over time. To address these aims the following objectives were met:

1. Assess the effects of cold storage on platelet parameters including platelet count, shape and size.
2. Determine the effect of cold storage on resting activation status of the platelets.
3. Determine the effect of cold storage on platelet procoagulant activity and thrombin generation.
4. Determine the effect of cold storage on platelet aggregation responses to a range of platelet agonists.

3.3 Methods

The methods described in this chapter are summaries of the more detailed methods in Chapter 2.

3.3.1 Collection and sampling of platelet concentrates

PC were collected and prepared as outlined in section 2.1, with a double dose of apheresis platelets bled from each donor, pooled into a single pack and mixed before separating into two separate packs. One pack was stored at 22 ± 2°C with gentle agitation and termed RTP and the second pack was stored at 4 ± 2°C with no agitation and termed CSP.

3.3.2 Visual assessment of platelet concentrates

Visual assessment of PC was performed by assessing and scoring the swirling phenomenon and the presence of aggregates, as described in 2.2.2.

3.3.3 Standard quality parameters

The standard quality parameters stipulated by JPAC for apheresis platelets were performed, including unit volume, platelet count, MPV, platelet yield, residual white cell counting and end of storage sterility (2.2.3 – 2.2.6). In addition, a platelet count was performed before running the CSP through an infusion kit and afterwards to assess the platelet loss due to micro-aggregates (2.2.7).

3.3.4 Extent of shape change and hypotonic shock response

The ESC was performed to determine the ability of the platelets to change from a discoid to a spherical shape in response to ADP (2.3.3) and the HSR was performed to test the membrane integrity and metabolism (2.3.4).

3.3.5 Platelet activation assays

CD62P is released from α-granules when platelets are activated and becomes exposed on the platelet membrane. It has also been shown to be secreted from platelets in a soluble form. CD62P on the surface of platelets was measured using a CD62P MoAb conjugated to the fluorescent dye PE as described in 2.4.2. The soluble form of CD62P was measured using an ELISA kit as described in 2.4.3. In addition, two

assays to detect surface PS exposure were performed using flow cytometry. These were Annexin V binding (2.4.2) and Lactadherin, both conjugated to FITC (2.4.4).

3.3.6 Thrombin generation

The ability of platelets to generate thrombin was assessed using the CAT as described in 2.3.5.

3.3.7 Light transmission aggregometry (LTA)

To determine the functionality of the platelets and their ability to induce aggregation, LTA was performed using the agonists ADP, collagen and TRAP-6 as described in 2.3.2.

3.3.8 Statistical analysis

Statistical analysis was performed as described in section 2.6. The p values for the statistical analysis of each timepoint compared to baseline values are shown in Appendix II

.

3.4 Results

The results in this chapter compare the effects of cold storage with standard room temperature storage on platelet count, morphology and activation in PC. The baseline results shown for all assays are samples of the apheresis unit in PAS on the day it was donated (day 0), prior to the unit being split and stored at the two different temperatures. Only the CSP groups were tested on day 21 of shelf life meaning that there is no comparison of results for this day of storage. PC were tested throughout shelf life on day bled (day 0), day 2, day 8, day 14 and day 21. These are referred to in the text as D0, D2, D8, D14 and D21.

3.4.1 Indicators of component quality

3.4.1.1 Visual assessment of platelet concentrates

Platelets with a normal discoid shape scatter light in such a way as to produce a 'swirling' phenomenon when a PC is held up to a light source. Once platelets undergo shape change and become spherical, they lose their ability to change orientation and scatter light in the same direction giving a dull unchanging appearance.

All PC were scored according to the method described by Fratantoni et al (Fratantoni, Poindexter and Bonner, 1984), shown in Table 3-1.

Table 3-1: Scoring method for platelet swirling , as described by Fratantoni et al (Fratantoni, Poindexter and Bonner, 1984)

Score	Swirling Description
0	No swirling, sample appears homogenously turbid (same before rotating as afterwards)
1	Some inhomogeneity, but contract poor and only observed in a few places
2	Swirling inhomogeneity throughout the bag with good contrast
3	Swirling in homogeneity throughout the bag with contrast observable as fine detail

Swirling was well conserved in the RTP with the mean results for all units having the maximum swirling score of 3 throughout the 14-day storage period (Table 3-2). In

contrast, there was an absence of swirl in CSP once they are stored at 4 ± 2°C, with all CSP scoring a 0.

Table 3-2: Swirling Results , mean score for each day, n = 12

Swirling - mean scores					
Day tested	D0	D2	D8	D14	D21
RTP	3	3	3	3	N/A
CSP	3	0	0	0	0

All PC were scored for aggregates as described in Table 3-3.

Table 3-3: Scoring method for platelet aggregates.

Score	Aggregate Description
0	No aggregates
1	Minor aggregates (a few small aggregates)
2	Moderate (>10 obvious aggregates)
3	Extensive aggregates (large clumps)

Table 3-5) with more aggregates seen early in the study (D0 & D2) than later (D8-D21). Slightly more CSP units had aggregates on D2 compared to RTP (Table 3-4). The D0 units were observed for aggregates after splitting into two units and prior to being placed in their storage temperature.

Table 3-4: Aggregate results, mean scores for each day, n = 12

Aggregates - mean scores					
Day tested	D0	D2	D8	D14	D21
RTP	1	0	0	0	N/A
CSP	1	1	0	0	1

Table 3-5: Total number of units with aggregates by day, n = 12

Total number of units with aggregates					
Day tested	D0	D2	D8	D14	D21
RTP	8	4	3	3	N/A
CSP	8	6	3	3	6

3.4.1.2 Unit volume and platelet yield

All PC were within the volume range specified by JPAC Guidelines for the Blood Transfusion Services for 'Platelets, Apheresis, Leucocyte Depleted' required for clinical use (within the range 150 mL to 380 mL) (JPAC, 2021), i.e. they would still be viable units at the end of the study, in terms of volume (Table 3-6). The mean percentage volume loss of the RTP from the beginning of the study, D0 (pre-sampling), to the end of the study, D14 (post sampling), was 15% whereas the mean percentage loss of volume for the CSP was 12% to D14 and 18% to D21.

Table 3-6: Platelet Volume prior to sampling . Data presented as mean ± SD, n=12.

Day of Storage	Volume (mL)	
	RTP	CSP
D0	218.6 ± 5.6	217.9 ± 5.4
D2	217.2 ± 5.8	218.0 ± 5.4
D8	201.7 ± 5.6	204.3 ± 5.0
D14	185.7 ± 6.6	191.6 ± 4.6
D21	n/a	179.3 ± 5.3

At the start of the study all units met the specification for platelet yield of ≥ 240 x 10^9/unit laid out by the JPAC Guidelines for the Blood Transfusion Services for 'Platelets, Apheresis, Leucocyte Depleted'. The platelet yield declined throughout storage, as the units were sampled and the platelets begin to fragment, with the CSP units maintaining a statistically significant higher platelet yield than RTP at D8 and D14 ($p = 0.0095$ and $p = 0.0002$). The mean percentage loss of yield for the RTP from the beginning of the study, D0 (pre-sampling), to the end of the study, D14 (post sampling), was 37% whereas the mean percentage loss of yield for the CSP was 18% to D14 and 29% to D21.

3.4.1.3 Platelet concentration and mean platelet volume

Platelet concentration was similar in both RTP and CSP (Figure 3-1 A), with no statistical difference seen until D14 of shelf life ($p = 0.0002$) when there is a clear decline in the RTP concentration compared to the CSP concentration. At D21 CSP still have a higher mean platelet concentration than the RTP measured on D14. The mean platelet concentration on D14 for CSP was 94% of the starting concentration, compared to 74% for the RTP units. The platelet concentration was significantly

lower in comparison to the baseline result for both RTP and CSP by D14 with respective p values of <0.0001 and 0.0003 (all p values are shown in Appendix II).

The MPV increased for RTP from D2 throughout storage from a mean of 7.9 ± 0.9 fL on D2 to a mean of 9.2 ± 0.9 fL on D14 (Figure 3-1 B). Conversely, the CSP results showed a decline in MPV throughout storage from a mean of 8.0 ± 0.9 fL on D2 to a mean of 7.5 ± 0.8 fL on D21. A statistically significant difference was seen between the RTP and CSP groups on D8 and D14 (p=0.0009 and p=<0.0001).

A significant decrease in MPV was seen from baseline value by D8 for CSP (p=0.0430), while for RTP, significance was only reported at D14 and this was an increase in MPV rather than a decrease (p=0.0233) (all p values are shown in Appendix II).

In addition, the platelet count of the CSP units was assessed pre and post filtration through a transfusion set. The mean platelet concentration for the CSP pre-filtration was 1194.7 ± 189.8 x 10^9/L and post filtration was 1111.9 ± 168.1 x 10^9/L. This equated to a mean platelet concentration loss of 7% when transfusing.

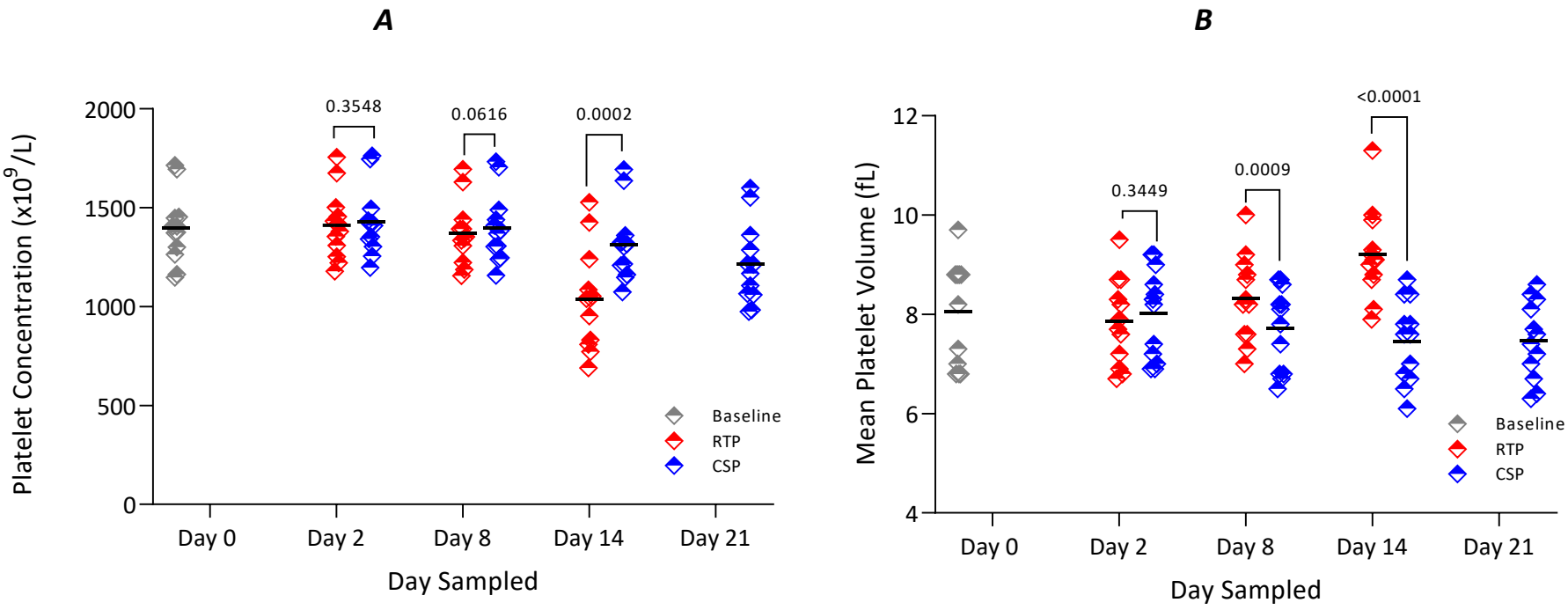

Figure 3-1: Relevant full blood count results of platelet concentrations in Room Temperature Platelets (RTP) and Cold Stored Platelets (CSP).A: Platelet concentration results. B: Mean platelet volume (MPV) results. Data are expressed as absolute values with the means represented by the black lines. Statistical comparisons were made using the two-way repeated ANOVA test and p values are presented. $p < 0.05$ was considered significant, $n = 12$.

3.4.1.4 *Residual white cell counting and end of storage sterility*

All PC were within the residual white cell count range specified by the JPAC Guidelines for the Blood Transfusion Services for 'Platelets, Apheresis, Leucocyte Depleted' required for clinical use (<1 x 10^6/unit) (JPAC, 2021). In addition, none of the study units grew bacteria when cultured at the end of study period.

3.4.2 Platelet activation assays

3.4.2.1 *Expression of CD62P by flow cytometry*

CD62P is a component of the α-granule membrane of resting platelets that is rapidly mobilised to the platelet surface upon activation where it plays a central role in platelet, leucocyte and endothelial interactions. Quantification of CD62P on the surface of platelets by FC is used as an indicator of their activation state.

Figure 3-2 shows overlay histograms for a single donation throughout storage for both the RTP and CSP groups. A unit was chosen that had results similar to the mean results shown in Figure 3-3. Comparison of Figure 3-2A and Figure 3-2B shows that for this sample, CD62P steadily increased throughout storage for RTP but for CSP is higher from D2 and remains high with a further step increase at D14.

The percentage of platelets expressing CD62P increased throughout storage for both RTP and CSP (Figure 3-3A) from 40% on D2 for RTP to 76% on D14 and from 51% on D2 for CSP to 76% on D14 and 78% on D21. The only statistical difference between the two groups was on D2 suggesting that CSP are more activated than RTP early in their shelf life. All of the results were significantly higher compared to the baseline result ($p = <0.0001$).

The MFI of CD62P also increased progressively with storage (Figure 3-3B) in both storage conditions with the only statistical difference between the two groups being at D2, where the CSP MFI of CD62P was slightly higher (2505 ± 530 MFI) than for RTP (2125 ± 381 MFI). All results, with the exception of RTP D2 ($p = 0.4314$) were significantly higher than the baseline result (all p values are shown in Appendix II).

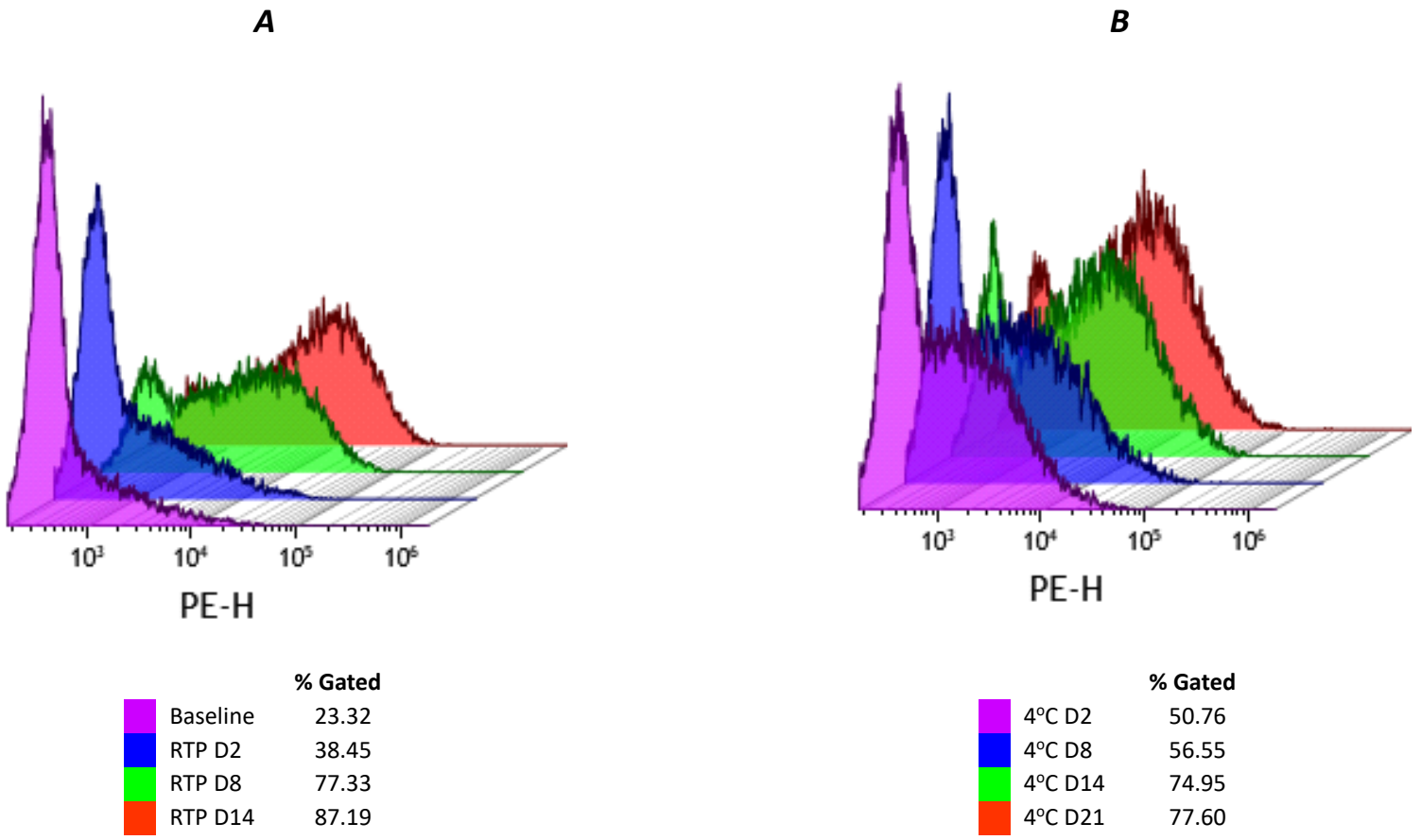

Figure 3-2: Representative plot of overlaid histograms for CD62P % positive for a single unit throughout shelf life , demonstrating the change in fluorescence as the platelets age. A: RTP; B: CSP. Representative unit chosen as overlay had results closest to the mean results seen in Figure 3-3.

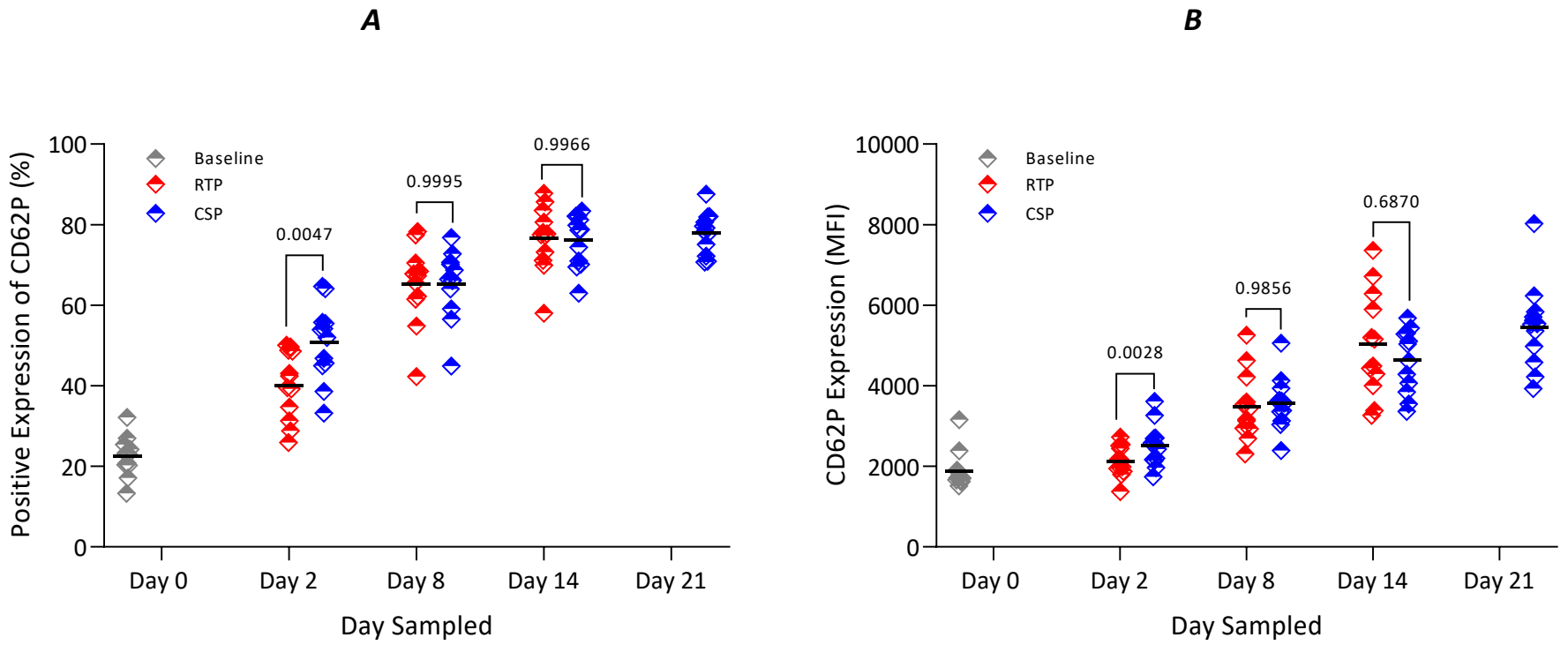

Figure 3-3: Expression of CD62P results of platelet concentrations in Room Temperature Platelets (RTP) and Cold Stored Platelets (CSP).A: Positive expression of CD62P (%) by flow cytometry. B: Median fluorescence intensity (MFI) of CD62P by flow cytometry. Data are expressed as absolute values with the means represented by black lines. Statistical comparisons were made using the two-way repeated measures ANOVA test and p values are presented. $p < 0.05$ was considered significant, $n = 12$.

3.4.2.2 Soluble CD62P

A soluble form of CD62P is secreted from activated platelets and can be measured using an ELISA assay.

Soluble CD62P (sCD62P) levels increased over storage time for both the RTP and CSP groups with the mean RTP results being statistically significantly higher than CSP throughout storage and considerably higher by D14 (RTP 197 ± 43 ng/mL vs CSP 94 ± 28 ng/mL) (Figure 3-4). All of the results were significantly higher than the baseline ($p = <0.0001$) with the exception of the RTP ($p = 0.1263$) and CSP D2 ($p = 0.9977$) results.

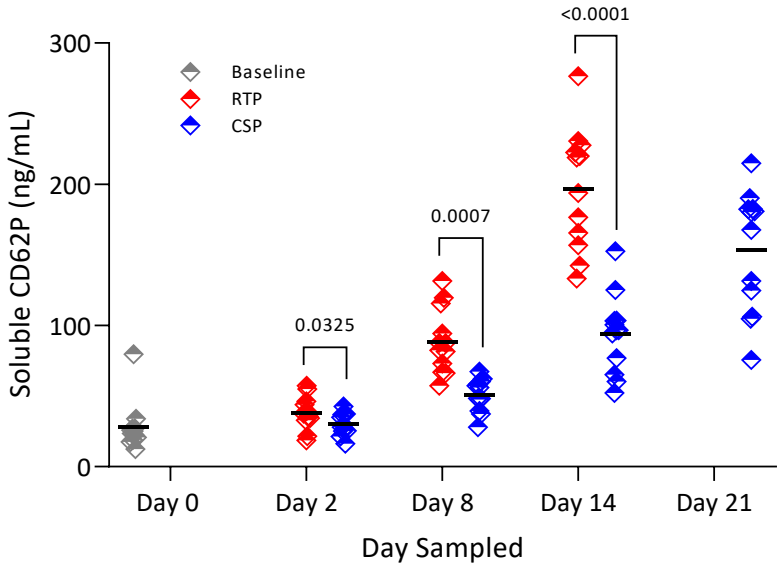

Figure 3-4: Soluble CD62P results of platelet concentrations in Room Temperature Platelets (RTP) and Cold Stored Platelets (CSP). Data are expressed as absolute values with the means represented by the black lines. Statistical comparisons were made using the two-way repeated measures ANOVA test and p values are presented. $p < 0.05$ was considered significant, $n = 12$.

3.4.2.3 Expression of phosphatidyl serine using Annexin V stain

Phosphatidyl serine is exposed on the surface of platelets following activation and can be identified by increased binding of the Ca^{2+} dependent fluorescein-Annexin V labelled stain.

The % Annexin V binding for a single donation throughout storage for both RTP and CSP were compared in an overlap histogram (Figure 3-5) as a representation of how the levels change. A unit was chosen that had results similar to the mean results

shown in Figure 3-7A. Comparison of Figure 3-6A and Figure 3-6B shows that for this sample, the % of Annexin V binding is initially higher in CSP than RTP for D2 and D8 but that RTP rises to a higher level than CSP by D14 (RTP 78.84% compared to CSP 48.49%). This is further demonstrated by the overlay histogram Figure 3-5, where the CSP D21 Annexin V levels are compared to the D14 RTP levels from the same donation.

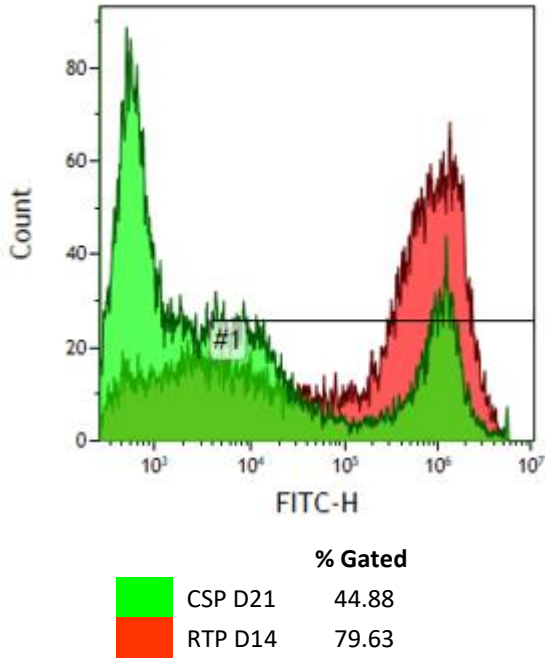

Figure 3-5: Representative plot of overlaid histograms for Annexin V binding, comparing the CSP D21 levels with RTP D14 levels in samples from the same donor.

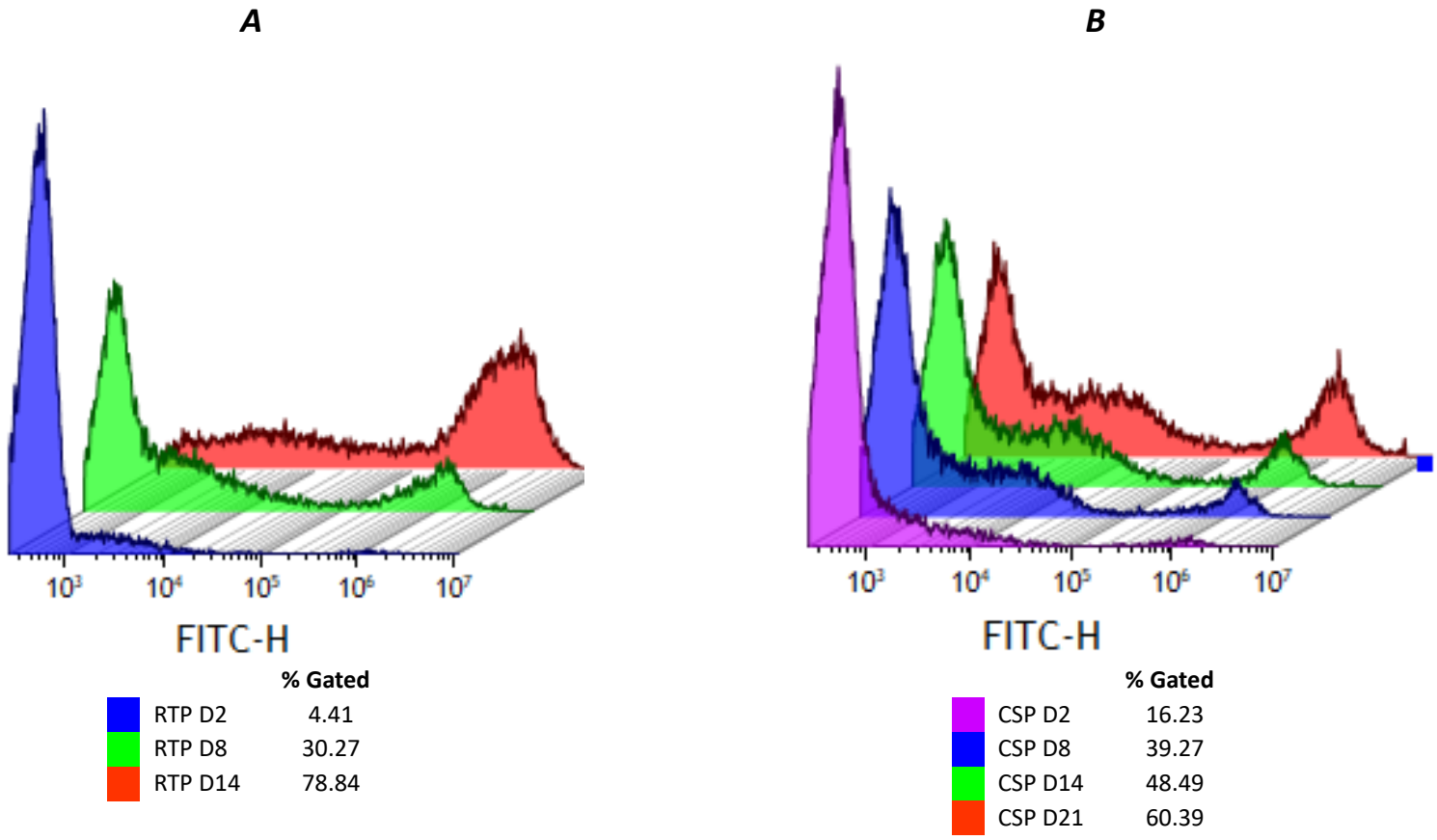

Figure 3-6: Representative plot of overlaid histograms for Annexin V binding % positive for a single unit throughout shelf life, demonstrating the change in fluorescence as the platelets age. A: RTP; B: CSP. Unit chosen for overlay had results closest to the mean results seen in Figure 3-7A.

The percentage of cells expressing bound Annexin V was initially very low at baseline (D0) with only 2.39 ± 1.13 % of cells showing positive expression but rose steadily for both RTP and CSP throughout storage (Figure 3-7A). The level of Annexin V binding increased throughout storage for RTP from a mean of around 2% on D2 to 43% by D14 compared to mean values of approximately 9% on D2 to 40% on D21 for CSP. The levels of Annexin V binding were statistically significantly higher for CSP than RTP on D2 and D8. However, by D14 the RTP group had a higher mean % positive than CSP at both D14 and D21, although no statistically significant difference was seen between the two groups at D14. All of the results were significantly higher than the baseline results (all p values are shown in Appendix II).

Annexin V binding expressed as the MFI was low for both RTP and CSP on D2 and D8, although with some high-level outliers for the RTP (Figure 3-7). The RTP test group levels rose considerably by D14 (122,922 ± 245,805 MFI), which could be PS as a result of apoptotic pathway rather than activation pathway, indicating that the platelets may be marked for destruction/phagocytosis once transfused into the circulation. The levels of Annexin V in CSP did not rise until D21 and were at a lower level than D14 RTP (65,659 ± 231,494 MFI). For both RTP D14 and CSP D21 there is a wide spread of results in the data.

There is minimal statistical significance seen from baseline data with only RTP D14 ($p=0.0237$) and CSP D21 ($p=0.0140$) showing a significant increase (all other p values are shown in Appendix II).

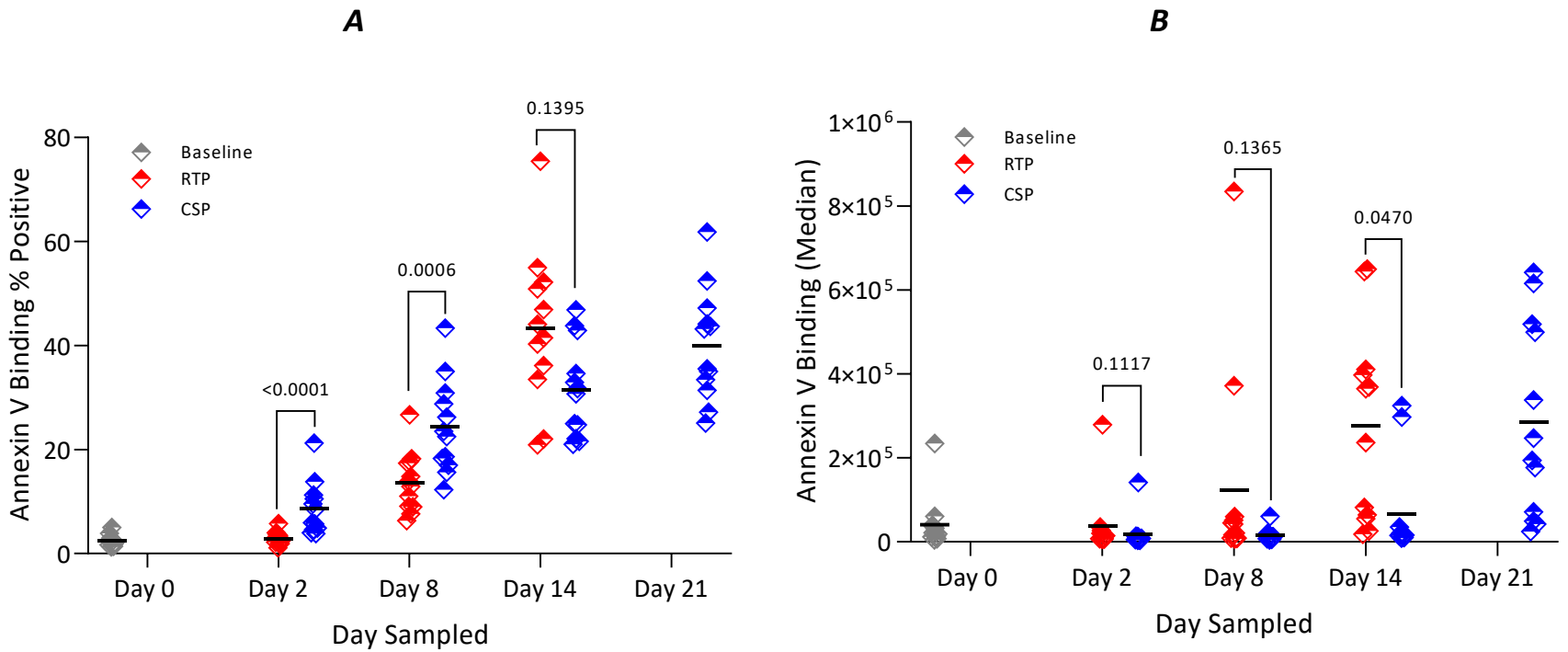

Figure 3-7: Expression of Phosphatidyl Serine using Annexin V stain on Room Temperature Platelets (RTP) and Cold Stored Platelets (CSP) . A: Annexin V % positive platelets; B: Median values of Annexin V binding on platelets. Data are expressed as absolute values with the means represented by the black lines. Statistical comparisons were made using the two-way repeated measures ANOVA test for Annexin V Binding % Positive and using the non-parametric Friedman test for Annexin V Binding (Median) and p values are presented. $p < 0.05$ was considered significant, n = 12. ***N.B*** *The Rout method was used to identify outliers in the above data with a Q value of 1% (maximum desired false discovery rate (FDR)). Eight outliers were identified, and the two-way ANOVA was re-run on the condensed dataset. Although exact p values were altered, the overall statistical significance identified between the groups remained unchanged.*

3.4.2.4 *Expression of phosphatidyl serine using lactadherin stain*

PS can also be identified by increased binding of the Ca^{2+} independent fluorescein-labelled lactadherin stain.

The percentage of cells expressing PS through Lactadherin binding were initially fairly low at baseline (D0) with only 12.85 ± 0.53 % of cells showing positive expression but rose steadily for both RTP and CSP throughout storage (Figure 3-8) . The level of PS increased throughout storage for RTP from a mean of around 13% on D2 to 52% by D14. The level of % PS positive cells in the CSP group increased from around 25% on D2 to 50% on D21. No statistically significant difference was detected between the two groups at any time point. There was a significant increase above baseline at RTP D8 (p = 0.0118) and D14 (p = <0.0001) and between CSP D2 (p = 0.0237), D14 (p = 0.0066) and D12 (p = <0.0001).

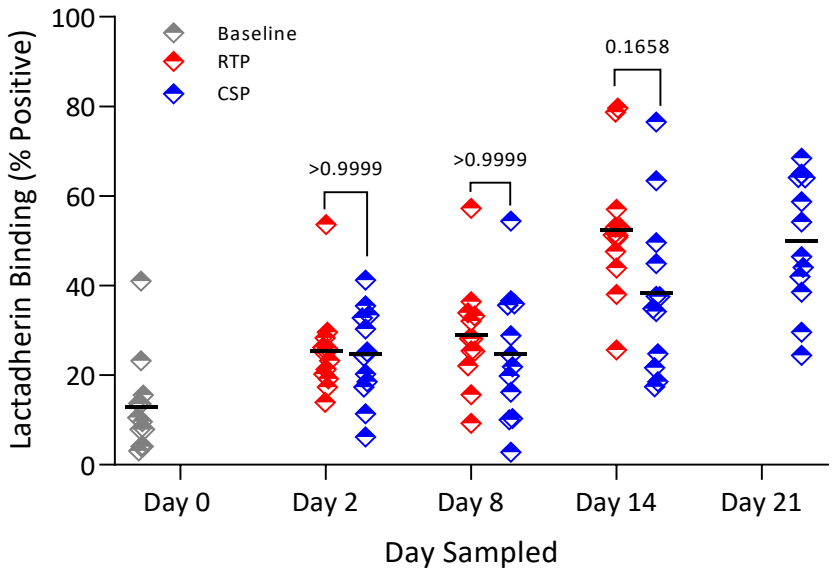

Figure 3-8: Expression of Phosphatidyl Serine using Lactadherin stain on Room Temperature Platelets (RTP) and Cold Stored Platelets (CSP) . Data are expressed as absolute values with the means represented by the black lines. Statistical comparisons were made using the non-parametric Friedman test. p < 0.05 was considered significant, n = 12.

3.4.2.5 Comparison of phosphatidylserine binding of Annexin V and lactadherin

Annexin V and lactadherin bind to PS on the surface of platelets and can be used as markers of the number of cells expressing PS. There is evidence to suggest that lactadherin is a more sensitive PS-binding probe than Annexin V and is also able to bind in a calcium independent manner. The WBS has not previously used lactadherin as a PS-binding probe and this study as an opportunity to compare the two probes. Figure 3-9A and Figure 3-9B compare the % binding of Annexin V and Lactadherin to PS in the RTP and CSP platelets at each timepoint throughout the study. For both RTP and CSP at all timepoints the % binding is higher with lactadherin although it is only a statistically significantly higher in RTP at D0, D2 and D8 and in CSP at D0 and D2. The largest difference between Annexin V binding of PS and lactadherin binding of PS is seen on D0 and on D2 for both RTP, where Annexin V shows a mean of approximately 3% binding vs Lactadherin which shows 25% binding and on D2 for CSP where Annexin V shows a mean of approximately 9% binding and lactadherin shows 25% binding.

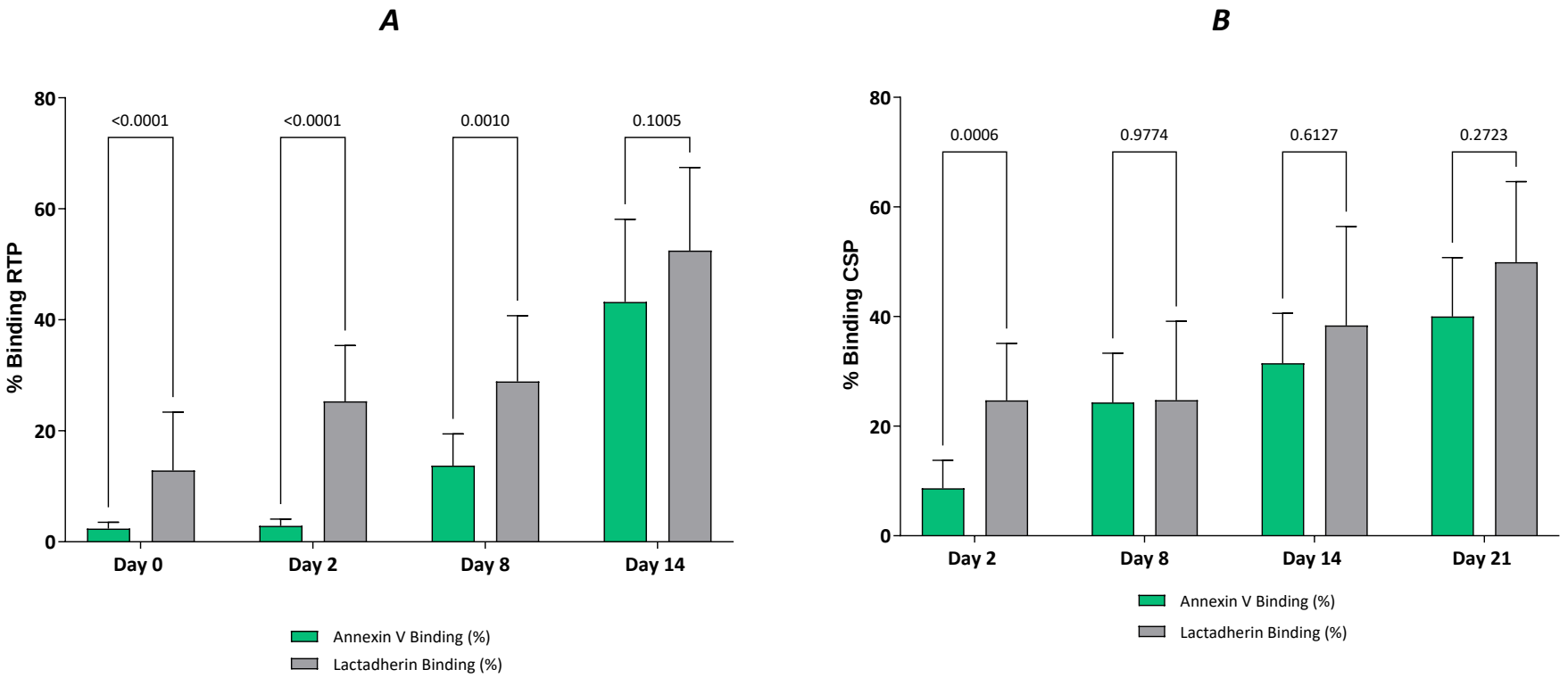

Figure 3-9: Comparison of Annexin V phosphatidylserine binding and lactadherin phosphatidylserine binding. A: Room Temperature Platelets (RTP); B: Cold Stored Platelets (CSP). Data are expressed as mean values with error bars. Statistical comparisons were made using the Man-Whittney test and p values are presented. p<0.05 was considered significant, n = 12.

3.4.3 Functional analysis

3.4.3.1 Extent of shape change and hypotonic shock response

The ESC measures the platelets' ability to change shape from disc to sphere in response to ADP and the HSR measures their ability to extrude water and regain normal volume (% recovery).

The ESC results (Figure 3-10A) showed an initial increase in % recovery from the D0 baseline to D2 (28.6 ± 2.2 % to 31.2 ± 2.9 % respectively) followed by a decline throughout storage from approximately 31% recovery on D2 to 6% recovery on D14. A statistically significant difference was seen between RTP compared to CSP on D2 and D8 but with no statistical difference on D14. The % recovery for ESC in CSP was immediately low at approximately 7% on D2 falling further to approximately 3% on D21. It was noted that 'excessive drift' was seen for four results on D14 and three results for D21 for CSP and no result was recorded. All results were significantly lower than the baseline with the exception of RTP on D2 (all p values are shown in Appendix II).

The HSR was compared between RTP and CSP at different timepoints (Figure 3-10B). There was an initial rise in % recovery for RTP from the D0 baseline to D2 (76.7 ± 11.6 % to 88.3 ± 11.4 % respectively) with a decline seen from D2 to D14 in the RTP ability to recover from hypotonic shock.

In the CSP group, the ability to recover from hypotonic shock decreased throughout storage and was depressed compared to RTP, with statistically significant differences seen between the two groups at D2 and D8 of approximately 88% compared to 57% on D2 and 28% compared to 15% on D14. It was noted that 'excessive drift' was seen for one result on D14 and one result for D21 for CSP and therefore no result was recorded.

All of the RTP and CSP results were significantly lower than the baseline result, particularly for CSP where a large decline was seen from a 57% mean response at baseline to a 6% mean response by D21 (all p values are shown in Appendix II).

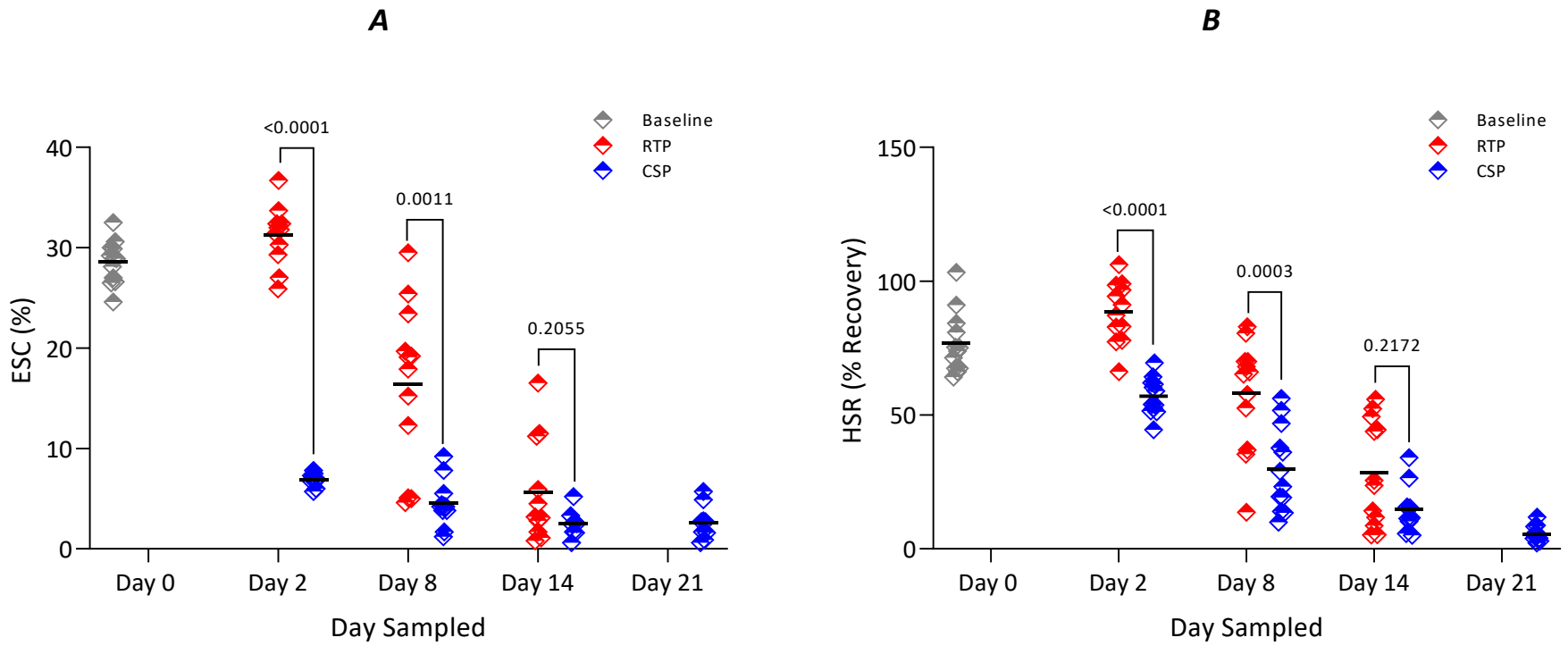

Figure 3-10: Extent of shape change (ESC) and hypotonic shock response (HSR) results of Room Temperature Platelets (RTP) and Cold Stored Platelets (CSP).A: ESC; B: HSR. Data are expressed as absolute values with the means represented by black lines. Statistical comparisons were made using Šídák's multiple comparisons analysis rather than by repeated measures ANOVA due to missing values with test and p values presented. $p < 0.05$ was considered significant, $n = 12$.

3.4.3.2 Thrombin generation

Thrombin generation was assessed using a fluorogenic substrate in the presence of exogenous TF and Ca^{2+}, using the calibrated automated thrombogram (CAT).

The mean ETP for CSP was slightly higher on D2 than RTP although this was not a significant difference; however prolonged cold storage enhanced thrombin generation and the ETP was significantly higher for CSP on D8 and D14 than for RTP, shown by the higher mean ETP values (Figure 3-11A). Other than for CSP at D14 ($p=0.0418$) none of the other results were significantly different to the baseline results (all p values are shown in Appendix II).

Peak thrombin generation was enhanced throughout storage for both RTP and CSP (Figure 3-11B) but was significantly higher for CSP than RTP at all the time points measured. From D8 onwards in the CSP group the results were significantly higher from the baseline, whereas for RTP the results were significantly higher for D14 only (all p values are shown in Appendix II).

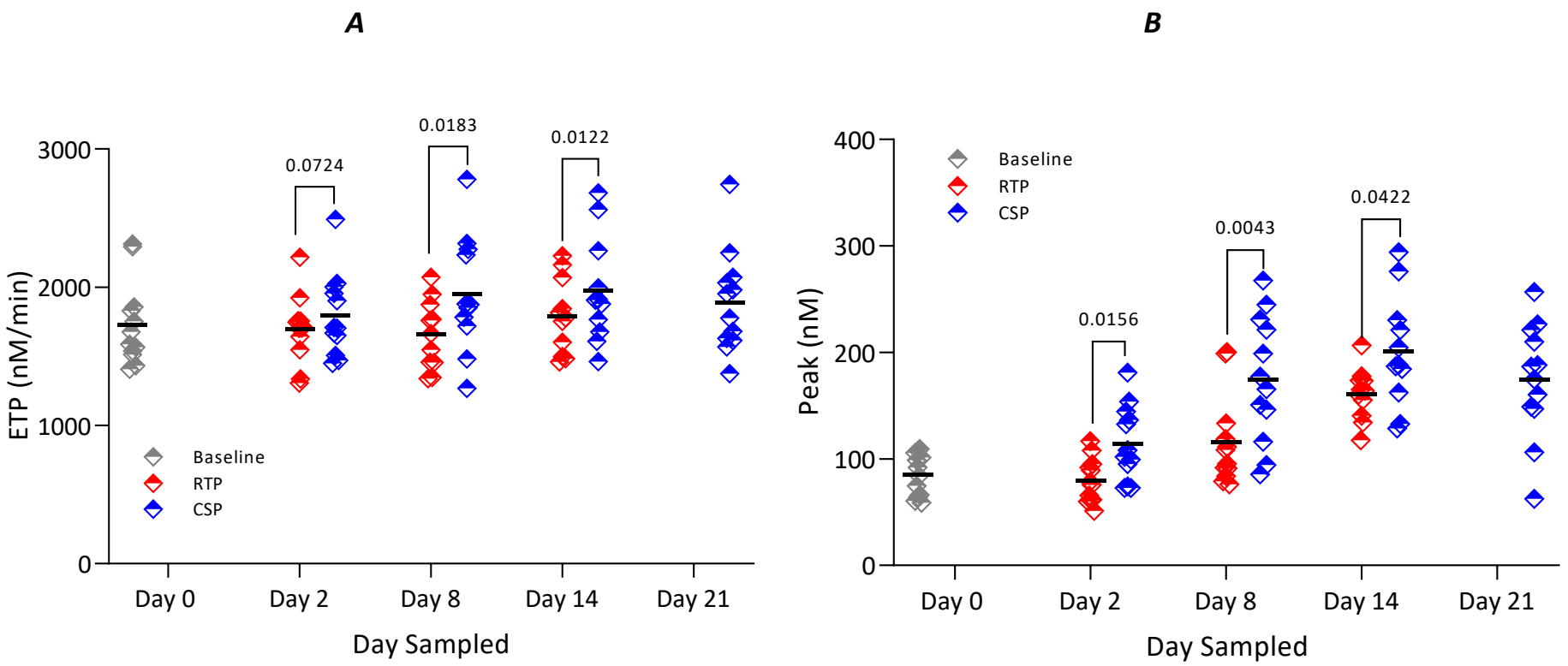

Figure 3-11: Thrombin generation results of platelet concentrations in Room Temperature Platelets (RTP) and Cold Stored Platelets (CSP).A: Endogenous thrombin potential (ETP); B: Peak height of thrombin curve. Data are expressed as absolute values with the means represented by the black lines. Statistical comparisons were made using Šídák's multiple comparisons analysis rather than by repeated measures ANOVA due to missing values with test and p values presented. $p < 0.05$ was considered significant, $n = 12$.

A statistically significant decrease in lag time was seen in CSP compared to RTP at D2 and D8 (Figure 3-12). All results at all timepoints were significantly lower than the baseline results (p values are shown in Appendix II).

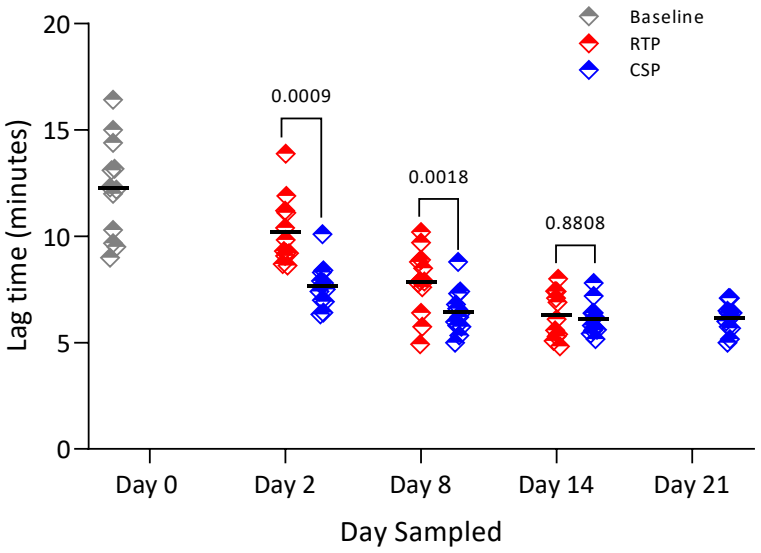

Figure 3-12: Thrombin generation lag time results of platelet concentrations in Room Temperature Platelets (RTP) and Cold Stored Platelets (CSP). Data are expressed as absolute values with the means represented by the black lines. Statistical comparisons were made using Šídák's multiple comparisons analysis rather than by repeated measures ANOVA due to missing values with test and p values presented. $p < 0.05$ was considered significant, $n = 12$.

The differences in thrombin generation between RTP and CSP can be further demonstrated by comparing the mean 'end of shelf life' results of D8 RTP with the potential end of shelf-life results for CSP D21 (Figure 3-13). It can be seen that CSP has a shorter lag time and a higher peak thrombin time than RTP.

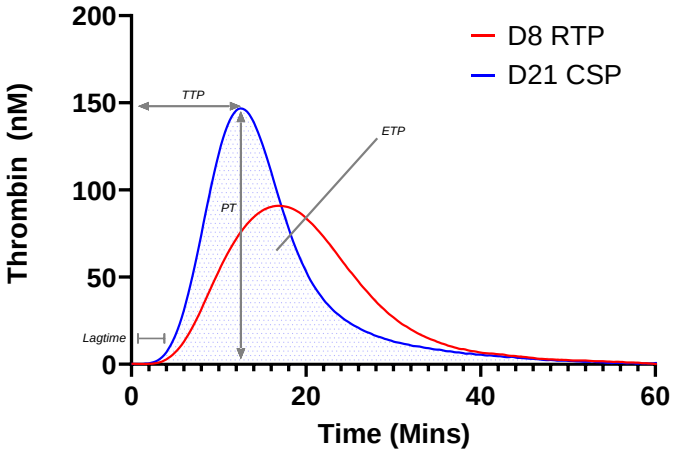

Figure 3-13: Traces of the mean thrombin generation results for room temperature (RTP) D8 (end of shelf life) and cold stored platelets (CSP) D21 (potential end of shelf life). TTP = Time to Peak; PT = Peak Thrombin; ETP = Endogenous Thrombin Potential.

3.4.3.3 Light transmission aggregometry (LTA)

To determine whether platelet functional responses are altered in cold stored PC, platelet aggregation assays were compared between RTP and CSP in response to 20 µM ADP (Figure 3-14A), 10 µg/ml collagen (Figure 3-14B) and a high (50 µM) and low (25 µM) concentration of TRAP-6 (Figure 3-15 A & B).

A weak aggregation response to ADP was seen in RTP with % aggregation dropping from a baseline of 28% (28 ± 23 %) to a mean of 9% (9 ± 8 %) by D2 and remaining low. The response was stronger for CSP with a slight increase in response from D0 (28 ± 23 %) to D2 (30 ± 18 %) and with the response rising from D14 to a high of 36% ±8 by D21. The difference between RTP and CSP results were all statistically significant although only RTP D2 showed a significant decrease compared to the baseline (p=0.0342).

The aggregation response to collagen decreased with storage for both RTP and CSP from D2 with no statistical difference observed between the groups at D2 and D8. At

D14, the mean maximum aggregation seen for RTP was 26 ± 12 % and for CSP was significantly higher at 56 ± 15 %. The results for both RTP and CSP from D8 onwards were significantly lower in comparison to the baseline result (p values are shown in Appendix II).

TRAP-6 was performed at two concentrations as the response can be very strong, making it difficult to see differences in the data (Figure 3-15). At 50 µM a downward trend in % aggregation is seen throughout storage with RTP dropping from 94 ± 5 % on D2 to 38 ± 25 % on D14 and CSP dropping from 87 ± 10 % on D2 to 60 ± 15 % on D14, and 52 ± 12 % on D21. The results from D8 onwards for both RTP and CSP are significantly lower in comparison to the baseline result (all p values are shown in Appendix II).

At 25 µM of TRAP-6 a similar downward trend in % aggregation is seen throughout storage with RTP dropping from 88 ± 9 % on D2 to 21 ± 16 % on D14 and CSP dropping from 68 ± 19 % on D2 to 41 ± 12 % on D14 and 40 ± 8 % on D21. Although the data look as though CSP maintains its response for longer than RTP on both dilutions of TRAP-6, there was no statistically significant difference between the RTP and CSP results. All of the results with the exception of RTP D2 show significantly reduced aggregation responses compared to the baseline result (p values are shown in Appendix II).

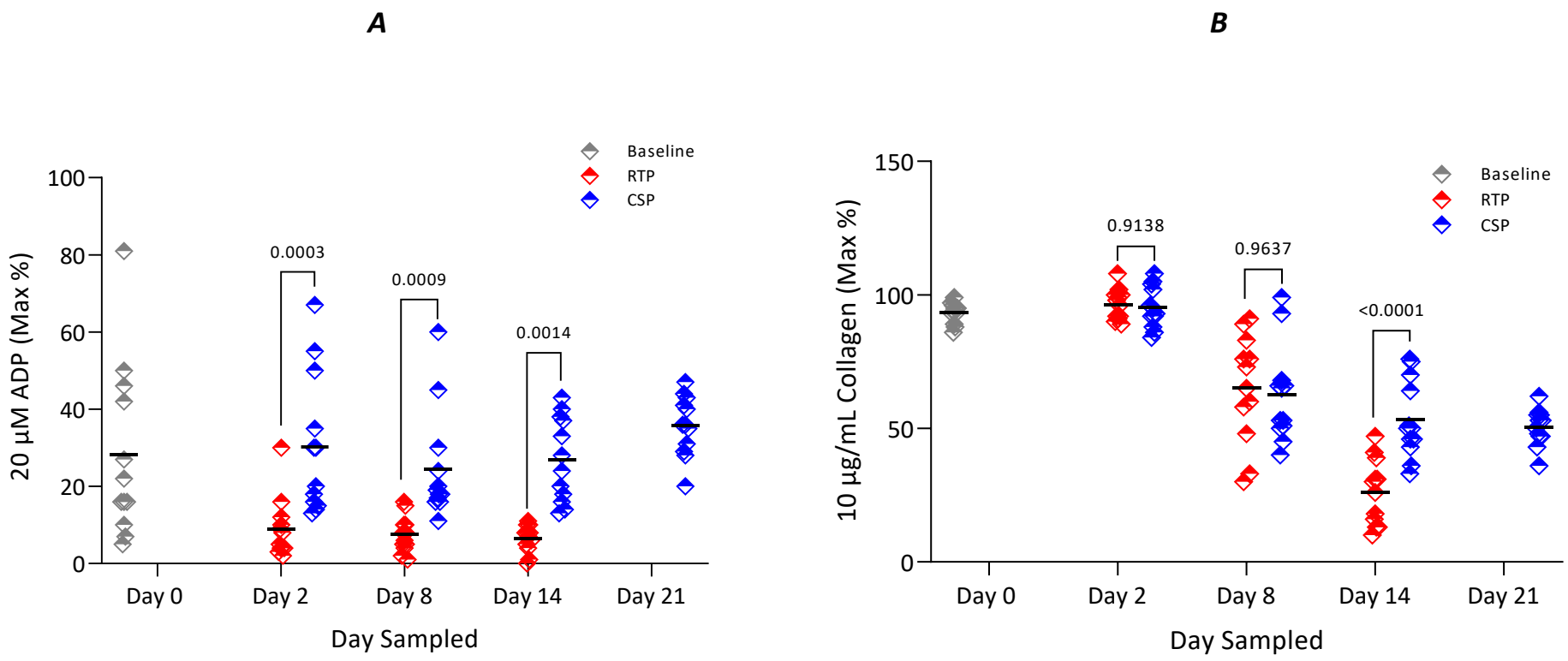

Figure 3-14: Aggregometry results of Room Temperature Platelets (RTP) and Cold Stored Platelets (CSP) using different agonists. A: ADP (20 µM). B: Collagen (10 µg/mL). Data are expressed as absolute values with the means represented by black lines. Statistical comparisons were made using the two-way repeated measures ANOVA test for collagen and using the non-parametric Friedman test for ADP. p values are presented. $p < 0.05$ was considered significant, $n = 12$.

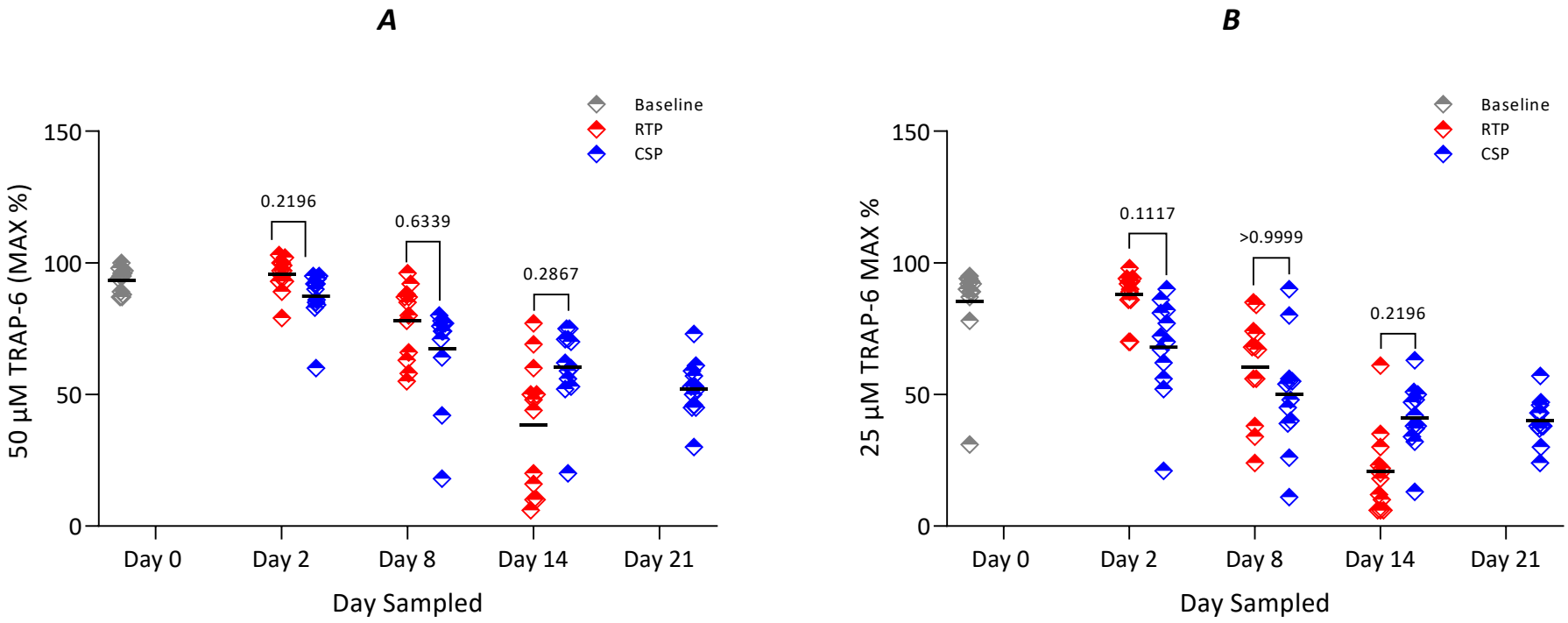

Figure 3-15: Aggregometry results of Room Temperature Platelets (RTP) and Cold Stored Platelets (CSP) using different agonists.A: TRAP-6 (50 µM). B: TRAP-6 (25 µM). Data are expressed as absolute values with the means represented by black lines. Statistical comparisons were made using the non-parametric Friedman test for TRAP-6 (50 µM) and TRAP-6 (25 µM) and p values are presented. $p < 0.05$ was considered significant , $n = 12$.

3.5 Discussion

The aim of this chapter was to investigate the impact of prolonged cold storage (4 ± 2°C) on the functional ability of platelets, compared to the current standard PC product that is stored at room temperature (22 ± 2°C) with gentle agitation. A paired study design was utilised with double apheresis PC split into two separate adult therapeutic doses, one stored at 4 ± 2°C and one at 22 ± 2°C with gentle agitation. The units were sampled and tested throughout storage on days 0, 2, 8 and 14 (with CSP also being tested on day 21) to assess their functional ability. A panel of quality assessment assays were employed including platelet morphology, expression of activation markers on the platelet surface, response to hypotonic shock, extent of shape change, response to agonists and thrombin generation.

Although storage temperature was not the only variable, as the RTP were also gently agitated whereas CSP were not, agitation has been demonstrated by others through comparison of agitated and non-agitated CSP, to have no impact on the platelets' functional ability when stored in the cold (Shea, Spinella and Thomas, 2022; Reddoch *et al.*, 2014; NasrEldin, 2017).

3.5.1 Indicators of Component Quality

Visual observation of PC for swirling and aggregates are the only quality assessments performed on all PC prior to issue to a patient. Swirling results from discoid shaped platelets scattering incident light in different directions. Once platelets have undergone a morphological shape change from a disc to a sphere, the light is scattered in one direction and swirling is no longer observed (Maurer-Spurej and Chipperfield, 2007). In RTP, lack of the swirling phenomenon can indicate that the platelets are not viable or can be an indicator of bacterial contamination (Vit, Klüter and Wuchter, 2020) and this would prevent the unit from being transfused.

A loss of swirl was identified in all CSP units in the study once placed into cold storage at 4 ± 2°C, indicating a shape change from disc to sphere had occurred, whereas all RTP maintained swirling throughout. Shape change in platelets stored in the cold is an established phenomenon with early studies on CSP in plasma demonstrating that

they change shape within a few minutes of being stored in the cold (Becker *et al.*, 1973; Zucker and Borrelli, 1954; Murphy and Gardner, 1969).

At low temperatures platelets become less able to maintain their energy-dependent calcium pumps (which function to maintain low cytosolic calcium levels, preventing activation) which leads to a rise in free cytosolic calcium (Hoffmeister *et al.*, 2003; Hoffmeister *et al.*, 2001; Davlouros *et al.*, 2016). This rise in calcium results in significant reorganization of the cytoskeletal proteins within the platelet with disassembly of the microtubule ring, actin polymerization and shape change (Figure 1-3).

In addition to causing shape change, cold-induced calcium leak leads to a conformational change of the extracellular part of the fibrinogen receptor, αIIbβ3, enabling it to bind fibrinogen (Davlouros *et al.*, 2016; Getz *et al.*, 2016). This results in aggregate formation in PC stored in 100% plasma at 4^{o}C due to the high fibrinogen concentration in plasma. However, it has been demonstrated that reducing plasma levels to 35% or less in CSP with a PAS dilutes the level of fibrinogen in the suspension medium sufficiently to reduce aggregate formation (Getz *et al.*, 2016). There are also other benefits associated with using PAS including improved mitochondrial support through the substrate sodium acetate (Getz *et al.*, 2016).

A high percentage of units in the study had visible macro-aggregates on day 0 (8/12, 67%), which dispersed following storage for longer periods, with only 25% (3/12) still having visible aggregates for both CSP and RTP from Day 8 onwards. Two units from both groups had an aggregate score of >1 at the end of the study (the cut-off value for clinical use). However, overall, no differences were seen in aggregate formation between RTP & CSP. In addition, the CSP units were passed through an infusion device to mimic transfusion in order to assess the number of platelets that may be lost due to micro-aggregates being caught in the filter. This was determined to be minimal with only 7% of the total platelets lost during 'infusion'.

Platelet concentration remained stable in both RTP and CSP until D14 when a significant drop was seen in RTP (to 74% of baseline concentration) compared to CSP

which remained at 94% of baseline concentration. This could reflect more rapid use of cellular metabolites in RTP resulting in earlier apoptosis of the platelets.

It might be expected that when platelets become spherical (as they do in the cold) that the MPV would increase rather than decrease. This study found no significant difference between the MPV for RTP and CSP on D2, however a gradual decline was seen in CSP from D8, suggesting that the platelets were becoming smaller. A slight increase in MPV was seen in RTP throughout the study suggesting they were becoming larger. These results are in contrast to other CSP studies where no difference in MPV was observed (Reddoch *et al.*, 2014), or where an increase in MPV was reported (Hornsey *et al.*, 2008; Johnson *et al.*, 2016). Hornsey et al. (2008), focused on CSP in 100% plasma and only examined MPV until D5 and D7 respectively. In the present study, the difference in MPV was not apparent until D8, which may explain the conflicting findings results. Johnson *et al* focused on PC in PAS and tested up to D21, however the study used buffy coat derived PC rather than apheresis platelets as used in this study, which may be the reason for the difference in results. A more comparable study was performed by (Reddoch-Cardenas *et al.*, 2019b) which involved apheresis platelets in T-PAS+ over 18 days of storage. This study reported a slight increase in MPV on D3 and D5 of storage but then a return to the baseline result for the remainder of the 18 days.

A possible explanation for the reduction in MPV in CSP could be due to extracellular vesicle (EV) formation. EV's are produced by platelets upon activation and bud off from the platelet plasma membraneand have the potential, if produced in sufficient numbers to reduce the size of the platelets in a CSP. Indeed, in red cells, EV formation has been shown to reduce cell membrane by 20% with an accompanying decrease in cell volume and an increase in cell density (Leal, Adjobo-Hermans and Bosman, 2018), and it is plausible that EV formation could have the same effect on platelet volume. CSP have been shown to produce significantly larger EVs than RTP from day 4 of storage onwards (Nash *et al.*, 2023) as well as significantly more EVs by day 20 compared to day 7 RTP (Stolla *et al.*, 2020). This could account for the significant size decrease in CSP observed compared to RTP from D8 in this study.

The differences resulting from the study when compared to the present study could also be down to different haematology analysers utilising different technologies to calculate the MPV. Despite the difference, the mean MPV at all time points for both CSP and RTP were within the normal adult range (7.0-11.0 fL).

3.5.2 Platelet shape change and response to hypotonic shock

The ESC assay can be used to assess discoid shape of platelets through the use of the agonist ADP, where the extent of shape change is directly related to the percentage of discoid platelets (Holme, Moroff and Murphy, 1998). The ESC results from this study demonstrated that RTP maintain their discoid shape until D2 with a large decline seen by D8 (ESC ~29% at baseline, declining to ~16% by D8). CSP however, as demonstrated by their loss of swirling, have lost almost all of their discoid shape by D2 (ESC ~7%, dropping further to 3% by D21). No other studies examining shape change by the ESC assay were found in the literature.

The HSR assay measures platelets' ability to extrude water when exposed to an osmotic challenge by measuring the transmitted light through a sample. Where normal membrane integrity and energy metabolism are maintained, platelets should be able to regain their normal volume (Holme, Moroff and Murphy, 1998). Loss of HSR has been associated with a loss of platelet viability *in vivo* with studies demonstrating a correlation between HSR and loss of viability where a HSR below 60% is seen (Holme, 1998; Valeri, Feingold and Marchionni, 1974).

Both RTP and CSP demonstrated a progressive depression of HSR throughout storage with more of a significant decline in CSP than RTP at D2 (RTP ~88%, CSP 57%) and D8 (RTP ~59%, CSP ~30%). These results are in concordance with other CSP studies that have reported a decrease in the HSR over time (Kim and Baldini, 1974; Handin, Fortier and Valeri, 1970; Johnson *et al.*, 2016; Hornsey *et al.*, 2008).

3.5.3 Platelet activation

The activation state of the PC in the study were monitored by measuring the expression of CD62P on the surface of the platelets, the amount of soluble CD62P in the plasma and the expression of PS on the surface of the platelets.

CD62P is a component of the α-granule membrane that becomes surface expressed upon activation of platelets (Badlou *et al.*, 2005) and provides a sensitive marker for platelet activation status *in vitro* (Curvers *et al.*, 2008). The expression of CD62P on the surface of the platelets in this study increased from baseline during storage for both RTP and CSP, with the greatest incremental change seen early during storage between baseline and D2. At D2, the % positive expression of CD62P on CSP were statistically significantly higher than RTP, with 50% of platelets showing positive expression of CD62P compared with 40% of RTP. However, at the other time points in storage (D8 & D14) there was no statistically significant difference between the two groups. In addition, the mean fluorescent intensity (MFI) of the CD62P increased throughout storage for both groups suggesting that not only do more cells express CD62P but that the levels on each cell of CD62P become progressively higher with storage. As with the % positive expression, the only significant difference between the two groups in terms of MFI was seen on D2 where CD62P MFI in CSP was statistically significantly higher than seen in RTP.

The expression of CD62P on the surface of RTP has been shown in other studies to increase with storage (Metcalfe *et al.*, 1997; Palmer *et al.*, 1998; Dumont *et al.*, 2002) and has also been compared with that in CSP (Reddoch *et al.*, 2014; Wood *et al.*, 2016; Reddoch-Cardenas *et al.*, 2019b). The study by Wood *et al* showed approximately two-fold higher CD62P levels in CSP compared with RTP up to 18 days of storage (Wood *et al.*, 2016). This was not seen in our study, where there was only a statistically significant higher amount of CD62P in CSP at D2. The platelets prepared in the Wood *et al* study were buffy coat derived. Buffy coat derived platelets undergo more centrifugation steps and are stored in whole blood at ambient temperature for 24 hours before being separated into components, which could result in them becoming more activated.

Reddoch *et al* (2014) observed a significant increase in CD62P on CSP compared with RTP, but this was only measured on D1, D4 and D5 (Reddoch *et al.*, 2014) which are not timepoints included in this study. In addition, Reddoch *et al* (2019) measured CD62P expression on CSP made from apheresis platelets in T-PAS+ up to D18 (not compared with RTP) and reported a large increase between day 0 and day 3 levels.

This was similar to the difference seen in our study between D0 and D2 (Reddoch-Cardenas *et al.*, 2019b). They also showed a levelling off of CD62P levels from D14 – D16, similar to that seen between D14 and D21 in this study.

The increase in CD62P levels in CSP has historically been thought to be a poor indicator of platelet quality and a reflector of the platelet storage lesion in RTP, resulting in rapid clearance of platelets from the circulation once transfused (Albanyan, Harrison and Murphy, 2009; Badlou *et al.*, 2005). Although correlation between the amount of CD62P and shortened recovery has been demonstrated in a rabbit model (Leytin *et al.*, 2004), length of time in the circulation and platelet functional ability *in vivo* are not necessarily related. In fact, conversely, there is evidence from *in vitro* and *in vivo* studies which suggests that an increased activation state may help promote faster clot formation in bleeding patients, as the platelets are 'primed' ready to function upon transfusion (Nair *et al.*, 2017; Reddoch *et al.*, 2014; Strandenes *et al.*, 2016; Stubbs *et al.*, 2017).

The soluble form of CD62P (sCD62P) is released into the plasma by active cleavage from the platelet surface or is released from the platelets by direct secretion (Choudhury *et al.*, 2007). It was observed that an increase in the percentage of CD62P-positive cells during storage was followed by an increased concentration of sCD62P in the plasma, with both RTP and CSP sCD62P levels increasing throughout storage. A correlation between increased expression of CD62P on the platelet surface during storage with increased concentration of sCD62P in the plasma in RTP has been demonstrated previously by others (Skripchenko *et al.*, 2008) (Kostelijk *et al.*, 1996). However, in contrast to the surface expression of CD62P on RTP and CSP, the levels of sCD62P in CSP were statistically significantly lower than RTP at all timepoints, data mirrored by Johnson and colleagues study (Johnson *et al.*, 2021). This suggests that CD62P may be better preserved on the surface of platelets stored in the cold (not shed into the plasma to the same extent) compared to platelets stored at 22 ± 2^{o}C.

Another frequently used platelet activation marker is PS. PS is an anionic phospholipid which in a resting platelet is predominantly asymmetrically distributed on the inner leaflet of the plasma membrane (Albanyan *et al.*, 2009). Upon platelet activation with agonists that induce a rise in intracellular calcium, the asymmetric

orientation of membrane phospholipids is rapidly re-disrupted and PS is translocated via a 'flip-flop' mechanism to the outer leaflet of the platelet (Lhermusier, Chap and Payrastre, 2011). On the outer leaflet, PS acts as a procoagulant surface for coagulation factors to assemble and accelerates thrombin generation (Albanyan *et al.*, 2009). The role of PS exposure in coagulation is confirmed by the moderate/severe bleeding tendency in patients with the rare congenital disorder Scott syndrome where the PS cannot translocate to the outer platelet leaflet (Lhermusier, Chap and Payrastre, 2011; Reddy *et al.*, 2018). In addition to its function in promoting blood coagulation, PS exposure also plays a pivotal role in the recognition and removal of apoptotic cells through a PS-recognizing receptor on phagocytic cells (Zwaal, Comfurius and Bevers, 2005).

The proportion of platelets expressing PS on the PC examined in this study were measured using two different PS-binding probes: Annexin V and Lactadherin. Previous studies performed by the WBS have utilised Annexin V to detect PS translocation on the outer leaflet of cells (Saunders, Pearce and George, 2022; Saunders, 2012), however Annexin V is not sensitive to low-level PS exposure and can only bind to the platelet membrane when the PS content is >8% and calcium is present (Shi *et al.*, 2006). Annexin V can also be internalized by stressed cells even when there is no PS exposure and can bind to other lipids on the surface (Hou *et al.*, 2011), meaning that the extent to which Annexin V represents the true amount of PS on the surface of stored PC is unknown. Lactadherin, an opsonin that bridges PS exposing apoptotic cells to macrophages, has been identified as an alternative probe for PS levels on platelets (Hou *et al.*, 2011; Albanyan *et al.*, 2009). It can detect low levels of PS (0.5%) in a calcium free manner and has been shown to more sensitively detect PS-rich platelets than Annexin V (Shi *et al.*, 2006).

In this study Annexin V and lactadherin were separately probed to determine the % PS exposure during PC storage on RTP and CSP. Increasing PS exposure during storage compared to baseline (D0) results was observed using both Annexin V and lactadherin, although the statistical significance was greater using Lactadherin than Annexin V. In the Annexin V binding results, CSP bound significantly more Annexin V at D2 and D8 than RTP, suggesting that there is more PS expressed on CSP earlier in

the shelf life. No statistically significant difference was observed between the two groups at D14. These results are similar to those demonstrated by Wood *et al* who saw a significant, steady increase of Annexin V binding of PS throughout storage in CSP compared to RTP (Wood *et al.*, 2016). The significantly higher PS levels in D2 and D8 CSP indicate that the platelets within the PC will be able to facilitate increased thrombin generation compared to RTP, which is associated with an increased haemostatic effectiveness.

In the Lactadherin binding results no statistically significant differences were seen at any timepoint during storage between RTP and CSP. This is in contrast to the study by Reddoch *et al* which demonstrated a significant increase in Lactadherin binding of PS in CSP compared to RTP (over a study period of 5 days) (Reddoch *et al.*, 2014).

The results for Annexin V and Lactadherin were directly compared for each storage group at each timepoint (Figure 3-9), to determine if Lactadherin detected higher levels of PS than Annexin V. Significantly higher levels of Lactadherin binding compared to Annexin V binding were detected in RTP at D0, D2 and D8 and in CSP at D2 with no significant difference seen at the other timepoints. The difference in PS binding levels was more pronounced on D0 and D2 in RTP (D0 = ~ 2% for Annexin V vs ~ 13% for Lactadherin; D2, ~ 3% for Annexin V vs ~ 25% for Lactadherin) and on D2 for CSP (~ 9% for Annexin V vs ~ 25% for Lactadherin) suggesting that Lactadherin may be more sensitive at detecting PS at lower levels (i.e. earlier in storage) but that once levels rise (later in storage) there is no difference in Lactadherin 's ability to bind PS compared to Annexin V. This suggests that there may be an argument for the use of Lactadherin instead of Annexin V for PS detection, although Lactadherin did not detect the significant differences between RTP and CSP that were detected in this study and in other CSP studies (Reddoch *et al.*, 2014; Wood *et al.*, 2018).

An increase in procoagulant platelets throughout storage in CSP, as demonstrated by increased binding of Annexin V to PS in this study at D2 and D8 compared to RTP, in theory, should increase the ability of the platelets to generate thrombin. PS exposure turns the platelets into a two-dimensional reaction compartment in which absorbed clotting factors generate thrombin far more efficiently than in free solution (Hemker *et al.*, 2006).

3.5.4 Thrombin generation

In this study, thrombin generation (TG) was measured and the lag time, peak height and ETP were recorded. The lag time corresponds to the amount of time it takes for the initiation phase of coagulation to occur which is followed by a rapid 'burst' of TG on the surface of the platelets (Wolberg, 2007). Lag time decreased in both RTP and CSP throughout storage with a significant decrease seen in CSP compared to RTP on D0 and D8, suggesting that CSP are faster at forming thrombin than RTP, results mirrored in other CSP studies (Reddoch *et al.*, 2016).

During TG, the rate of TG and inhibition of free thrombin by antithrombin reach an equilibrium, resulting in a 'peak' in the amount of thrombin generated (Wolberg, 2007). The mean peak TG increased for both RTP and CSP throughout storage although the increase was only significantly higher compared to baseline for RTP at D14 and for CSP from D8 onwards. The peak TG was significantly higher in CSP compared to RTP at all time points measured, demonstrating the ability of CSP to achieve higher thrombin levels than RTP. The increase in lag time and peak time in CSP compared to RTP may be attributed to increased PS (as seen in our Annexin V binding results) and FVa on the surface of the platelets (Reddoch *et al.*, 2016).

The ETP reflects the amount of substrate that could be converted by the thrombin generated in the sample (Hemker *et al.*, 2006). Other studies (Nair *et al.*, 2017) have demonstrated that the ETP is similar in RTP and CSP, however we have shown that although the ETP remained fairly stable throughout the study for both RTP and CSP, the ETP in CSP was significantly higher than RTP at D8 and D14, suggesting that at these time points CSP produce more total thrombin than RTP. The differences in results are probably due to the different timepoints studied – the study by Nair and colleagues (Nair *et al.*, 2017) only examined CSP up to D5 whereas in this study we did not see a significant difference in the ETP until D8.

The concentration of thrombin present at the time of clot gelation has a profound physiological influence on the fibrin clot structure. It has been shown that when higher concentrations of thrombin are present, as we have demonstrated in CSP within this study, fibrin clots are produced that are composed of thinner, more tightly packed fibrin strands (Wolberg, 2007). Fibrin clot structure in CSP has been shown,

through morphological analysis, to consist of denser, thinner and straighter fibres with more cross-links than RTP and to generate significantly stiffer and stronger clots than those from RTP (Nair *et al.*, 2017).

Platelet response to stimulation

All of the assays described thus far assess the PC in their unstimulated/basal state. Light transmission aggregometry enables the probing of different pathways of platelet activation, assessing the ability of platelets within PC to function (aggregate) *in vitro* after stimulation with agonists. Interactions of platelets with agonists cause intracellular signalling that leads to the activation of the fibrinogen receptor, αIIbβ3. These interactions cause the fibrinogen receptor to change from a low-affinity to a high-affinity state that binds fibrinogen, resulting in cross-linking and aggregation between platelets (Dorsam and Kunapuli, 2004). In this study, we used the single agonists ADP, collagen and TRAP-6.

ADP, secreted from dense granules, is considered a mild platelet agonist and exerts its effect on platelets by binding to the $P2Y_1$ and $P2Y_{12}$ receptors (Dorsam and Kunapuli, 2004). $P2Y_1$ activation induces shape change and initiates primary wave platelet aggregation through calcium mobilisation (Zhou and Schmaier, 2005). However, without $P2Y_{12}$ activation, the result is small and reversible platelet aggregation. The $P2Y_{12}$ receptor is considered the major receptor mediating full platelet aggregation with its stimulation resulting in amplification and stabilization of the aggregation response (Gremmel, Frelinger and Michelson, 2016; Zhou and Schmaier, 2005). For this reason, $P2Y_{12}$ is the target of anti-platelet drugs such as clopidogrel, which is used to reduce the risk of heart disease and stroke (Koessler *et al.*, 2020).

As demonstrated by others (Choi and Pai, 2003; Becker *et al.*, 1973; Holme, Heaton and Courtright, 1987), a significant loss in response to ADP was demonstrated from baseline to D2 (28% ± 23% to 9% ± 8%) in RTP. In contrast, CSP maintained their ability to respond to ADP throughout the 21 days studied, with no significant difference observed to the baseline result and with maximum aggregation significantly greater ($p = <0.05$) than RTP at all timepoints studied.

Collagen is important for platelet adhesion and subsequent activation on the extracellular matrix (Zhou and Schmaier, 2005). The response to collagen in this study was variable with both RTP and CSP displaying a reduction in response compared to baseline from D8 onwards. At D14, the response from CSP was significantly higher than the RTP group (56% ± 15% vs 26% ± 12%) and was maintained at D21 (50% ± 17%). This is similar to results demonstrated by others (Johnson *et al.*, 2016; Getz *et al.*, 2016; Marini *et al.*, 2019).

Thrombin is the most potent physiological agonist of platelets and activates them through binding to the PAR-1 and PAR-4 receptors (Zhou and Schmaier, 2005). The PC ability to respond to TRAP-6 (thrombin), declined throughout storage for both RTP and CSP with no significant difference detected between the two groups at either 50 µM or 25 µM of TRAP-6. The CSP results are concordant with those demonstrated by Reddoch-Cardenas and colleagues (Reddoch-Cardenas *et al.*, 2019b). The decreasing response to TRAP-6 during storage is possibly due to the decreasing levels of PARs on platelets after 5 days storage as demonstrated by Schlagenhauf *et al* (Schlagenhauf *et al.*, 2012).

The aggregation results from this study with ADP and collagen demonstrated an improved function in CSP compared to RTP. It is possible that this is connected to the disruption of the actin cytoskeleton which results in the spherical shape of CSP as it has been shown that the actin cytoskeleton inhibits α-granule release in response to weak agonists. Once the actin cytoskeleton is disrupted (as they are in CSP), ADP has been shown to elicit significant secretion of α-granules (Flaumenhaft *et al.*, 2005).

In summary, we have performed a thorough assessment of the functional ability of CSP compared to RTP, utilising different methods to examine the basal state of platelets within the PC stored at different temperatures and their ability to generate thrombin and become activated under stimulation. Some of our results confirmed the findings of other studies on CSP whilst others expanded the current knowledge, providing a fuller picture of how CSP function up to 21 days in storage.

All PC in the study demonstrated increased activation profiles throughout storage for markers for CD62P, sCD62P and Annexin V, with CSP showing significantly higher

activation levels compared to RTP at certain timepoints (D2 CD62P and D2 & D8 Annexin V), suggesting that CSP are more 'primed' than RTP for function early during storage. CSP demonstrated a superior ability to aggregate in response to ADP compared to RTP throughout all timepoints measured and to collagen at D14, suggesting an improved function compared to RTP. In addition, we have demonstrated that CSP have increased thrombin potential, generate thrombin faster and reach higher peaks of thrombin than RTP meaning that CSP are likely to generate stronger clots than RTP.

Chapter 4: Platelet Metabolism and Bioenergetics

4.1 Introduction

Platelets undergo dramatic morphological shape changes when they are recruited to an injured vessel, including activation, spreading, clot formation and clot retraction (Fritsma, 2015). All of these processes require large amounts of chemical energy which is generated predominantly from the breakdown of glucose to produce ATP.

ATP exists as a highly charged molecule containing four negative charges and is the main energy source for platelets. Due to its negative charge ATP stores a large amount of energy in its phosphate bonds, with cleavage of one phosphate bond liberating -31kJmol^{-1} of energy (Judge and Dodd, 2020). There are two main pathways for liberating energy in the form of ATP from glucose within platelets: glycolysis and oxidative phosphorylation (OXPHOS).

The glycolytic pathway (glycolysis) involves the breakdown of glucose into two pyruvate molecules within the cytosol and can occur in the absence of oxygen. Glycolysis relies on the hydrogen carrier NAD^+ to accept electrons from glucose forming NADH and H^+ (Judge and Dodd, 2020). The subsequent fate of the pyruvate and NADH generated depends on whether O_2 is available.

Where O_2 is unavailable (anaerobic respiration), pyruvate is reduced to lactate (La^-) by lactate dehydrogenase (LDH) (Rogatzki *et al.*, 2015):

$$Pyruvate^- + NADH + H^+ \leftrightarrow Lactate^- + NAD^+$$

This reaction regenerates NAD^+ molecules for the continuation of glycolysis and the subsequent formation of two ATP molecules (Judge and Dodd, 2020). In PC, this reaction leads to acidification of the medium, which results in a reduced pH (depending on the buffering capability of the medium).

Under aerobic conditions, pyruvate generated from the glycolytic pathway is transported across the mitochondrial membrane and oxidised by pyruvate dehydrogenase (PDH) to form two molecules of acetyl CoA.

$$\text{Pyruvate} + \text{CoA} + NAD^+ \rightarrow \text{Acetyl CoA} + \text{NADH} + CO_2$$

The acetyl CoA molecules enter the citric acid cycle which harvests energy in the form of the reduced compounds NADH and $FADH_2$. NADH and $FADH_2$ then deposit their electrons into the ETC where they are transported through a series of complexes to the final electron acceptor O_2 (Judge and Dodd, 2020). As the electrons pump through the ETC they cause the release of H^+ into the intermembrane space (Figure 1-5) which drives ATP synthase to produce ATP (OXPHOS). The process of OXPHOS yields 30-32 ATP molecules (Judge and Dodd, 2020).

RTP are stored in a manner that enables them to be metabolically active – they have a medium that contains the substrates for metabolism (predominantly glucose) and are stored at room temperature (20-24^{o}C) with constant agitation, in gas permeable packs, allowing gaseous exchange. However, during storage at room temperature, RTP undergo a decline in function termed the platelet storage lesion, which results in glucose depletion, mitochondrial dysfunction and enhanced glycolysis with increased lactate production, all of which result in acidification of the PC medium and platelet death. It is for this reason that PC have a relatively short shelf life of 5-7 days. Cold storage of platelets slows down metabolism and has been shown to alter metabolic activity, reducing glycolytic metabolism and thus reducing glucose consumption and lactate production (Yang *et al.*, 2018). Despite this, there are still unanswered questions about the extent to which metabolism is reduced in CSP and how this relates to the maximum period of time that CSP can be stored before transfusion. By elucidating the effects of cold storage on platelet bioenergetics, it may be possible to propose a potential shelf life for CSP.

Platelet metabolism can be measured in PC by quantifying analytes that are by-products of metabolism in the extracellular medium; by measuring the function of the ETC via the mitochondrial membrane potential ($\Delta\psi_m$) and through directly measuring the bioenergetic profiles of live, intact platelets through the O_2 consumption rate and the extracellular acidification rate.

4.2 Aims

The aim of this chapter was to study the metabolic profiles of PC following cold storage (4 ± 2 ^{o}C) compared to PC stored under standard room temperature conditions (22 ± 2 ^{o}C) to enable the assessment of the effect of cold storage on platelet metabolism over time. To address these aims the following objectives were met:

- Assess the effects of cold storage on standard platelet metabolic parameters including glucose, lactate, pO2, pCO2, pH and bicarbonate.
- Determine the effect of cold storage on extracellular ATP levels.
- Determine the effect of cold storage on the mitochondrial membrane potential.
- Determine the effect of cold storage on bioenergetic profiles of PC as a measure of mitochondrial function and platelet ability to respond to increased metabolic demands.
- To establish the potential shelf life of PC stored in the cold based on the bioenergetic profile.

4.3 Methods

The methods described in this chapter are summaries of the more detailed methods in Chapter 2.

4.3.1 Glucose, lactate, pO_2, pCO_2 and pH

Glucose, Lactate, pO_2, pCO_2 and pH were performed using an ABL800 blood gas analyser, as described in 2.5.1.2.

4.3.2 Calculation of bicarbonate levels

Bicarbonate levels were calculated from the CO_2 and pH results as described in 2.5.2.2.

4.3.3 ATP levels

ATP levels were measured as described in 2.5.3.1.

4.3.4 Mitochondrial membrane potential ($\Delta\psi_m$)

The mitochondrial membrane potential ($\Delta\psi_m$) was measured using two cationic fluorescent dyes, TMRM and JC-1, as described in 2.5.4.

4.3.5 Bioenergetic profiling

The bioenergetic profile assays 'ATP rate assay' and 'Mito stress test' were performed using an Agilent Seahorse XF HS Mini Analyser as described in 2.5.5.

4.3.6 Statistical analyses

Statistical analyses were performed as described in section 2.6.

4.4 Results

This chapter investigated the difference in metabolic profile and mitochondrial function in PC which were cold stored compared to those stored under standard room temperature conditions. The baseline results shown for all assays are samples of the apheresis unit in PAS on the day of donation (Day 0), prior to the unit being split and stored at the two different temperatures. Only the CSP units were tested on day 21 of shelf life meaning that there is no comparison of results for this day of storage. PC were tested throughout shelf life on day bled (day 0), day 2, day 8, day 14 and day 21. These are referred to in the text as D0, D2, D8, D14 and D21.

4.4.1 Glucose, lactate, pO_2, pCO_2, pH and bicarbonate levels

The electrolytes glucose, lactate, pO_2, pCO_2 and pH were measured using a blood gas analyser and the bicarbonate levels were calculated from the pCO_2 and pH. These are indirect measurements of metabolism that have traditionally been utilised in transfusion science to assess PC function and are recommended by JPAC (JPAC, 2021) for the evaluation of PC produced by new methodologies, for example use of new additive solution or a new storage temperature.

The metabolites glucose and lactate were compared between RTP and CSP at different timepoints (Figure 4-1 A & B). The glucose levels in RTP rapidly dropped during storage from a mean glucose level at baseline of 6.5 mmol/L to 0.8 mmol/L on Day 8. In contrast, glucose levels were well maintained in CSP and significantly higher than for RTP, with mean glucose levels at D14 of 2.5 mmol/L and only dropping to low levels on D21 (0.5 mmol/L). Lactate levels increased throughout storage for both RTP and CSP, with a larger significant increase in RTP compared to CSP, especially on D8 and D14. All results (RTP and CSP) for glucose were significantly lower than baseline, while all results for lactate were statistically higher than baseline results ($p = <0.0001$).

Mean pO_2 (Figure 4-2A) levels increased steadily throughout the period of storage for both RTP and CSP, with CSP showing significantly higher levels at all time points ($p = <0.001$). Mean pCO_2 levels (Figure 4-2B) declined throughout storage for both RTP and CSP with the only significant difference seen between the groups on D2 (p =

0.0025) where CSP has a slightly higher mean pCO_2 (2.36 kPa) compared to RTP (2.59 kPa). All results for pO_2 were significantly higher than baseline, with the exception of the pO_2 results for RTP on D8, while all pCO_2 levels were statistically lower than baseline results (p values shown in Appendix II).

The pH (Figure 4-3A) values were all within range for the JPAC specification for PC at end of shelf life (≥6.4) and remained between a mean of 7.0 and 7.2 throughout shelf life for RTP and for CSP until D14 when a steep decline was observed for CSP to 6.9 and then further to 6.7 by D21. The only significant difference between RTP and CSP was on D14 (p=<0.001). None of the RTP results were significantly different compared to the baseline, whereas all of the CSP results were significantly lower, with the exception of CSP at D2 (p values shown in Appendix II).

Bicarbonate levels (Figure 4-3B) decreased during storage for both RTP and CSP from the baseline mean of 7.82 mmol/L to 4.24 mmol/L on D14 for RTP and to 2.00 mmol/L on D21 for CSP. No significant differences were seen between the two groups although all of the results were significantly lower than the baseline result (p values shown in Appendix II).

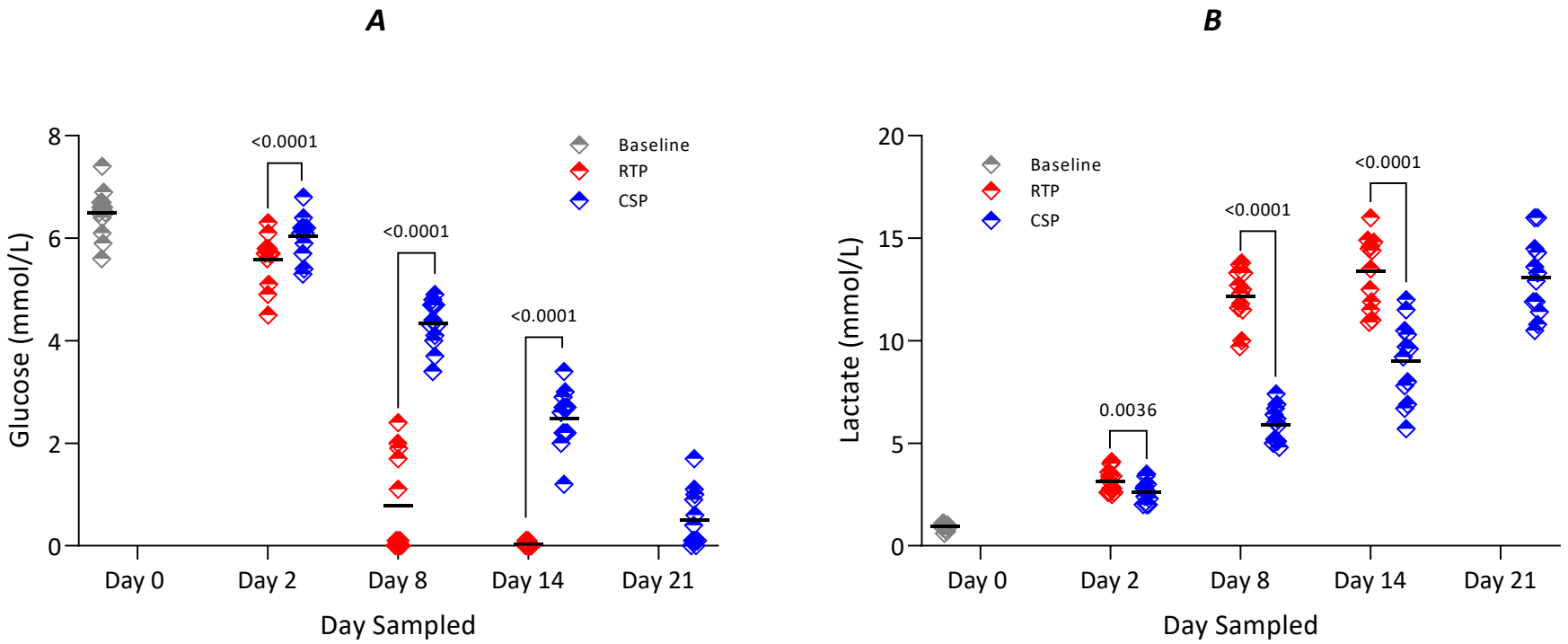

Figure 4-1: Metabolic assay results for Room Temperature Platelets (RTP) and Cold Stored Platelets (CSP). A: Glucose; B: Lactate. Data are expressed as absolute values with the means represented by the black lines. Statistical comparisons were made using the two-way repeated measures ANOVA; p values are presented. $p < 0.05$ was considered significant, $n = 12$.

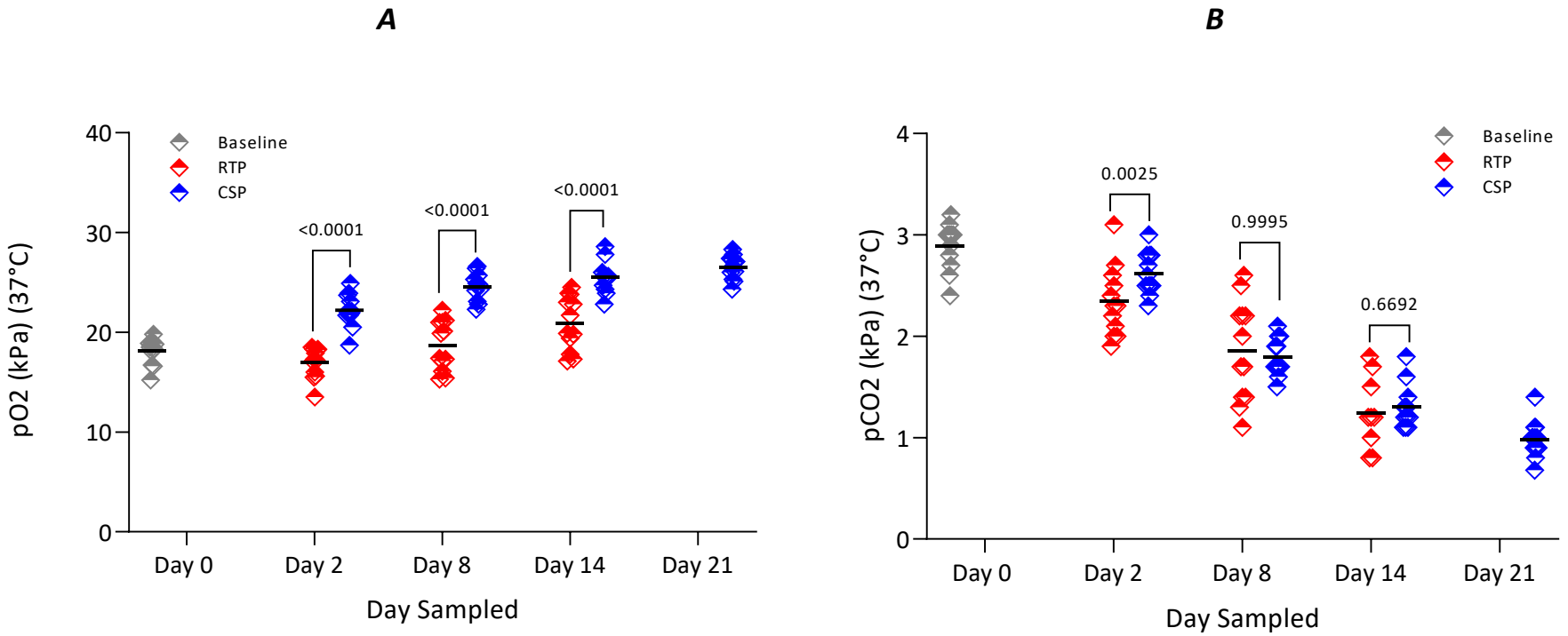

Figure 4-2: Metabolic assay results for Room Temperature Platelets (RTP) and Cold Stored Platelets (CSP). A: pO_2 at 37°C; B: pCO_2 at 37°C. Data are expressed as absolute values with the means represented by the black lines. Statistical comparisons were made using the two-way repeated measures ANOVA test for PO_2 and via Šídák's multiple comparisons analysis for pCO_2; p values are presented. $p < 0.05$ was considered significant, n = 12.

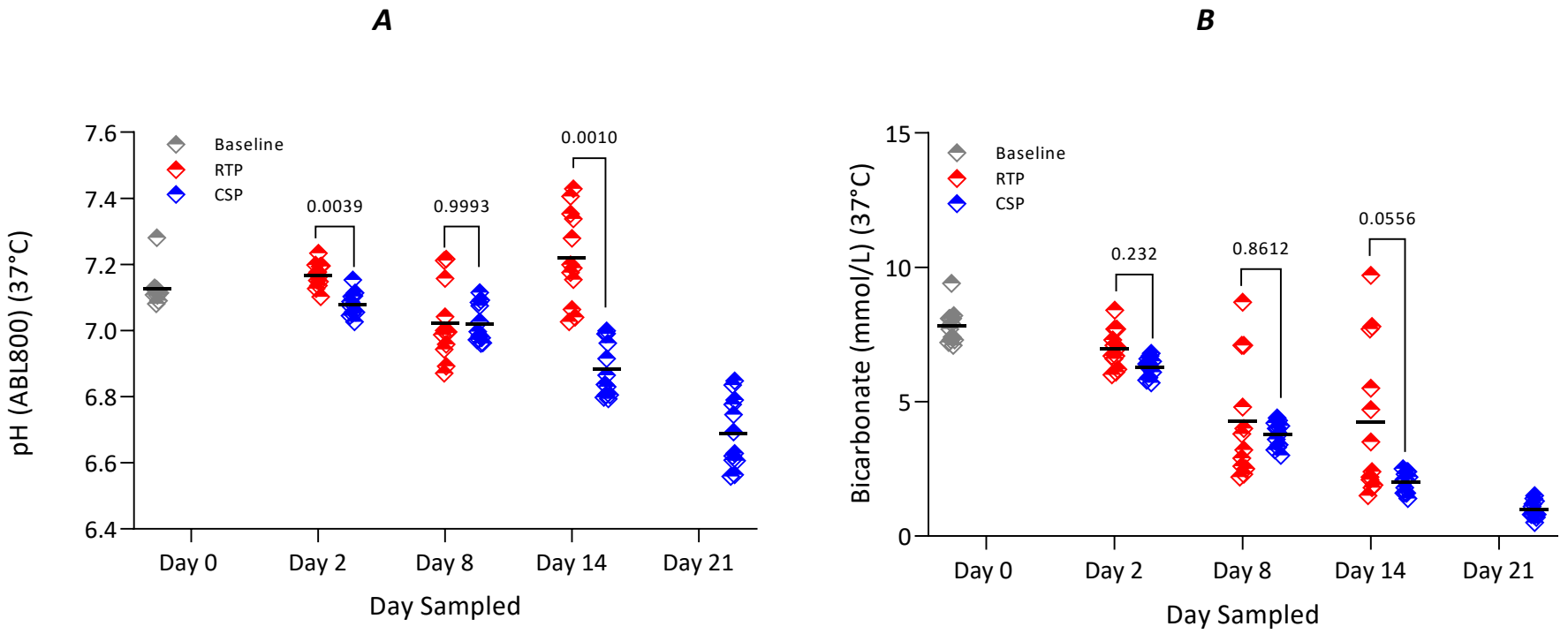

Figure 4-3: Metabolic assay results for Room Temperature Platelets (RTP) and Cold Stored Platelets (CSP). A: pH at 37°C; B: Bicarbonate. Data are expressed as absolute values with the means represented by the black lines. Statistical comparisons were made using the two-way repeated measures ANOVA Bicarbonate and via the Friedman non-parametric test for pH; p values are presented. $p < 0.05$ was considered significant, n = 12.

4.4.2 ATP levels

ATP levels steadily declined throughout storage for both groups (Figure 4-4), with all timepoints measured being statistically significantly different compared to the baseline result, with the exception of D2 RTP (p values shown in Appendix II). Statistically significant lower levels of ATP were initially observed in D2 CSP compared to RTP (2.00 ± 0.59 µmol/10^{11} platelets compared to 2.46 ± 0.54 µmol/10^{11} platelets), with no difference between the two groups by D8. However, by D14, CSP had statistically significantly higher levels of ATP than RTP (1.72 ± 0.45 µmol/10^{11} platelets compared to 1.09 ± 0.52 µmol/10^{11} platelets) (Figure 4-4).

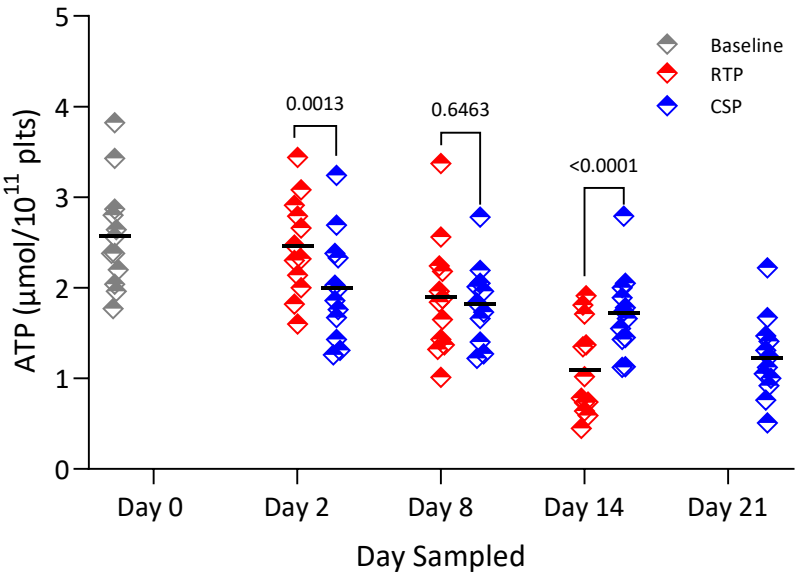

Figure 4-4: ATP level results for Room Temperature Platelets (RTP) and Cold Stored Platelets (CSP). Data are expressed as absolute values with the means represented by the black lines. Statistical comparisons were made using a mixed-effects analysis (Šídák's multiple comparisons test) rather than by repeated measures ANOVA, due to missing values, with test and p values presented. $p < 0.05$ was considered significant, n = 12.

4.4.3 Mitochondrial membrane potential ($\Delta\psi_m$)

Changes in $\Delta\psi_m$, which relate to the platelets' capacity to generate ATP by OXPHOS, were measured in CSP and RTP throughout storage time using the lipophilic cationic dyes TMRM and JC-1. An increase in the $\Delta\psi_m$ leads to a greater accumulation of the positively charged dyes within the mitochondrial matrix.

Figure 4-5 shows the uptake of TMRM and JC-1 during the storage time of the study, with changes in the $\Delta\psi_m$ expressed as percentage of TMRM fluorescence emitting

cells (Figure 4-5A) and the percentage of cells with JC-1 aggregates (Figure 4-5B). It was not possible to perform statistical analysis on the comparison of RTP and CSP TMRM results due to missing values in the data set. However, a decline in $\Delta\psi_m$ (expressed as TMRM % positive platelets) was observed between D8 and D14 for both RTP and CSP. The mean values are similar for both RTP and CSP groups for D2 and D8 whereas on D14, the mean for RTP is lower (approximately 63% of cells positive for TMRM) than for CSP (approximately 77% of cells positive for TMRM) and of a similar level to CSP at D21 (approximately 64% positive). The only significant difference between the results and the baseline result was for CSP on D21, which was significantly lower ($p=0.0082$, all p values shown in Appendix II).

No statistically significant differences were observed between the RTP and CSP groups (Figure 4-5B) for the JC-1 samples. However, there was more of a downward trend observed throughout storage for RTP than CSP with the mean % JC-1 positive cells for RTP on D14 being approximately 62% whereas for CSP, the mean result was approximately 86%. The results for RTP D14 ($p = 0.0002$) and CSP D14 ($p = 0.0002$) and D21 ($p = <0.0001$) were all significantly lower than the baseline results.

A CCCP challenge test was run alongside each control with the aim of demonstrating successful disruption of the ETC, showing that the dye does not bind independently to the mitochondria in any detectable amount (Perry *et al.*, 2011). Unfortunately, these challenge tests did not work as intended with some changes in dot plots visualised but not clear evidence that the $\Delta\psi_m$ was completely depolarised. As a result of this the dot plots for each day throughout storage were analysed using the D0 gating strategy for the unit to ensure that changes between the storage days could be detected.

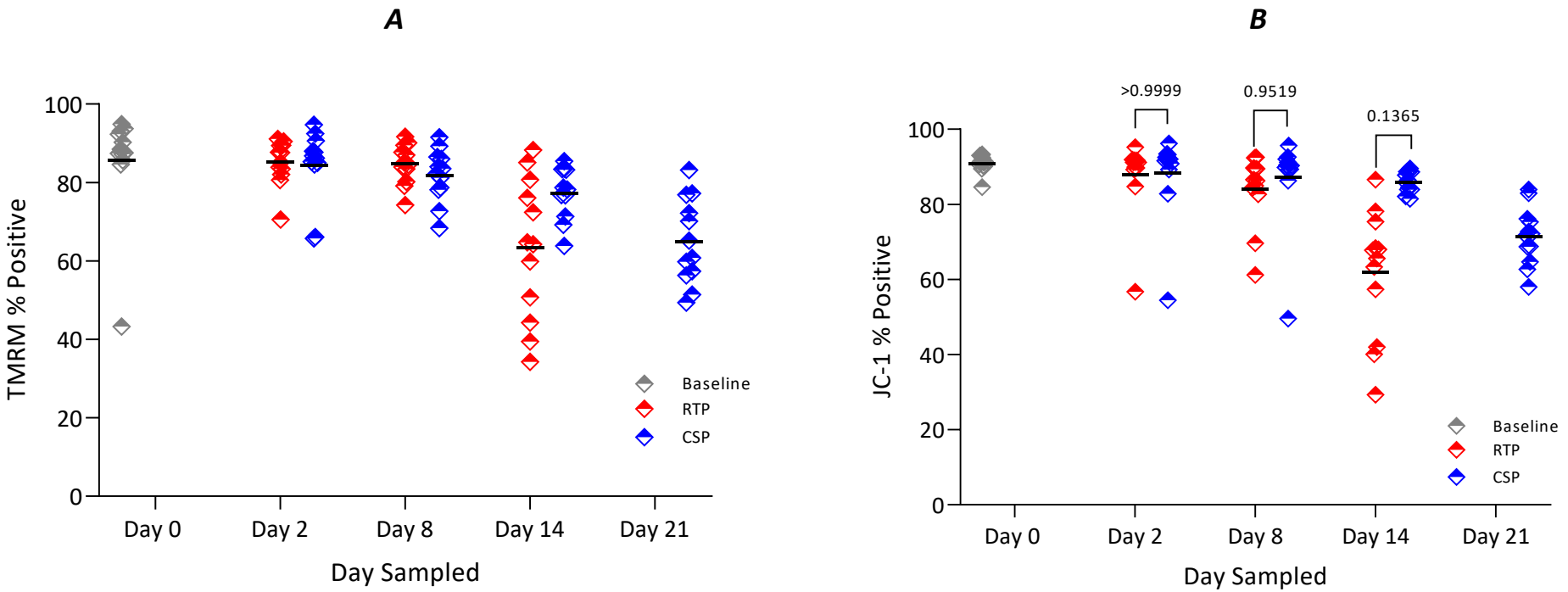

Figure 4-5: Mitochondrial Membrane Potential ($\Delta\psi_m$) results for Room Temperature Platelets (RTP) and Cold Stored Platelets (CSP).A: Percentage of TMRM fluorescence emitting cells. B: Percentage of cells with JC-1 aggregates. Data are expressed as absolute values with the means represented by the black lines. Statistical comparisons were made using the Friedman non-parametric test for JC-1 and p values are presented. $p < 0.05$ was considered significant. Unable to perform two-way ANOVA on TMRM as data not normal unable to perform other statistical analysis (Friedman test) due to one missing value, n = 12.

4.4.4 Bioenergetic profiling

The bioenergetic profiles of RTP and CSP were determined throughout storage time using the Agilent Seahorse XF HS Mini Analyser.

4.4.4.1 Mito stress test

The mito stress test (MST) measures the oxygen consumption rate (OCR) of live platelets from PC and how they respond to the sequential addition of the modulators of respiration oligomycin, FCCP and rotenone/antimycin A. A representative example of the graphical results for RTP and CSP from one of the donations in the study following the addition of the modulators is shown in Figure 4-6. In the example shown in this figure, it can be seen that at D2 mitochondrial respiration (OXPHOS) is similar in RTP and CSP with the basal respiration being slightly higher in the CSP and the maximal respiratory capacity being slightly higher in the RTP.

Throughout storage it can be seen that basal respiration and maximal respiration start to separate between the two groups with CSP having a greater basal and maximal respiratory capacity than RTP in this sample.

A downward trend in basal respiration was observed throughout storage in both RTP and CSP (Figure 4-7A), with CSP appearing to have a higher rate than RTP, although no significant difference is seen between the two data sets. When comparing the mean results to the mean baseline result (D0) the only significant differences were seen in RTP at D14 ($p=0.0413$) and CSP at D21 ($p=0.0060$) (all p values shown in Appendix II).

A downward trend was also observed in ATP production coupled respiration for both RTP and CSP throughout storage from D2, with CSP values appearing to be higher than RTP (Figure 4-7B). The only statistically significant value is the difference between RTP and CSP on D2 where the RTP value is 31 ± 23 pmol/min and the CSP value is 49 ± 28 pmol/min. When comparing the mean results to the mean baseline result (D0) the only significant differences were seen in RTP at D14 ($p=0.0238$) and CSP at D21 ($p=0.0124$) (all p values shown in Appendix II).

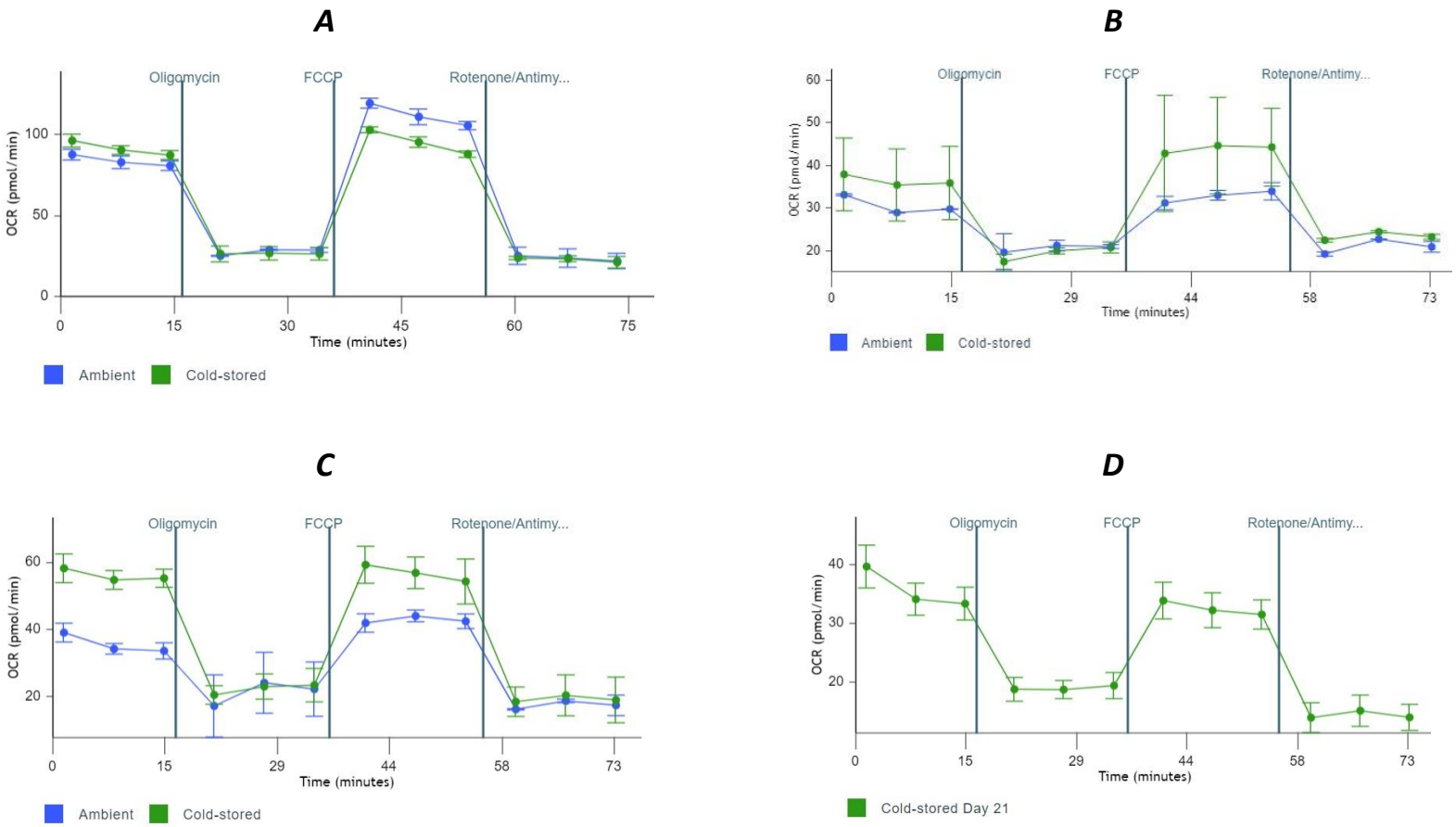

Figure 4-6: A representative example of the comparison of mitochondrial respiration in Room Temperature Platelets (RTP) and Cold Stored Platelets (CSP) throughout storage following injection of the modulators of respiration: oligomycin, FCCP and rotenone/antimycin A. ***A****: Day 2;* ***B:*** *Day 8;* ***C:*** *Day 14;* ***D:*** *Day 21. Once the basal rate of respiration is established, oligomycin is injected. This inhibits ATP synthase and allows the rate of ATP-linked production to be estimated. The injection of FCCP dissipates the Δp and enables the maximum activity of the ETC. Finally, the inhibitors of complex I and complex III (rotenone & antimycin A) are injected to halt electron transfer through the ETC, correcting for O_2 consumption from non-mitochondrial oxidases. Ambient = RTP, Cold-stored = CSP.*

No statistically significant differences were seen between RTP and CSP for the maximal respiration rate (Figure 4-8A) throughout storage although CSP appear to have slightly higher levels than RTP, with both groups observing a slight downward trend throughout storage. When comparing the mean results to the mean baseline result (D0) the only significant difference was seen in CSP at D21 ($p=0.0141$, all p values shown in Appendix II).

The data for proton leak showed no statistically significant differences between RTP and CSP (Figure 4-8B) although the results for CSP appear to be slightly higher than RTP at all timepoints and particularly at D2. When the mean results were compared to the baseline result (D0) there were no significant differences seen in either RTP or CSP (all p values shown in Appendix II).

No statistically significant differences were seen in the spare respiratory capacity (SRC) of RTP compared to CSP throughout storage (Figure 4-9A) with both groups showing a downward trend with storage time and significant differences were seen when comparing the mean results to the mean baseline result (all p values shown in Appendix II).

The non-mitochondrial OCR showed a slight downward trend throughout storage for both RTP and CSP with no statistical difference between the two arms (Figure 4-9B). In addition, when the mean results at each timepoint were compared to the mean baseline result, no statistical differences were observed (all p values shown in Appendix II).

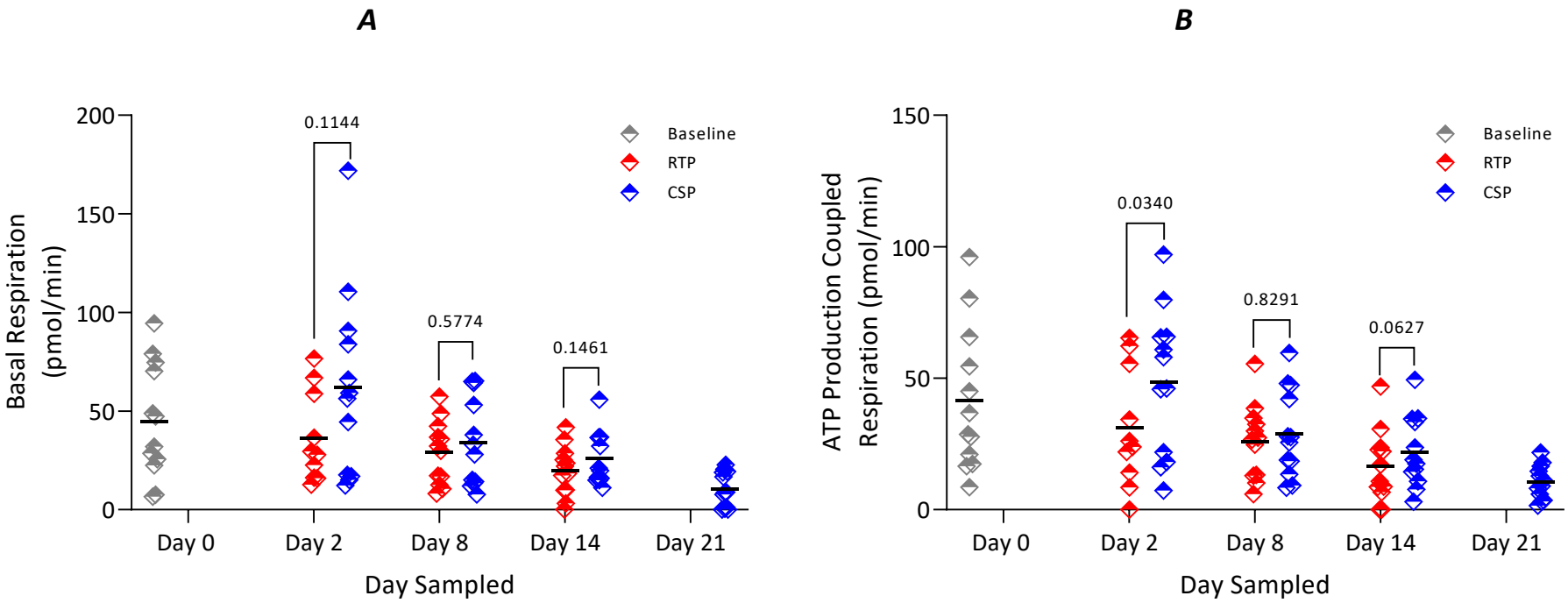

Figure 4-7: Mito stress test assay results of platelet concentrations in Room Temperature Platelets (RTP) and Cold Stored Platelets (CSP).A: Basal respiration B: ATP production coupled respiration. Data are expressed as absolute values with the means represented by the black lines. Statistical comparisons were made using a mixed-effects analysis (Šídák's multiple comparisons test) rather than by repeated measures ANOVA due to missing values with test and p values presented. $p < 0.05$ was considered significant, $n = 12$.

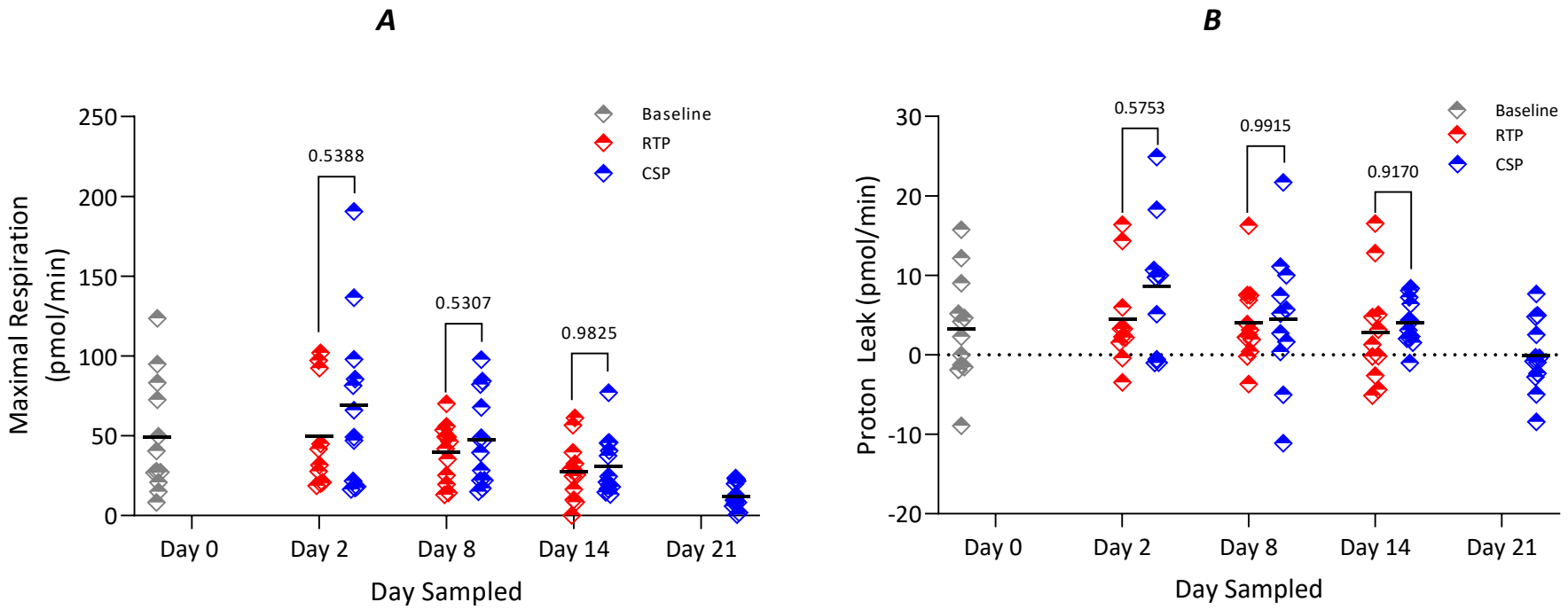

Figure 4-8: Mito stress test assay results of platelet concentrations in Room Temperature Platelets (RTP) and Cold Stored Platelets (CSP).A: Maximal respiration B: Proton Leak. Data are expressed as absolute values with the means represented by the black lines. Statistical comparisons were made using a mixed-effects analysis (Šídák's multiple comparisons test) rather than by repeated measures ANOVA due to missing values with test and p values presented. $p < 0.05$ was considered significant, $n = 12$.

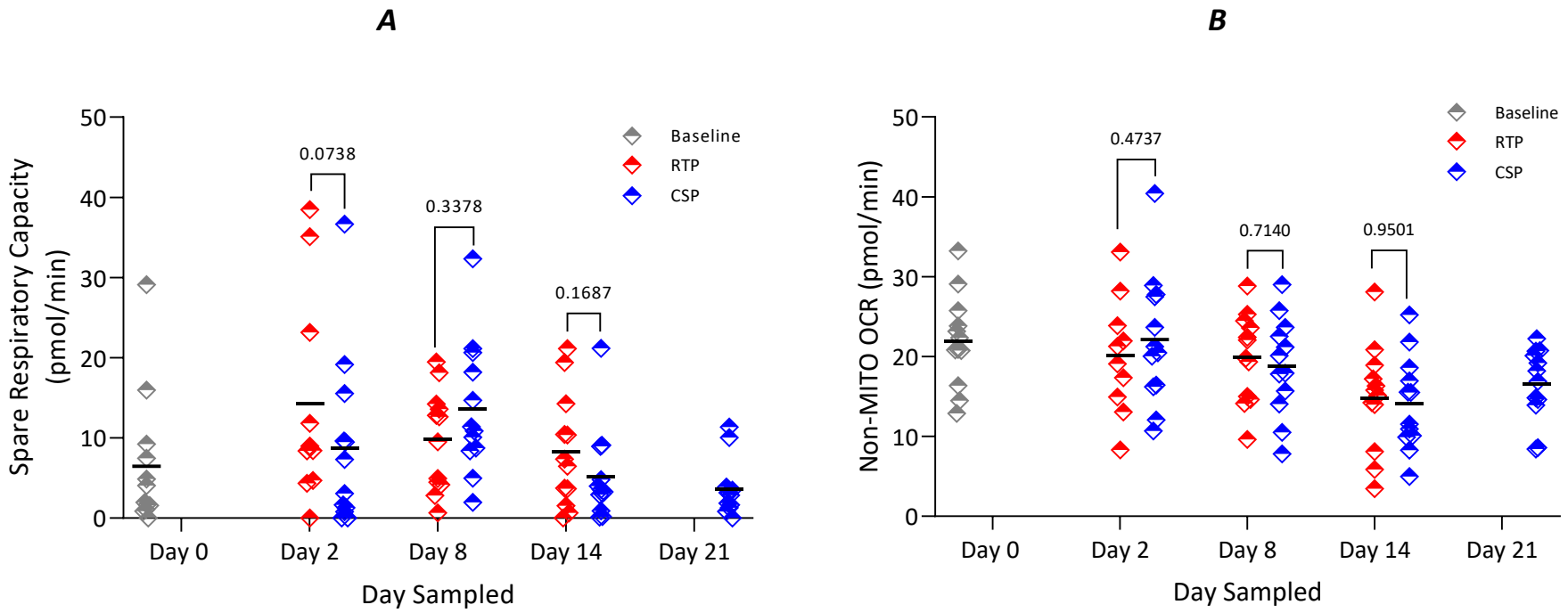

Figure 4-9: Mito stress test assay results of platelet concentrations in Room Temperature Platelets (RTP) and Cold Stored Platelets (CSP). A: Spare Respiratory Capacity B: Non-mitochondrial OCR. Data are expressed as absolute values with the means represented by the black lines. Statistical comparisons were made using a mixed-effects analysis (Šídák's multiple comparisons test) rather than by repeated measures ANOVA due to missing values with test and p values presented. $p < 0.05$ was considered significant, $n = 12$.

4.4.4.2 ATP Rate Assay

The XFp Real-Time ATP Rate Assay (Agilent Technologies, Texas, USA) measures the cellular rate of ATP production through the flux of both H^+ production (ECAR) and O_2 consumption (OCR) and is able to distinguish between the fractions of ATP that are produced from mitochondrial OXPHOS and glycolysis.

Figure 4-10 shows the total ATP production rate of RTP compared to CSP throughout storage. There is a downward trend in the ATP production rate in the RTP group throughout storage, whereas CSP reduced from baseline to D8 before rising again slightly at D14. The only significant difference between RTP and CSP was seen on D14 where the ATP production rate is higher in the CSP group than the RTP group. When comparing the mean results to the mean baseline result (D0), other than the D2 CSP all of the results were significantly lower, with the strongest significance seen in RTP D14 (p=0.0001) and CSP D21 (p=<0.0001) (all p values shown in Appendix II).

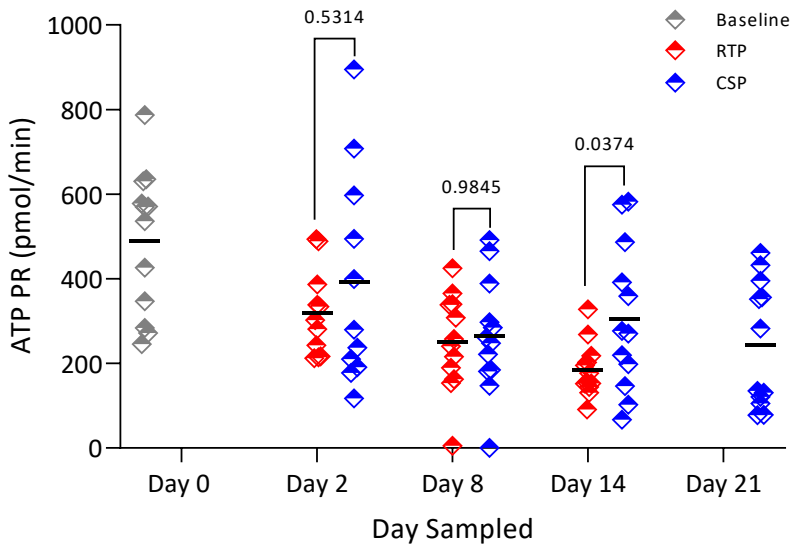

Figure 4-10: ATP Production Rate (PR) assay results of platelet concentrations in Room Temperature Platelets (RTP) and Cold Stored Platelets (CSP). Data are expressed as absolute values with the means represented by the black lines. Statistical comparisons were made using a mixed-effects analysis (Šídák's multiple comparisons test) rather than by repeated measures ANOVA due to missing values with test and p values presented. $p < 0.05$ was considered significant, n = 12.

Figure 4-11A shows the MITO ATP production rate of RTP compared to CSP throughout storage. There is a downward trend in the MITO ATP production rate in both groups throughout storage, with CSP showing slightly larger mean results than

RTP. Due to data not being a normal distribution and missing values in the dataset, no statistical analysis could be performed between the groups. However, the mean results were compared to the mean baseline result (D0) - other than the D2 CSP and D2 RTP, all of the results were significantly different from the baseline with the strongest significance seen in RTP D14 ($p=0.0004$) and CSP D21 ($p=<0.0002$).

Figure 4-11B shows the GLYCO ATP production rate of RTP compared to CSP throughout storage. There is a slight downward trend in the ATP production rate in the RTP group throughout storage, whereas the CSP group drops slightly from D2 to D14 before rising to higher than the baseline on D14. Due to data not being normally distributed and missing values in the dataset, no statistical analysis could be performed between the groups. The mean results were compared to the mean baseline result (D0) and no significant difference was seen between any storage timepoint and the baseline.

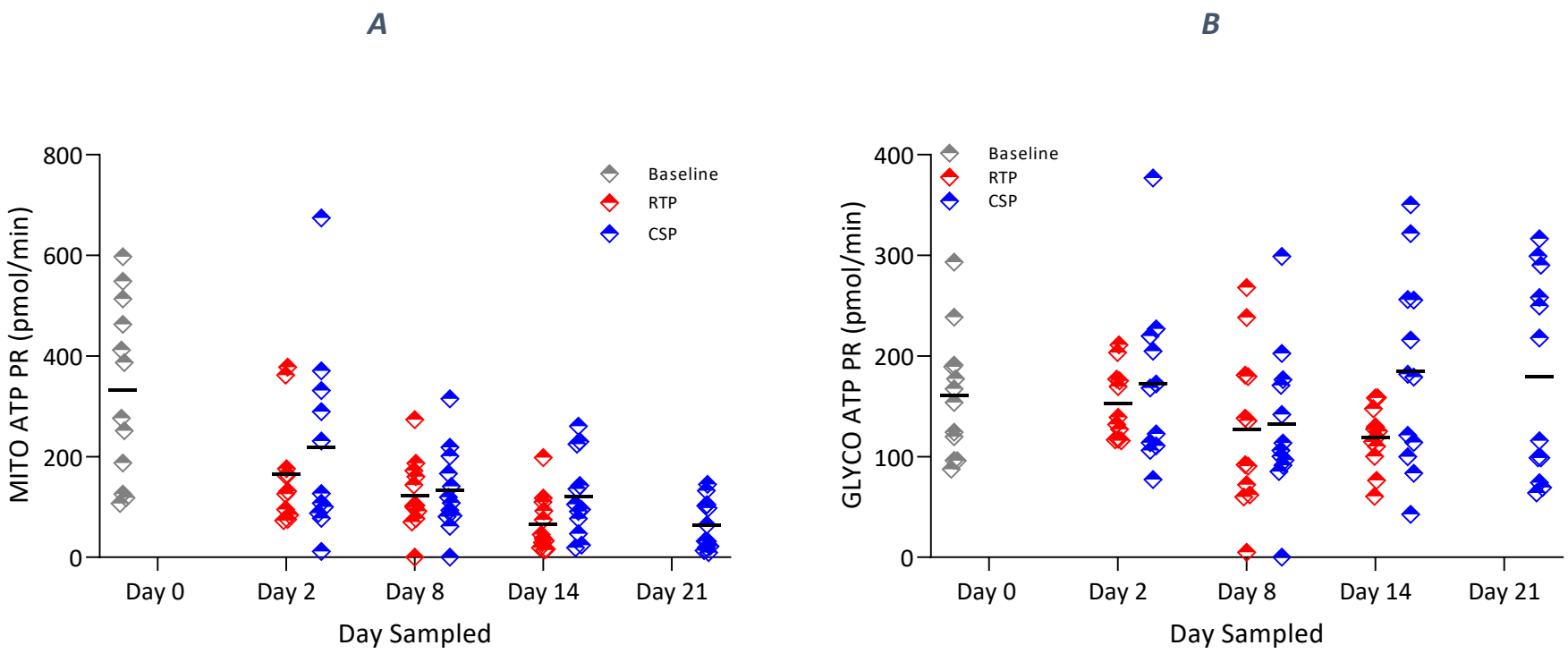

Figure 4-11: ATP Production Rate (PR) assay results of platelet concentrations in Room Temperature Platelets (RTP) and Cold Stored Platelets (CSP).A: MITO ATP PR; B: GLYCO ATP PR. Data are expressed as absolute values with the means represented by the black lines. Unable to perform statistical analysis on MITO ATP PR and GLYCO ATP PR as data not normal and unable to perform non-parametric test due to missing values in data, no p values shown, n = 12.

The ATP production rate of RTP and CSP during storage are also represented as a histogram of the mean results for each storage timepoint, with the SD shown as error bars (Figure 4-12A). The total amount of ATP being produced per minute for RTP shows a statistically significant decline during storage (D2, $p = 0.0499$, D8, $p = 0.0076$, D14, $p = 0.0001$) whereas the rate of ATP production is higher at all timepoints in the CSP group (although only statistically significantly higher at D14), and although ATP production is lower than baseline, it is not a significant decline by D2 ($p = 0.6352$). A significant decline is seen in the subsequent CSP storage days (D8, $p = 0.0166$, D14, $p = 0.0226$, D21, $p = <0.0001$) compared to baseline although overall the levels appear better maintained than RTP with a statistically significantly higher level of ATP production at D14. In addition, the D21 CSP ATP mean rate is similar to the D8 RTP ATP rate.

The percentage of ATP produced at each timepoint for RTP and CSP that is derived from mitochondrial respiration (OXPHOS) and from glycolysis is represented in histogram Figure 4-12B. The percentage of ATP that is produced by mitochondrial respiration reduces in both RTP and CSP throughout storage. Both groups start with an approximately 50:50 split of mitochondrial and glycolytic ATP production at D2 and move to a predominantly glycolytic phenotype throughout storage. Mitochondrial respiration in CSP appears to be slightly better conserved by D14 than RTP with approximately 35% of RTP ATP production being produced form OXPHOS compared to 45% in CSP at the same timepoint.

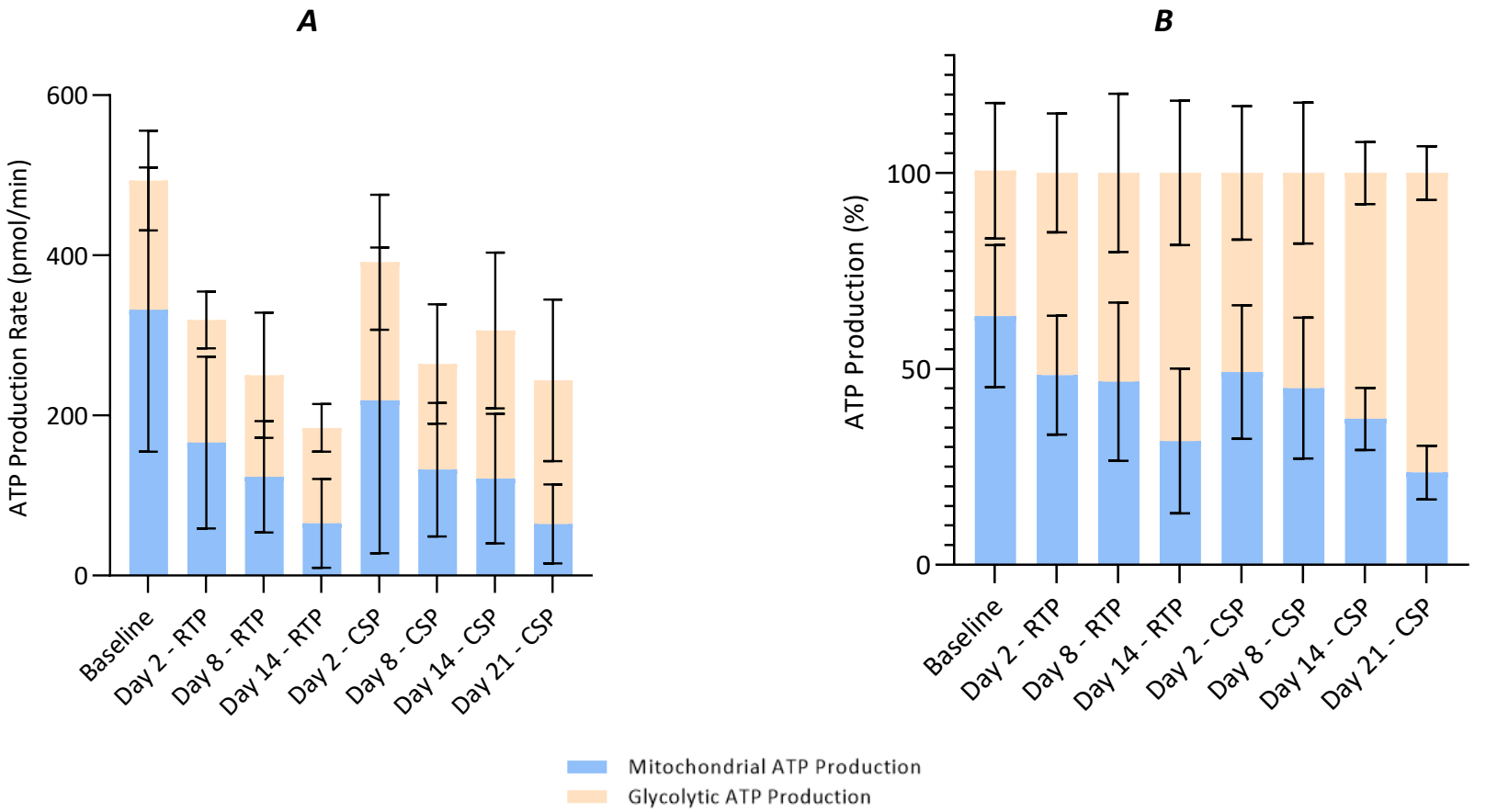

*Figure 4-12: Proportion of ATP that is derived from the mitochondrial pathway and the glycolytic pathway. **A:** Mean ATP production rates for the mitochondrial and glycolytic pathways for RTP and CSP during storage. **B:** Mean results for the % of ATP production that is from the mitochondrial and the glycolytic pathways for RTP and CSP during storage. Error bars demonstrate the SD of the results, n = 12.*

4.5 Discussion

The aim of this chapter was to investigate the impact of prolonged cold storage (4 ± 2°C) on platelet metabolism, compared to the current standard PC product that is stored at room temperature (22 ± 2°C), with gentle agitation. A paired study design was utilised with double apheresis PC donations split into two separate adult therapeutic doses, one stored at 4 ± 2°C and one at 22 ± 2°C with gentle agitation. The units were sampled and tested throughout storage on days 0, 2, 8 and 14 (with CSP also being tested on day 21) to assess their metabolic ability. Metabolism of the platelets within the PC was examined through indirect/endpoint assays measuring metabolites (glucose/lactate) and by-products of metabolism (O_2/CO_2 and bicarbonate), through direct measurement of the ability of mitochondria to function and through direct measurement of the bioenergetic profiles of the live platelets.

Stored PC metabolize glucose by breaking it down into pyruvate which either enters the glycolytic pathway in the absence of sufficient O_2, resulting in lactate formation and free hydrogen ions or in the presence of O_2 enters the electron transport chain, generating ATP through OXPHOS.

The glucose and lactate results from this study suggest that the storage of PC at 4°C ± 2°C significantly reduces metabolism compared to storage at 22 ± 2°C. Glucose levels in RTP drop rapidly during storage from a mean glucose concentration of 5.6 ± 0.5 mmol/L on D2 to a mean glucose concentration of 0.8 ± 1.0 mmol/L on D8 (with 4/12 results having no detectable glucose) and a mean concentration of 0.0 ± 0.0 mmol/L by D14. Conversely, glucose levels remain high in CSP throughout storage until D14 with a dip seen on D21 with a mean glucose concentration of 0.5 ± 0.6 mmol/L (2/12 results had no detectable glucose at D21).

These findings are in accordance with other studies on CSP (Sandgren *et al.*, 2007; Yang *et al.*, 2018; Getz *et al.*, 2016; Reddoch-Cardenas *et al.*, 2019b) and demonstrate that platelets in RTP are significantly more metabolically active than platelets in CSP. This is further supported by the lactate results which rise throughout storage in both groups but are significantly higher in RTP compared to CSP. Lactate is a by-product of glycolysis, and its increase is concomitant with increased glycolytic turnover,

suggesting that significantly more glycolysis is occurring in RTP compared to a CSP. It has been demonstrated that PC with a reduced lactate production during storage have an increased lifespan compared to those with high lactate production (Murphy and Gardner, 1969; Paulus *et al.*, 1981).

When PC are stored in 100% plasma, the accumulation of lactate has a direct effect on the pH, as free hydrogen ions (H^+) are produced when pyruvate is broken down to lactate in glycolysis. These H^+ ions are buffered by bicarbonate in the plasma which binds to them, creating carbonic acid (H_2CO_3) which in turn is converted into CO_2 (extruded through the gas permeable pack) and H_2O (Nash, Saunders and George) in the following reversible equation:

$$CO_2 + H_2O \longleftrightarrow H_2CO_3 \longleftrightarrow HCO_3^- + H^+$$

Due to the gas permeable nature of the pack with CO_2 being drawn out of the pack, the equation is driven towards CO_2 generation and bicarbonate breakdown.

Bicarbonate levels decreased throughout storage in both RTP and CSP, as it performed its buffering function, binding to H^+ produced during glycolysis, but with no statistically significant difference seen between the two groups. When all of the bicarbonate is exhausted in a PC, H^+ accumulates and results in the pH falling to levels that affect the functional ability of the platelets (Farrugia, 1994). The buffering capability in both CSP and RTP were maintained in this study with the pH of all PC, at all timepoints, meeting the JPAC criteria for pH_{22oC} at end of storage of ≥ 6.4. This is likely due to the additional buffering capacity of acetate in the PAS which is oxidised by platelets under storage into acetic acid, producing bicarbonate ions in the process (Bertolini *et al.*, 1992) and also due to the buffer, phosphate, in the PAS (T-PAS+) (Nash, Saunders and George).

The measurement of pH is used to determine the acid-base balance of PC. Below a level of pH 6.4, platelets within PC undergo morphological alterations which affect their viability *in vivo* (Farrugia, Baron and Zammit, 2023) and should not be transfused. A decline in pH was observed in CSP throughout storage, from 7.1 ± 0.0 on D2 to 6.7 ± 0.1 by D21 and were statistically significantly lower than RTP on D2

and D14, despite the lactate levels being significantly lower than RTP at these time points (and therefore pH expected to be lower). It was unexpected that CSP would have a lower pH than RTP as it suggests that cold storage had not reduced metabolism, although similar findings have been demonstrated by others (Farrugia, Baron and Zammit, 2023; Braathen *et al.*, 2019; Johnson *et al.*, 2016). The lower pH in CSP could be linked to the concentration of the buffer bicarbonate in CSP which appears to decline at a greater rate than in RTP (Figure 4-3) although the difference between the two groups was not significant. In addition, the PAS used in this study was validated by the manufacturer for use in RTP, not CSP, so it may be that the buffering capacity of the solution is reduced at lower temperatures. pH levels can also be affected by bacterial contamination as microorganisms carry out metabolic reactions which produce CO_2 as an acidic by-product (Farrugia, Baron and Zammit, 2023). Sterility testing was performed on all units at the end of the study and no bacterial contamination was detected, so it was unlikely that this would be the cause of the lower pH.

It is important to note however that all PC in this study had a pH ≥ 6.4 and therefore would have been suitable for transfusion under JPAC guidelines (JPAC, 2021).

The RTP consumed more O_2 than the CSP, with significantly higher levels of pO_2 in CSP at all timepoints measured. This correlates with other studies (Sandgren *et al.*, 2007) (Lorusso *et al.*, 2023) and suggests that more OXPHOS is occurring in RTP than CSP, consuming more O_2. It is interesting to note that the pO_2 levels measured in CSP were above atmospheric O_2 levels (21kPa (Carreau *et al.*, 2011)) from D2 onwards, rising to a high of 26.5 kPa ± 1.2 by D21. The high pO_2 levels may be at least partially due to the higher solubility of oxygen at lower temperatures (Christmas and Bassingthwaighte, 2017). This suggestion was confirmed by an additional experiment that measured pO_2 levels in the additive solution, stored in isolation in a gas-permeable platelet storage pack (results not shown). CO_2 levels decreased during storage in both groups, with the only significant difference being at D2, where CSP was significantly higher than RTP.

ATP levels decreased throughout storage in both RTP and CSP, suggesting that metabolism of the platelets reduces throughout shelf life, producing less ATP, which

is in line with the increase of O_2 and decrease in CO_2 seen in this study throughout storage. Initially RTP platelets produced more ATP than CSP at D2 (2.46 ± 0.54 µmol/10^{11} platelets compared to 2.00 ± 0.59 µmol/10^{11} platelets) which suggests that RTP are more metabolically active early in shelf life, generating more ATP. However, by D14 of storage, the level of ATP produced by CSP is higher than that for RTP (1.72 ± 0.45 µmol/10^{11} platelets compared to 1.09 ± 0.52 µmol/10^{11} platelets) which is likely to be due to many of the platelets in RTP being dead by D14 and no longer metabolising. This is the same pattern seen by Sandgren and colleagues (Sandgren *et al.*, 2007) who demonstrated CSP ATP levels to be 3.61 ± 0.28 µmol/10^{11} platelets on D14 and RTP ATP levels to be 1.69 ± 0.32 µmol/10^{11} platelets by D14.

Changes to the $\Delta\psi_m$ during storage at different temperatures were measured using two different fluorophores, TMRM and JC-1. Although missing values in the dataset prevented statistical analysis, the $\Delta\psi_m$ appeared to be well maintained in both groups on D2 and D8 with no statistical difference observed from the baseline and the results were maintained between 82-85% positive during D2 and D8 for TMRM.

A loss of $\Delta\psi_m$ (depolarisation) was observed at D14 in both groups, which was more severe in RTP (approximately 63% positive for TMRM) compared to CSP (approximately 77% positive for TMRM). This was mirrored in the JC-1 $\Delta\psi_m$ results where there was no statistically significant difference between RTP and CSP at any time point but the results at D14 suggest that RTP had a lower % of JC-1 positive cells (approximately 62%) compared to CSP (approximately 86%). It may be that statistical significance was not observed between these results due to the large spread of the data for RTP, whereas the CSP were all consistently of a similar value with minimal data spread (Figure 4-5). In addition, the D21 CSP results showed a large significant decline from baseline in both TMRM (baseline 86%, D21 65%) and JC-1 (baseline 91%, D21 71%), suggesting that the mitochondria in D21 CSP are not functioning as well. Stolla and colleagues performed a similar experiment comparing RTP and CSP in plasma that demonstrated a markedly reduced $\Delta\psi_m$ using JC-1 that remained significant up to day 20 of storage for CSP (Stolla *et al.*, 2020).

A similar pattern was seen in the results for the total ATP levels where a statistically significant drop in RTP levels compared to CSP was observed at D14 (Figure 4-4). This

suggests that there is increasing depolarisation of mitochondria in RTP by D14 with loss of function, followed by a reduction in the amount of ATP produced through the ETC on the inner mitochondrial membrane. This depolarisation may result from the formation of the mitochondrial permeability transition pore which reduces the potential for ATP synthesis (Shimizu *et al.*, 2001).

In addition, decreased $\Delta\psi_m$ has been directly linked to PS exposure (Leytin *et al.*, 2004) (Cookson *et al.*, 2010) which is seen in this study (Figure 3-7) where there is a significant increase in % Annexin V binding by D14 of storage. Although there is not a significant difference between RTP and CSP (again possibly due to the large spread of RTP data), the value of % Annexin V on RTP at D14 is higher than that for CSP (approximately 43% compared to 31%).

It has been demonstrated previously (Verhoeven *et al.*, 2005) that decreases in platelet $\Delta\psi_m$ correlate with an increase in lactate production, as was observed in this study. It is likely that when the $\Delta\psi_m$ becomes depolarised during storage, the platelets begin to switch from OXPHOS to glycolysis, to compensate for the decrease in mitochondrial ATP production, resulting in lactate production as the end product (Verhoeven *et al.*, 2005) as borne out by our results.

Loss of $\Delta\psi_m$ is known to occur in prolonged storage of RTP (Leytin *et al.*, 2008; Verhoeven *et al.*, 2005) but there are limited studies on depolarisation of the $\Delta\psi_m$ in CSP. Johnson and colleagues (Johnson *et al.*, 2016) determined $\Delta\psi_m$ using the red-orange dye tetramethylrhodamine (TMRE) and found that the $\Delta\psi_m$ of CSP (in 100% plasma) was more depolarised compared to RTP (in 100% plasma). However, Reddoch-Cardenas and colleagues have more recently shown (Reddoch-Cardenas *et al.*, 2021) with CSP and RTP in PAS, stained with the dye 3, 3'-dihexyloxacarboncynanine iodide ($DIOC_6$) that the mitochondria in both RTP and CSP become increasingly depolarised during storage for 15 days and that RTP are depolarised to a greater extent than CSP; similar results to those seen in this study.

Mitochondrial function was further assessed in RTP and CSP using the Seahorse XF analyser to quantify mitochondrial function and perform bioenergetic profiling. The Seahorse utilised intact platelets rather than isolating individual mitochondria from

the platelets as performed in other techniques, thus providing greater physiological relevance and an undisturbed cellular environment, with none of the artefacts generated through isolation (Brand and Nicholls, 2011).

The Oxygen Consumption Rate (OCR) was measured using fluorophores to assess energy metabolism due to the coupling of ATP synthesis and oxygen consumption during OXPHOS. The basal respiration rate is strongly controlled by mitochondrial phosphorylation (ATP turnover) and partly by proton leak, where the inner membrane is permeable to protons, resulting in some of the $\Delta\psi_m$ generated by oxidation reactions being dissipated by protons 'leaking' back across the mitochondrial inner membrane without yielding ATP (Ainscow and Brand, 1999), uncoupling the respiratory chain activity from ATP production (Divakaruni *et al.*, 2014).

In this study, there was no statistically significant differences observed between the basal respiration rate of RTP and CSP at any timepoint, although a significant decline was observed in D14 RTP (20 ± 13 pmol/min compared to 45 ± 29 pmol/min, 56% decline) and D21 CSP (10 ± 9 pmol/min compared to 45 ± 29 pmol/min, 78% decline) from the baseline result, suggesting that respiration in the PC was reduced by these timepoints.

Measurement of the respiratory rate after the addition of the ATP synthase inhibitor, oligomycin, enabled direct measurement of the portion of the basal respiration rate that was due to proton leak (Figure 2-13 and Figure 4-8). Protons continuously 'leak' back across the mitochondrial inner membrane, consuming the membrane potential in a manner that is independent of ATP synthesis and as such is sometimes referred to as 'inefficient respiration'. In physiological conditions proton leak is minimal but a significant increase can indicate mitochondrial membrane damage (Braganza, Annarapu and Shiva, 2020). No significant difference was observed between RTP and CSP or between the mean results at each timepoint compared to the baseline result. Several negative results were observed in the data. As proton leak is calculated from (Minimum rate measurement after Oligomycin injection) – (Non-Mitochondrial Oxygen Consumption), this suggests that there has been either a lack of complete inhibition following Rot/AA injection, resulting in a higher non-mitochondrial oxygen consumption or

an over inhibition from oligomycin which could both be collectively underpinned by dysfunctional or damaged mitochondria in the preparation. In the case of the non-mitochondrial oxygen consumption a significant switch from mitochondrial sources when examining the levels post Rot/AA cannot be discounted. The results could also be due to an artefact or idiosyncrasy of the protocol or equipment.

Through measuring the decrease in respiration after inhibition of ATP synthase, the rate of mitochondrial ATP synthesis (ATP production coupled respiration) could be derived (Brand and Nicholls, 2011). As with the basal respiration rate, no statistically significant difference was observed between RTP and CSP throughout storage, although a significant decrease was observed in RTP D14 (17 ± 14 pmol/min compared to 41 ± 28 pmol/min, 59% decline) and CSP D21 (11 ± 6 pmol/min compared to 41 ± 28 pmol/min, 73% decline) as with the basal respiration measurement. This decline could be due to mitochondrial death/dysfunction due to aging although a corresponding significant increase in proton leak was not seen as an indicator of mitochondrial membrane damage.

The basal rate of respiration does not reflect the ability of platelet respiration to respond to an increased energy demand, for example during platelet activation. In order to estimate the maximum respiratory capacity of platelets in the PC, the uncoupler FCCP was added, which allows protons re-entry to the mitochondrial matrix, dissipating the Δ*p*, resulting in maximal activity of the ETC to maintain the protonmotive force and an uncoupling of respiratory chain activity from ATP synthesis (Divakaruni *et al.*, 2014). No statistically significant difference was observed between RTP and CSP throughout storage, although a significant decline in CSP at D21 was observed compared to the baseline result (12 ± 8 pmol/min compared to 49 ± 36 pmol/min, 76% decline), suggesting that CSP have a reduced ability to increase their energy requirements on demand by D21.

This was not however mirrored in the results for spare respiratory capacity which showed no statistical difference between the two groups (RTP and CSP) or any statistical difference between the different timepoints and the baseline, including D21 of CSP. This appears to be out of line with the results seen for basal respiration, ATP coupled respiration and maximal respiration where the D21 CSP results show a

statistically significant decline compared to baseline. It is possible that the spare respiratory capacity, D21 CSP statistical results are due to a statistical artifact as there are two points in the data set which appear to be outliers (Figure 4-7A) compared to the tight datasets seen for the other D21 CSP results and this may be skewing the data.

Overall, for the Seahorse Mito stress test (MST), no significant difference was observed between the RTP and CSP group. It was expected that the basal respiration would be lower in CSP compared to RTP initially during storage due to reduced metabolic rate in CSP and that later in storage CSP may be greater than RTP as mitochondria become dysfunctional in RTP and the platelets begin to die. This was seen by Bynum and colleagues, who demonstrated similar routine respiration rates in RTP and CSP until D7 when the RTP were significantly lower than the CSP (Bynum *et al.*, 2016). In addition, Bynum and colleagues found that maximal mitochondrial oxygen consumption was better preserved in CSP than RTP (statistically significantly higher at D7) (Bynum *et al.*, 2016). The differences in this study's results compared to that of Bynum and colleagues, could be due to the different methodology used by Bynum to measure oxygen consumption (using a high-resolution respirometer (HRR)). In HRR the platelets are treated differently in comparison to the Seahorse MST as they are continuously stirred during the assay whereas in the Seahorse assay the platelets are fixed to the well (and at least partial mechanical activation cannot be excluded), which may lead to differences in results between the two methodologies. In addition, platelet respiratory rates have been demonstrated to be higher in the Seahorse assay compared to the HRR assay (Jedlička, Radovan and Kuncova, 2021). It is also possible that the differences observed between this study and the study by Bynum and colleagues could mean that our XF technique requires further optimisation.

Of particular interest in our results is the significant difference demonstrated between baseline and CSP D21 results. The basal respiration, ATP coupled respiration and maximal respiration results all demonstrated a large significant decline compared to the baseline results by D21 of storage (78%, 73% & 76% declines

respectively), which raises questions about the level of mitochondrial dysfunction by D21 and whether CSP should be used as a clinical product at this age.

The Seahorse XF technology was also used to quantify the amount of ATP produced in the two groups throughout storage, using the ATP rate assay. This assay measures the flux of both H+ production (ECAR) and OCR simultaneously under basal conditions and after serial addition of the mitochondrial inhibitors oligomycin and rotenone/antimycin A. This enables total cellular ATP production rates as well as pathway-specific mitoATP and glycoATP production rates to be measured (Agilent, 2019). The initial baseline results for the PC in the study suggest that the amount of ATP supplied by glycolysis and by OXPHOS in a basal state is approximately 60% : 40% which is in line with that suggested by Wang and colleagues (Wang *et al.*, 2017), although others have suggested different balances (Kilkson, Holme and Murphy, 1984)

The total ATP production rates statistically significantly reduced during storage compared to baseline in both RTP and CSP, suggesting that the platelets within the PCs ability to metabolise was reducing. By D14, RTP was statistically significantly lower than D14 CSP which mirrors the results seen in the total ATP assay, further corroborating that RTP are less able to metabolise and produce ATP by D14 than CSP. A general downward trend was observed in both groups for mitoATP production rates with all results from D8-D21 for both groups being statistically significant compared to baseline, suggesting that the ability of the platelets to generate ATP through OXPHOS diminishes during storage; whereas glycoATP levels appeared to be fairly stable, with a slight trend down observed in RTP and a slight increase seen at D14 and D21 for CSP. None of the results were statistically significantly different compared to the baseline for glycoATP. The switch towards a glycolytic phenotype during storage is seen in Figure 4-12B where increasingly more of the ATP produced is from glycolytic ATP production. When cells switch to glycolysis alone it indicates that the mitochondria are damaged or dysfunctional and unable to provide ATP via OXPHOS. In addition, whilst glycolysis alone is able to produce enough energy for resting cells, it cannot produce enough energy for activated cells (Reddoch-Cardenas *et al.*, 2019a).

In summary, this work allowed a comprehensive metabolic profile of RTP and CSP to be developed through the measurement of indirect by-products of metabolism which represent the platelets' energy state, as well as through direct measures of mitochondrial function in intact cells.

Overall, cold storage of PC resulted in a reduction in metabolic activity demonstrated by reduced glucose utilisation as a substrate for metabolism, and reduced lactate production as a by-product of glycolysis. Although ATP levels (both total ATP and the ATP PR rate) decreased throughout storage in both RTP and CSP they were both demonstrated to be significantly higher in CSP at D14 and whilst statistical analysis could not be performed for the GlycoATP and MitoATP results, both RTP and CSP showed a trend towards a more glycolytic phenotype (RTP more so than CSP) during storage. This switch towards a glycolytic phenotype indicates that the mitochondria in the PC are becoming dysfunctional – more so in the RTP than in the CSP. This is supported by the $\Delta\psi_m$ results, where a loss of $\Delta\psi_m$ (depolarisation) was observed in both groups but to a greater extent in RTP than CSP at D14.

Mitochondrial function was further assessed with the mito stress test which did not demonstrate statistically significant differences between RTP and CSP in terms of their ability to respire. However, the results did demonstrate significant decline in basal respiration and ATP coupled respiration in D14 RTP and a significant decline in basal respiration, maximal respiration and ATP coupled respiration in D21 CSP. Alongside this the results for the $\Delta\psi_m$ were markedly decreased by D21 and glucose levels were very low. As the lifespan of mitochondria likely determine the lifespan of the platelets, these results raise important questions about prolonging the shelf life of CSP to 21 days as it does not appear to be supported by these results.

Chapter 5: Discussion

5.1 General discussion

Platelet transfusion is an essential medical treatment used for its haemostatic abilities, either prophylactically to prevent bleeding or therapeutically to halt bleeding. When platelet transfusion was first introduced in the 1960's, PC were stored in the cold at 4^{o}C with a very limited shelf life (Filip and Aster, 1978). Following several critical studies demonstrating that RTP survived longer than CSP in the circulation post-transfusion (Filip and Aster, 1978; Murphy and Gardner, 1969; Valeri, Feingold and Marchionni, 1974), CSP were abandoned globally in favour of the RTP product.

RTP are logistically challenging to store as they must be kept at 20-24^{o}C with constant gentle agitation, which requires bulky incubators and agitators. They have a limited shelf life of 5-7 days due to the risk of bacterial contamination and the decline in function seen over storage time, known as the platelet storage lesion. The short shelf life of RTP creates problems in maintaining supply, especially in rural areas and in the pre-hospital and military setting.

In recent years there has been a revival in interest in CSP, driven by a reduction in platelet transfusion for prophylactic reasons and an increase in the use of PC for the treatment of acute bleeding in traumatic haemorrhage resuscitation and surgery (Cap and Reddoch-Cardenas, 2018). Cold storage of PC is an attractive option as it greatly reduces the chance of bacterial growth, preserves haemostatic function of the platelets and simplifies the supply chain (CSP can be stored refrigerated with red cells, without agitation) (Johnson *et al.*, 2023). In addition, these advantages enable the shelf life of PC to be extended beyond 5-7 days of storage.

CSP derived from single donor apheresis have been licensed for use in the US by the FDA (suspended in 100% plasma or an FDA-approved PAS), for a maximum of 14 days, for '*the treatment of active bleeding when conventional platelets are not available or their use is not practical*' (FDA, 2023). They are also licensed in Norway for a maximum of 14 days, for use as mitigation for blood shortages (Braathen *et al.*,

2022). Although CSP are licensed in both of these countries, their shelf life is currently limited to 14 days as well as having restrictions on the clinical scenarios in which they can be utilised. This is due to unanswered questions about the maximum shelf life CSP could be extended to and a lack of clinical trials to provide evidence-based decisions on where CSP can provide benefit to patients. The first of these can be answered, at least in part through *in vitro* studies whilst the second requires clinical trial data. It is also worth noting that CSP are not currently licensed for use in the UK under the Medicines and Healthcare products Regulatory Agency (MHRA).

The overall objective of this study was to characterise the bioenergetic profiles of CSP and RTP, determining if they accurately reflect platelet function and whether they can be used to inform the maximum shelf life for CSP. This study utilised an extra-cellular flux methodology to simultaneously monitor mitochondrial function (OXPHOS) and glycolysis, creating bioenergetic profiles of RTP and CSP throughout prolonged storage. Previous studies have examined metabolic characteristics of RTP and CSP utilising endpoint assays such as glucose and lactate, but this is the first study to describe the bioenergetic profiles of RTP and CSP through the detection of metabolic function in real time using an extracellular flux technology.

5.1.1 Bioenergetic profiles of RTP and CSP

Analysis of the bioenergetic profiles from the mito stress test showed no significant difference in basal respiration, ATP coupled respiration, maximal respiration and spare respiratory capacity between RTP and CSP during the storage period. This suggests that in a basal state there is no difference in the ability of the platelets in RTP and CSP to utilise O_2 (OCR) through OXPHOS, that their maximum capacity to perform OXPHOS (respond to an increased energy demand such as activation) is the same and that CSP do not have any additional spare respiratory capacity. It was expected that if CSP are more quiescent/metabolically suppressed by the cold then early in shelf life (D2) the RTP may have displayed a higher OCR in a basal state than CSP as they are not metabolically suppressed by the cold and that as RTP age and their mitochondria become dysfunctional later in storage that the basal rate of CSP may begin to be higher than RTP and that due to metabolic suppression CSP, would have a greater spare respiratory capacity. These results are at odds with CSP having

significantly higher pO_2 than RTP, which suggests less O_2 is being used for OXPHOS (and therefore less OXPHOS is taking place) in CSP.

Analysis of the bioenergetic profiles using the ATP rate assay enabled the metabolic profiles of CSP and RTP to be determined and showed no significant difference between the ATP levels produced between CSP and RTP until D14 when the level was significantly higher in CSP, suggesting that their metabolic capability by this timepoint is greater than in RTP. This differs from the results seen in the mito stress test where no difference was seen, probably because the mito stress test only measures OXPHOS whereas the ATP rate assay measures ATP generated from both OXPHOS and glycolysis.

At D14 both the MITO ATP PR (OXPHOS) and the GLYCO ATP PR RTP results were lower than the CSP results, with a large difference seen in the GLYCO ATP PR, suggesting that there is a reduction of both OXPHOS and glycolysis in RTP compared to CSP by this timepoint. Not only was the ATP production rate of RTP significantly lower that CSP at D14, but the metabolic phenotype also showed that a lower percentage of the total ATP was produced by OXPHOS (35% OXPHOS : 65% Glycolysis) compared to CSP on D14 (45% OXPHOS : 55% Glycolysis), with platelets switching to a predominantly glycolytic phenotype. This indicates greater mitochondrial dysfunction in RTP by D14 than CSP (Bynum *et al.*, 2016) and whilst glycolysis alone is able to produce enough energy for resting cells, it is not sufficient to provide the energy required for activation (Reddoch-Cardenas *et al.*, 2019b). This is supported by the light transmission aggregometry results of the study where an increased ability to aggregate in response to collagen was seen by CSP at D14 and an increased ability to respond to ADP from D2-D14 in CSP. Significantly higher glucose levels were also seen in CSP compared to RTP along with lower lactate levels which suggests that RTP are more metabolically active than CSP.

5.1.2 Determining the maximum shelf life for CSP

A shelf life of 21 days has been postulated for CSP with several *in vitro* studies measuring up to this timepoint (Farrugia, Baron and Zammit, 2023; Shea *et al.*, 2023; Yang *et al.*, 2018). In addition, clinical trials are currently underway (Zantek *et al.*, 2023) which are examining a range of CSP storage durations in a step wise manner, up to 21 days storage to establish if there is non-inferiority compared to D5 RTP. In this study, the bioenergetic profiles have shown a significant decline throughout storage in the ability of CSP to perform OXPHOS compared to the baseline result and particularly by D21 a 78% decline in basal respiration, a 73% decline in ATP coupled respiration and a 76% decline in maximal respiration was observed. This data suggests that there is a high level of mitochondrial dysfunction by D21 in CSP, supported by the significant drop in mitochondrial membrane potential observed with both TMRM and JC-1 dyes by D21, suggesting significant mitochondrial depolarisation by this point in storage. In addition, the metabolic phenotype seen in the ATP rate assay is approximately 25% OXPHOS and 75% glycolysis, which is below that observed in D14 RTP and raises the question as to whether the platelets would have sufficient metabolic capability for activation when transfused.

In addition, glucose levels are very low in CSP by D21 (0.5 ± 0.6 mmol/L) with 2/12 results having no detectable glucose. This is particularly important as there has recently been an update to the blood component monographs for PC in PAS by the European Directorate for the Quality of Medicines and Healthcare (EDQM), moving away from the measurement of pH at end of shelf life (>6.4), to glucose measurement at end of shelf life. This is due to the buffering capacity of PAS preventing pH drops below 6.4 and rendering it no longer a good marker of platelet function, with EDQM stating that the glucose level must be above the limit of quantification (LoQ) of the analytical method (EDQM, 2023). In turn, the use of glucose instead of pH, as an end of shelf-life quality marker for PC in PAS in the UK has been suggested by the Special Advisory Committee of Blood Components (SACBC), who advise JPAC on the specifications of blood components for the UK, with potentially a limit of ≥ 1.0 mmol/L at the end of shelf life being set (personal correspondence, 2024). If this becomes the specification in the UK, only three of the

12 CSP units tested in this study would have passed end of shelf-life testing, which would be an unacceptable level for quality control processes.

In terms of measured functional ability at D21, CSP maintained their ability to aggregate in response to ADP and collagen and showed minimal changes in their superior ability to generate thrombin (compared to RTP), suggesting that their function is retained to D21 despite signs of metabolism reducing by this timepoint.

CSP function and metabolism *in vitro* is complex and must be linked to *in vivo* function to be able to determine a maximum storage shelf life. Although CSP are known to be rapidly cleared from the circulation post-transfusion, the rate at which they are cleared has been demonstrated to increase the longer they are stored pre-transfusion (Stolla *et al.*, 2020). It has been demonstrated with 111-Indium Oxine radiolabelled CSP that CSP % recovery compared to fresh platelets (2 hours post transfusion) shows a step wise decrease from day 5 to day 20 with day 20 CSP having half the recovery of day 5 CSP (Stolla *et al.*, 2020; Six, Compernolle and Feys, 2020). Whilst the purpose of CSP is to be transfused in trauma and actively bleeding patients and long survival in the circulation is not of high importance, severe trauma cases and surgeries with massive blood loss can take hours. It is unclear how efficacious CSP stored for 20 or 21 days will be in maintaining haemostasis in trauma and actively bleeding patients, despite functional *in vitro* assays suggesting functional superiority to Day 5/7 RTP and clinical trial data of CSP use at different timepoints is required.

5.2 Conclusions

The findings of this study have added new insights to the bioenergetic profile of CSP and RTP during prolonged storage and highlighted the importance of examining mitochondrial function when using *in vitro* studies to determine the shelf life of PC. Although the profiles did not show a significant difference between RTP and CSP, a significant decline in metabolic function was observed in D21 CSP compared to the baseline, suggestive of mitochondrial dysfunction by this timepoint, alongside very low and in some examples, no glucose. This decline in metabolic capability was not reflected in the platelets ability to aggregate and to generate thrombin at D21 but does raise concerns about extending the shelf life of CSP further from the 14 days

licence currently in place in the US and in Norway. There is no single *in vitro* assay that can be used to determine the likely effectiveness of a PC when transfused but assessment of mitochondrial function should be central to any testing strategy. Ultimately, to understand whether the reduced metabolic ability at D21 in CSP translates into a clinically inferior product, compared to CSP stored for shorter periods of time, data from randomised controlled clinical trials, such as the CHIlled Platelet study (CHIPS) in the US, is required.

5.3 Limitations of current research

This study was a pooled and split design where double clinical PC doses were bled via single donor apheresis, with one stored at 20-24^{o}C (RTP) and one stored in the cold at 2-6^{o}C (CSP). The PC were repeatedly tested to destruction and as such were removed from the clinical supply chain. Due to the expense and stock issues of removing apheresis platelets from clinical use (24 units in total for this study @ approx. £250/unit), only n = 12 paired units were studied in total. Although this is comparable to other PC published studies and in line with the JPAC recommendations for phase 0 *in vitro* studies of novel blood components (JPAC, 2021), it does limit the power of the study due to the small sample size. A wide variability of results between donors was seen in some assays as a result of natural individual human to human (or donor to donor) variability. If more replicates had been tested, statistical significance may have been seen in more aspects of the study, particularly in the bioenergetic assays where a large variation between samples was observed.

The testing timeframes (D0, D2, D8 , D14, D21) were selected to represent key timepoints in PC shelf life: day bled, early shelf life (D2), end of current UK shelf life of 7 days (D8) and end of potential extended shelf lives (D14 and D21). However, when comparing the study results to other CSP studies in the literature, many of them had examined D5, (probably because PC have a shelf life of 5 days in other countries) and a lack of data at this timepoint in this study limited some of the comparisons that could be made.

There were a few assay specific limitations identified. The light transmission aggregometry was performed using single agonists and although in some groups the response to agonists was demonstrated to decline during storage *in vitro*, this may not be an accurate reflection of how they would act *in vivo* where their function can be partially restored (Rinder *et al.*, 2003). In addition, stimulation of platelets with a single agonist is not reflective of mechanisms of platelet activation and aggregation *in vivo* where activation is the product of many signals originating from many receptors (Dorsam and Kunapuli, 2004). For future studies it is worth considering stimulating with multiple agonists for these assays (Cardigan and Williamson, 2003), although when comparing to other CSP studies in the literature many of them used single agonists, allowing effective comparisons to be drawn between this study and others.

The CCCP challenge test, used to confirm that directional changes in the dye signal are interpreted appropriately in the $\Delta\psi_m$ assay, did not work on all samples tested with TMRM and JC-1. This is a limitation of these results as there was no way to control that the dyes only enter the mitochondria when the $\Delta\psi_m$ exists (i.e. when they are polarized). To mitigate for this the gates were set based on the dot plot from D0 which was then used as the gating throughout storage for that sample to ensure changes could be quantified. A further limitation of the results for these assays was that normalisation of the data was not performed and therefore observed decline in fluorescence could be due to a loss of overall mitochondrial content through for example, mitophagy, rather than membrane depolarization.

A large amount of variability was seen in the Seahorse results, with datapoints spread over a wide range with some outliers. This could be due to real variation between the donors, for example, age-related changes have been demonstrated in mitochondrial function (Braganza, Annarapu and Shiva, 2020), with the donors in this study ranging in age from 44 - 67 years (mean age 55.5 years). This is the first study where our laboratory has utilised the Seahorse technology and itis possible that further optimisation of the assay is required, particularly around how normalisation of the data to cellular parameters is performed. Normalisation in this study was performed through quantitative platelet counting during sample preparation and

adding a known number of platelets into each well (0.2 x 10^6/µL) and by checking for confluence on the seeded plate using a microscope. More precise methods of normalisation could be considered for future work, including counting of cells in each well of the microplate via direct imaging of the cells or potentially through counting mitochondrial DNA copy number (although this is likely to be very low due to the small number of mitochondria in platelets). It would be interesting to perform a similar study utilising pooled platelets (where the buffy coats of four donors are pooled to make a PC) to see if this reduces the variation compared with that seen in individual single donor apheresis PC donations. This may help determine if the variability is due to the methodology, requiring further optimisation, or due to genuine donor variation.

Finally, this work was conducted *in vitro* and is therefore lacking the complexity of cell to cell interactions and milieu seen *in vivo*. This can make it difficult to draw conclusions about the effectiveness of the PC in haemostasis once transfused. Nevertheless, the experimental design has been effective for providing a solid basis to define a maximum shelf life for CSP.

5.4 Future work

This study has highlighted the extensive potential benefits of CSP for bleeding patients and for the logistics of blood supply chains worldwide. Within the UK, there are several areas for future work:

5.4.1 Further *in vitro* studies

This study has questioned whether the metabolic function of CSP by D21 is sufficient to support function *in vivo* by examining CSP at the timepoints D2, D8 , D14 and D21. A 14 day and 21-day shelf life were selected as convenient timepoints as it works out into complete weeks. However, there is the potential to examine CSP further between the timepoints D14 and D21, if D21 is too long a period in storage then it may be that for example, metabolic capability is better at day 18. Examining metabolic profiles at more time points between D14 and D21 for CSP may determine if there is a middle ground between D14 and D21 for shelf life.

Apheresis platelets in PAS were selected for this study to enable like for like comparison with the majority of published CSP studies. However, within the UK over 50% of all PC supplied for transfusion are pooled platelets. If the UK were to begin supplying CSP for clinical use interchangeably, then ideally both apheresis and pooled platelets would need to be used as is the case with the current RTP product. Pooled platelets are manufactured from the buffy coats of whole blood which is held overnight at ambient temperature before being processed into constituent components. Due to their different storage and manufacturing process, it is likely that their properties as CSP may be different to apheresis CSP. As such, pooled platelets need to be validated for use as CSP *in vitro* to establish if their properties are significantly different to apheresis. Depending on the results of these studies, the manufacturing process for pooled platelets may need to be amended from ambient overnight hold to either manufacture be on the day bled or possibly cold overnight hold of the whole blood and processing on day 1.

5.4.2 Licensing of CSP in the UK & *in vivo* clinical studies

To obtain a licence to transfuse CSP within the UK from the MHRA, an extensive *in vitro* validation needs to be performed that conforms to the specifications laid out in JPAC (JPAC, 2021). This study will form the body of that validation and enables an application to be made to the Special Advisory Committee for Blood Components (SACBC – a subgroup of JPAC) for approval of a trial specification for CSP. Once a trial specification has been approved, clinical trials can be performed using CSP within the UK.

In the UK the helicopter emergency medical services (HEMS) carry red cell concentrates and lyophilised plasma for transfusion to trauma patients pre-hospital. There is currently a pragmatic, randomised control trial (SWIFT trial) underway in the UK comparing whole blood (leucodepleted using the platelet sparing Terumo Imuflex SP filter) to the current standard of care – red cells and plasma, as a way to bring the benefits of platelet transfusion into the pre-hospital arena. However, this requires group O negative blood with a reduced shelf life due to the platelets that is often wasted if not used in the pre-hospital environment. This has the potential to add to already pressurise group O red cell supplies.

In addition, a significant proportion of platelets are lost when the whole blood is filtered so the units may not deliver a 'full' platelet dose. A proposed is to conduct a clinical trial to evaluate CSP alongside red cells and lyophilised plasma or leucodepleted whole blood (using a standard non-platelet sparing filter). These CSP can be stored with the red cells in transport boxes and would provide a larger dose of platelets to prevent bleeding in trauma patients.

5.4.3 Use of platelet bioenergetics as biomarkers for disease

Platelets have been shown to serve as biomarkers for mitochondrial dysfunction (Zharikov and Shiva, 2013) and changes in their bioenergetic profiles have been linked to sickle cell disease, asthma, Alzheimer's and Parkinson's disease (Chacko *et al.*, 2019; Braganza, Annarapu and Shiva, 2020). There is potentially scope to develop the extracellular flux assay for use in diagnostic and prognostic translational research through partnering with clinical colleagues in a hospital setting.

References

Agilent (2019) *Agilent Seahorse XFp Cell Mito Stress Test Kit*. https://www.agilent.com/cs/library/usermanuals/public/XFp_Cell_Mito_Stress_Test_Kit_User_Guide.pdf: Agilent Technologies Inc (Accessed: 27/11/2021.

Aibibula, M., Naseem, K. M. and Sturmey, R. G. (2018) 'Glucose metabolism and metabolic flexibility in blood platelets', *Journal of Thrombosis and Haemostasis,* 16(11), pp. 2300-2314.

Ainscow, E. K. and Brand, M. D. (1999) 'Top-down control analysis of ATP turnover, glycolysis and oxidative phosphorylation in rat hepatocytes', *European Journal of Biochemistry,* 263(3), pp. 671-685.

Albanyan, A. M., Harrison, P. and Murphy, M. F. (2009) 'Markers of platelet activation and apoptosis during storage of apheresis-and buffy coat–derived platelet concentrates for 7 days', *Transfusion,* 49(1), pp. 108-117.

Albanyan, A. M., Murphy, M. F., Rasmussen, J. T., Heegaard, C. W. and Harrison, P. (2009) 'Measurement of phosphatidylserine exposure during storage of platelet concentrates using the novel probe lactadherin: a comparison study with annexin V', *Transfusion,* 49(1), pp. 99-107.

Amorini, A. M., Tuttobene, M., Tomasello, F. M., Biazzo, F., Gullotta, S., De Pinto, V., Lazzarino, G. and Tavazzi, B. (2013) 'Glucose ameliorates the metabolic profile and mitochondrial function of platelet concentrates during storage in autologous plasma', *Blood transfusion = Trasfusione del sangue,* 11(1), pp. 61-70.

Árnason, N. Á. and Sigurjónsson, Ó. E. (2017) 'New strategies to understand platelet storage lesion', *ISBT Science Series,* 12(4), pp. 496-500.

Badlou, B. A., Ijseldijk, M. J. W., Smid, W. M. and Akkerman, J. W. N. (2005) 'Prolonged platelet preservation by transient metabolic suppression', *Transfusion,* 45(2), pp. 214-22.

Becker, G. A., Tuccelli, M., Kunicki, T., Chalos, M. K. and Aster, R. H. (1973) 'Studies of Platelet Concentrates Stored at 22 C and 4 C', *Transfusion,* 13(2), pp. 61-68.

Bertolini, F., Agazzi, A., Peccatori, F., Martinelli, G. and Sandri, M. T. (2000) 'The absence of swirling in platelet concentrates is highly predictive of poor posttransfusion platelet count increments and increased risk of a transfusion reaction', *Transfusion,* 40(1), pp. 121a-122.

Bertolini, F., Murphy, S., Rebulla, P. and Sirchia, G. (1992) 'Role of acetate during platelet storage in a synthetic medium', *Transfusion,* 32(2), pp. 152-156.

Bertolini, F., Murphy, S. and Transfusion, B. E. f. S. T. W. P. o. t. I. S. o. B. (1996) 'A multicenter inspection of the swirling phenomenon in platelet concentrates prepared in routine practice', *Transfusion,* 36(2), pp. 128-132.

Berzuini, A., Spreafico, M. and Prati, D. (2017) 'One size doesn't fit all: Should we reconsider the introduction of cold-stored platelets in blood bank inventories?', *F1000Research,* 6, pp. 95-95.

Bikker, A., Bouman, E., Sebastian, S., Korporaal, S. J. A., Urbanus, R. T., Fijnheer, R., Boven, L. A. and Roest, M. (2016) 'Functional recovery of stored platelets after transfusion', *Transfusion,* 56(5), pp. 1030-1037.

Braathen, H., Hagen, K. G., Kristoffersen, E. K., Strandenes, G. and Apelseth, T. O. (2022) 'Implementation of a dual platelet inventory in a tertiary hospital during the COVID-19 pandemic enabling cold-stored apheresis platelets for treatment of actively bleeding patients', *Transfusion,* 62, pp. S193-S202.

Braathen, H., Sivertsen, J., Lunde, T. H. F., Kristoffersen, E. K., Assmus, J., Hervig, T. A., Strandenes, G. and Apelseth, T. O. (2019) 'In vitro quality and platelet function of cold and delayed cold storage of apheresis platelet concentrates in platelet additive solution for 21 days', *Transfusion,* 59(8), pp. 2652-2661.

Braganza, A., Annarapu, G. K. and Shiva, S. (2020) 'Blood-based bioenergetics: An emerging translational and clinical tool', *Molecular Aspects of Medicine,* 71, pp. 100835.

Brand, Martin D. and Nicholls, David G. (2011) 'Assessing mitochondrial dysfunction in cells', *Biochemical Journal,* 435(2), pp. 297-312.

Brass, L. F. (2003) 'Thrombin and platelet activation', *Chest,* 124(3), pp. 18S-25S.

Brecher, M. E., Blajchman, M. A., Yomtovian, R., Ness, P. and AuBuchon, J. P. (2013) 'Addressing the risk of bacterial contamination of platelets within the United States: a history to help illuminate the future', *Transfusion,* 53(1), pp. 221-231.

Bynum, J. A., Meledeo, M. A., Getz, T. M., Rodriguez, A. C., Aden, J. K., Cap, A. P. and Pidcoke, H. F. (2016) 'Bioenergetic profiling of platelet mitochondria during storage: 4degreeC storage extends platelet mitochondrial function and viability', *Transfusion,* 56 Suppl 1, pp. S76-84.

Cap, A. P. and Reddoch-Cardenas, K. M. (2018) 'Can't get platelets to your bleeding patients? Just chill… the solution is in your refrigerator!', *Transfus Clin Biol,* 25(3), pp. 217-219.

Cardenas, J. C., Zhang, X., Fox, E. E., Cotton, B. A., Hess, J. R., Schreiber, M. A., Wade, C. E., Holcomb, J. B. and Group, o. b. o. t. P. S. (2018) 'Platelet transfusions improve hemostasis and survival in a substudy of the prospective, randomized PROPPR trial', *Blood Advances,* 2(14), pp. 1696-1704.

Cardigan, R. and Williamson, L. (2003) 'The quality of platelets after storage for 7 days', *Transfusion medicine,* 13(4), pp. 173-187.

Carreau, A., Hafny-Rahbi, B. E., Matejuk, A., Grillon, C. and Kieda, C. (2011) 'Why is the partial oxygen pressure of human tissues a crucial parameter? Small molecules and hypoxia', *Journal of Cellular and Molecular Medicine,* 15(6), pp. 1239-1253.

Chacko, B. K., Kramer, P. A., Ravi, S., Johnson, M. S., Hardy, R. W., Ballinger, S. W. and Darley-Usmar, V. M. (2013) 'Methods for defining distinct bioenergetic profiles in platelets, lymphocytes, monocytes, and neutrophils, and the oxidative burst from human blood', *Laboratory Investigation,* 93(6), pp. 690-700.

Chacko, B. K., Smith, M. R., Johnson, M. S., Benavides, G., Culp, M. L., Pilli, J., Shiva, S., Uppal, K., Go, Y.-M., Jones, D. P. and Darley-Usmar, V. M. (2019) 'Mitochondria in precision medicine; linking bioenergetics and metabolomics in platelets', *Redox Biology,* 22, pp. 101165.

Choi, J. W. and Pai, S. H. (2003) 'Influence of storage temperature on the responsiveness of human platelets to agonists', *Annals of Clinical & Laboratory Science,* 33(1), pp. 79-85.

Choudhury, A., Chung, I., Blann, A. D. and Lip, G. Y. (2007) 'Platelet surface CD62P and CD63, mean platelet volume, and soluble/platelet P-selectin as indexes of platelet function in atrial fibrillation: a comparison of “healthy control subjects” and “disease control subjects” in sinus rhythm', *Journal of the American College of Cardiology,* 49(19), pp. 1957-1964.

Christmas, K. M. and Bassingthwaighte, J. B. (2017) 'Equations for O2 and CO2 solubilities in saline and plasma: combining temperature and density dependences', *Journal of applied physiology,* 122(5), pp. 1313-1320.

Cohn, C. S., Stubbs, J., Schwartz, J., Francis, R., Goss, C., Cushing, M., Shaz, B., Mair, D., Brantigan, B. and Heaton, W. A. (2014) 'A comparison of adverse reaction rates for PAS C versus plasma platelet units', *Transfusion,* 54(8), pp. 1927-1934.

Cookson, P., Sutherland, J., Turner, C., Bashir, S., Wiltshire, M., Hancock, V., Smith, K. and Cardigan, R. (2010) 'Platelet apoptosis and activation in platelet concentrates stored for up to 12 days in plasma or additive solution', *Transfusion medicine (Oxford, England),* 20(6), pp. 392-402.

Cottet-Rousselle, C., Ronot, X., Leverve, X. and Mayol, J.-F. (2011) 'Cytometric assessment of mitochondria using fluorescent probes', *Cytometry Part A,* 79A(6), pp. 405-425.

Curvers, J., De Wildt-Eggen, J., Heeremans, J., Scharenberg, J., De Korte, D. and Van Der Meer, P. F. (2008) 'Flow cytometric measurement of CD62P (P-selectin) expression on platelets: a multicenter optimization and standardization effort', *Transfusion,* 48(7), pp. 1439-1446.

Davlouros, P., Xanthopoulou, I., Mparampoutis, N., Giannopoulos, G., Deftereos, S. and Alexopoulos, D. (2016) 'Role of calcium in platelet activation: novel insights and pharmacological implications', *Medicinal Chemistry,* 12(2), pp. 131-138.

Devine, D. V. and Serrano, K. (2010) 'The Platelet Storage Lesion', *Clinics in Laboratory Medicine,* 30(2), pp. 475-487.

Diagouraga, B., Grichine, A., Fertin, A., Wang, J., Khochbin, S. and Sadoul, K. (2014) 'Motor-driven marginal band coiling promotes cell shape change during platelet activation', *Journal of Cell Biology,* 204(2), pp. 177-185.

Diaz, F. and Moraes, C. T. (2008) 'Mitochondrial biogenesis and turnover', *Cell calcium,* 44(1), pp. 24-35.

Divakaruni, A. S., Paradyse, A., Ferrick, D. A., Murphy, A. N. and Jastroch, M. (2014) 'Chapter Sixteen - Analysis and Interpretation of Microplate-Based Oxygen Consumption and pH Data', in Murphy, A.N. and Chan, D.C. (eds.) *Methods in Enzymology*: Academic Press, pp. 309-354.

Dorsam, R. T. and Kunapuli, S. P. (2004) 'Central role of the P2Y 12 receptor in platelet activation', *The Journal of clinical investigation,* 113(3), pp. 340-345.

Dumont, L. J., AuBuchon, J. P., Whitley, P., Herschel, L. H., Johnson, A., McNeil, D., Sawyer, S. and Roger, J. C. (2002) 'Seven-day storage of single-donor platelets: recovery and survival in an autologous transfusion study', *Transfusion,* 42(7), pp. 847-854.

Duncan, E., Bonar, R., Rodgers, S., Favaloro, E., Marsden, K. and RCPA QAP in Haematology, H. C. (2009) 'Methodology and outcomes of platelet aggregation testing in Australia, New Zealand and the Asia-Pacific region: results of a survey from the Royal College of Pathologists of Australasia Haematology Quality Assurance Program', *International Journal of Laboratory Hematology,* 31(4), pp. 398-406.

Dunlop, L. C., Skinner, M. P., Bendall, L. J., Favaloro, E. J., Castaldi, P. A., Gorman, J. J., Gamble, J. R., Vadas, M. A. and Berndt, M. C. (1992) 'Characterization of GMP-140 (P-selectin) as a circulating plasma protein', *Journal of Experimental Medicine,* 175(4), pp. 1147-1150.

EDQM, E. C. P. A. o. B. T. (2023) *Guide to the preparation, use and quality assurance of blood components.* 21st edn.: European Directorate for the Quality of Medicines & Healthcare.

Estcourt, L., Birchall, J., Allard, S., Bassey, S. J., Hersey, P., Kerr, J. P., Mumford, A. D., Stanworth, S. J. and Tinegate, H. (2016) 'Guidelines for the use of platelet transfusions', *British journal of haematology,* 176(3).

Farrugia, A. (1994) 'Platelet Concentrates for Transfusion—Metabolic and Storage Aspects', *Platelets,* 5(4), pp. 177-185.

Farrugia, C., Baron, B. and Zammit, V. (2023) 'Platelet Storage: Time to Rethink the Cold', *International Blood Research & Reviews,* 14(4), pp. 57-69.

FDA (2023) *Alternative Procedures for the Manufacture of Cold-Stored Platelets Intended for the Treatment of Active Bleeding when Conventional Platelets Are Not Available or Their Use Is Not Practical*. Available at: https://www.fda.gov/regulatory-information/search-fda-guidance-documents/alternative-procedures-manufacture-cold-stored-platelets-intended-treatment-active-bleeding-when (Accessed: 07/05/2024.

Ferrer, F., Rivera, J., Lozano, M. L., Corral, J. and Garcia, V. V. (2001) 'Effect of cold-storage in the accumulation of bioreactive substances in platelet concentrates treated with second messenger effects', *Haematologica,* 86(5), pp. 530-536.

Filip, D. J. and Aster, R. H. (1978) 'Relative hemostatic effectiveness of human platelets stored at 4 degrees and 22 degrees C', *The Journal of laboratory and clinical medicine,* 91(4), pp. 618-624.

Flaumenhaft, R., Dilks, J. R., Rozenvayn, N., Monahan-Earley, R. A., Feng, D. and Dvorak, A. M. (2005) 'The actin cytoskeleton differentially regulates platelet α-granule and dense-granule secretion', *Blood,* 105(10), pp. 3879-3887.

Fratantoni, J. C., Poindexter, B. J. and Bonner, R. F. (1984) 'Quantitative assessment of platelet morphology by light scattering: a potential method for the evaluation of platelets for transfusion', *The Journal of laboratory and clinical medicine,* 103(4), pp. 620-631.

Fritsma, G. (2015) 'Platelet Structure and Function', *American Society for Clinical Laboratory Science,* 28, pp. 125-131.

George, M. J., Bynum, J., Nair, P., Cap, A. P., Wade, C. E., Cox, C. S., Jr. and Gill, B. S. (2018) 'Platelet biomechanics, platelet bioenergetics, and applications to clinical practice and translational research', *Platelets,* 29(5), pp. 431-439.

Getz, T. M., Montgomery, R. K., Bynum, J. A., Aden, J. K., Pidcoke, H. F. and Cap, A. P. (2016) 'Storage of platelets at 4°C in platelet additive solutions prevents aggregate formation and preserves platelet functional responses', *Transfusion,* 56(6), pp. 1320-8.

Ghoshal, K. and Bhattacharyya, M. (2014) 'Overview of Platelet Physiology: Its Hemostatic and Nonhemostatic Role in Disease Pathogenesis', *The Scientific World Journal,* 2014, pp. 781857.

Gil-Fernández, J. J., Alegre, A., Fernández-Villalta, M. J., Pinilla, I., Gómez García, V., Martinez, C., Tomás, J. F., Arranz, R., Figuera, A., Cámara, R. and Fernández-Rañada, J. M. (1996) 'Clinical results of a stringent policy on prophylactic platelet transfusion: non-randomized comparative analysis in 190 bone marrow transplant patients from a single institution', *Bone Marrow Transplant,* 18(5), pp. 931-5.

Gottschall, J., Wu, Y., Triulzi, D., Kleinman, S., Strauss, R., Zimrin, A. B., McClure, C., Tan, S., Bialkowski, W., Murphy, E., Ness, P., Epidemiology, f. t. N. R. and Study, D. E. (2020) 'The epidemiology of platelet transfusions: an analysis of platelet use at 12 US hospitals', *Transfusion,* 60(1), pp. 46-53.

Gremmel, T., Frelinger, A. L., 3rd and Michelson, A. D. (2016) 'Platelet Physiology', *Semin Thromb Hemost,* 42(3), pp. 191-204.

Handin, R., Fortier, N. and Valeri, C. (1970) 'Platelet response to hypotonic stress after storage at 4 C or 22 C', *Transfusion,* 10(6), pp. 305-309.

Handin, R. I. and Valeri, C. R. (1971) 'Hemostatic effectiveness of platelets stored at 22 degrees C', *N Engl J Med,* 285(10), pp. 538-43.

Heijnen, H. and Van der Sluijs, P. (2015) 'Platelet secretory behaviour: as diverse as the granules… or not?', *Journal of thrombosis and haemostasis,* 13(12), pp. 2141-2151.

Hemker, H., Giesen, P., AlDieri, R., Regnault, V., De Smed, E., Wagenvoord, R., Lecompte, T. and Beguin, S. (2002) 'The calibrated automated thrombogram (CAT): a universal routine test for hyper-and hypocoagulability', *Pathophysiology of haemostasis and thrombosis,* 32(5-6), pp. 249-253.

Hemker, H. C., Al Dieri, R., De Smedt, E. and Béguin, S. (2006) 'Thrombin generation, a function test of the haemostaticthrombotic system', *Thrombosis and haemostasis,* 96(11), pp. 553-561.

Hemker, H. C., Giesen, P., Al Dieri, R., Regnault, V., De Smedt, E., Wagenvoord, R., Lecompte, T. and Béguin, S. (2003) 'Calibrated automated thrombin generation measurement in clotting plasma', *Pathophysiology of haemostasis and thrombosis,* 33(1), pp. 4-15.

Hirayama, J., Fujihara, M., Akino, M., Homma, C., Kato, T., Ikeda, H. and Azuma, H. (2012) 'Influence of a 24-hour interruption of agitation on in vitro properties of platelets washed with M-sol during 7-day storage', *Transfusion,* 52(5).

Hoffmeister, K. M. (2011) 'The role of lectins and glycans in platelet clearance', *Journal of Thrombosis and Haemostasis,* 9(s1), pp. 35-43.

Hoffmeister, K. M., Falet, H., Toker, A., Barkalow, K. L., Stossel, T. P. and Hartwig, J. H. (2001) 'Mechanisms of cold-induced platelet actin assembly', *Journal of Biological Chemistry,* 276(27), pp. 24751-24759.

Hoffmeister, K. M., Felbinger, T. W., Falet, H., Denis, C. V., Bergmeier, W., Mayadas, T. N., von Andrian, U. H., Wagner, D. D., Stossel, T. P. and Hartwig, J. H. (2003) 'The clearance mechanism of chilled blood platelets', *Cell,* 112(1), pp. 87-97.

Hogge, D., Thompson, B. and Schiffer, C. (1986) 'Platelet storage for 7 days in second-generation blood bags', *Transfusion,* 26(2), pp. 131-135.

Holinstat, M. (2017) 'Normal platelet function', *Cancer and Metastasis Reviews,* 36(2), pp. 195-198.

Holme, S. (1998) 'Storage and Quality Assessment of Platelets', *Vox Sanguinis,* 74(S2), pp. 207-216.

Holme, S., Heaton, W. and Courtright, M. (1987) 'Improved in vivo and in vitro viability of platelet concentrates stored for seven days in a platelet additive solution', *British journal of haematology,* 66(2), pp. 233-238.

Holme, S., Moroff, G. and Murphy, S. (1998) 'A multi-laboratory evaluation of in vitro platelet assays: the tests for extent of shape change and response to hypotonic shock. Biomedical Excellence for Safer Transfusion Working Party of the International Society of Blood Transfusion', *Transfusion,* 38(1), pp. 31-40.

Holme, S., Sweeney, J. D., Sawyer, S. and Elfath, M. D. (1997) 'The expression of p-selectin during collection, processing, and storage of platelet concentrates: relationship to loss of in vivo viability', *Transfusion,* 37(1), pp. 12-17.

Hornsey, V. S., Drummond, O., McMillan, L., Morrison, A., Morrison, L., MacGregor, I. R. and Prowse, C. V. (2008) 'Cold storage of pooled, buffy-coat-derived, leucoreduced platelets in plasma', *Vox Sanguinis,* 95(1), pp. 26-32.

Hou, J., Fu, Y., Zhou, J., Li, W., Xie, R., Cao, F., Gilbert, G. and Shi, J. (2011) 'Lactadherin functions as a probe for phosphatidylserine exposure and as an anticoagulant in the study of stored platelets', *Vox sanguinis,* 100(2), pp. 187-195.

Italiano Jr, J. E., Bergmeier, W., Tiwari, S., Falet, H., Hartwig, J. H., Hoffmeister, K. M., André, P., Wagner, D. D. and Shivdasani, R. A. (2003) 'Mechanisms and implications of platelet discoid shape', *Blood,* 101(12), pp. 4789-4796.

Jedlička, J., Radovan, K. and Kuncova, J. (2021) 'Mitochondrial respiration of human platelets in young adult and advanced age–seahorse or O2k?', *Physiological Research,* 70(Suppl 3), pp. S369.

Johansson, P. I., Svendsen, M. S., Salado, J., Bochsen, L. and Kristensen, A. T. (2008) 'Investigation of the thrombin-generating capacity, evaluated by thrombogram, and clot formation evaluated by thrombelastography of platelets stored in the blood bank for up to 7 days', *Vox Sanguinis,* 94(2), pp. 113-118.

Johnson, L., Roan, C., Lei, P., Spinella, P. C. and Marks, D. C. (2023) 'The role of sodium citrate during extended cold storage of platelets in platelet additive solutions', *Transfusion,* 63(S3), pp. S126-S137.

Johnson, L., Tan, S., Wood, B., Davis, A. and Marks, D. C. (2016) 'Refrigeration and cryopreservation of platelets differentially affect platelet metabolism and function: a comparison with conventional platelet storage conditions', *Transfusion,* 56(7), pp. 1807-18.

Johnson, L., Vekariya, S., Wood, B., Tan, S., Roan, C. and Marks, D. C. (2021) 'Refrigeration of apheresis platelets in platelet additive solution (PAS-E) supports in vitro platelet quality to maximize the shelf-life', *Transfusion,* 61(S1), pp. S58-S67.

Josefsson, E. C., Ramström, S., Thaler, J., Lordkipanidzé, M., Agbani, E. O., Alberio, L., Bakchoul, T., Bouchard, B. A., Camera, M. and Chen, V. (2023) 'Consensus report on markers to distinguish procoagulant platelets from apoptotic platelets: Communication from the Scientific and Standardization Committee of the ISTH', *Journal of Thrombosis and Haemostasis,* 21(8), pp. 2291-2299.

JPAC (2021) *Joint UK Blood Transfusion and Tissue Transplantation Services Professional Advisory Committee - Guidelines for the Blood Transfusion Services.* https://www.transfusionguidelines.org/.

Judge, A. and Dodd, Michael S. (2020) 'Metabolism', *Essays in Biochemistry,* 64(4), pp. 607-647.

Kattlove, H. E. and Alexander, B. (1971) 'The effect of cold on platelets. I. Cold-induced platelet aggregation', *Blood,* 38(1), pp. 39-48.

Ketter, P. M., Kamucheka, R., Arulanandam, B., Akers, K. and Cap, A. P. (2019) 'Platelet enhancement of bacterial growth during room temperature storage: mitigation through refrigeration', *Transfusion,* 59(S2), pp. 1479-1489.

Kilkson, H., Holme, S. and Murphy, S. (1984) 'Platelet metabolism during storage of platelet concentrates at 22 C', *Blood,* 64(2), pp. 406-414.

Kim, B. K. and Baldini, M. G. (1974) 'The Platelet Response to Hypotonic Shock. Its Value as an Indicator of Platelet Viability After Storage', *Transfusion,* 14(2), pp. 130-138.

Koessler, J., Klingler, P., Niklaus, M., Weber, K., Koessler, A., Boeck, M. and Kobsar, A. (2020) 'The Impact of Cold Storage on Adenosine Diphosphate-Mediated Platelet Responsiveness', *TH Open,* 4(3), pp. e163-e172.

Kostelijk, E., Fijnheer, R., Nieuwenhuis, H., Gouwerok, C. and De Korte, D. (1996) 'Soluble P-selectin as parameter for platelet activation during storage', *Thrombosis and haemostasis,* 76(12), pp. 1086-1089.

Krailadsiri, P. and Seghatchian, J. (2000) 'Are All Leucodepleted Platelet Concentrates Equivalent?: Comparison of Cobe LRS Turbo, Haemonetics MCS+ LD, and Filtered Pooled Buffy–Coat–Derived Platelets', *Vox Sanguinis,* 78(3), pp. 171-175.

Kramer, P. A., Ravi, S., Chacko, B., Johnson, M. S. and Darley-Usmar, V. M. (2014) 'A review of the mitochondrial and glycolytic metabolism in human platelets and leukocytes: Implications for their use as bioenergetic biomarkers', *Redox Biology,* 2, pp. 206-210.

Kühlbrandt, W. (2015) 'Structure and function of mitochondrial membrane protein complexes', *BMC Biology,* 13(1), pp. 89.

Kunicki, T., Tuccelli, M., Becker, G. and Aster, R. (1975) 'A study of variables affecting the quality of platelets stored at “room temperature”', *Transfusion,* 15(5), pp. 414-421.

Leal, J. K. F., Adjobo-Hermans, M. J. W. and Bosman, G. (2018) 'Red Blood Cell Homeostasis: Mechanisms and Effects of Microvesicle Generation in Health and Disease', *Front Physiol,* 9, pp. 703.

Leeksma, C. H. W. and Cohen, J. A. (1956) 'Determination of the life span of human blood platelets using labelled diisopropylfluorophosphonate', *The Journal of Clinical Investigation,* 35(9), pp. 964-969.

Levy, J. H., Neal, M. D. and Herman, J. H. (2018) 'Bacterial contamination of platelets for transfusion: strategies for prevention', *Critical Care,* 22(1), pp. 1-8.

Leytin, V., Allen, D. J., Gwozdz, A., Garvey, B. and Freedman, J. (2004) 'Role of platelet surface glycoprotein Ibα and P-selectin in the clearance of transfused platelet concentrates', *Transfusion,* 44(10), pp. 1487-1495.

Leytin, V., Allen, D. J., Mutlu, A., Mykhaylov, S., Lyubimov, E. and Freedman, J. (2008) 'Platelet activation and apoptosis are different phenomena: evidence from the sequential dynamics and the magnitude of responses during platelet storage', *British journal of haematology,* 142(3), pp. 494-497.

Lhermusier, T., Chap, H. and Payrastre, B. (2011) 'Platelet membrane phospholipid asymmetry: from the characterization of a scramblase activity to the identification of an essential protein mutated in Scott syndrome', *Journal of Thrombosis and Haemostasis,* 9(10), pp. 1883-1891.

Li, J., Xia, Y., Bertino, A. M., Coburn, J. P. and Kuter, D. J. (2000) 'The mechanism of apoptosis in human platelets during storage', *Transfusion,* 40(11), pp. 1320-1329.

Lorusso, A., Croxon, H., Faherty-O'Donnell, S., Field, S., Fitzpatrick, Á., Farrelly, A., Hervig, T. and Waters, A. (2023) 'The impact of donor biological variation on the quality and function of cold-stored platelets', *Vox Sanguinis,* 118(9), pp. 730-737.

Marini, I., Aurich, K., Jouni, R., Nowak-Harnau, S., Hartwich, O., Greinacher, A., Thiele, T. and Bakchoul, T. (2019) 'Cold storage of platelets in additive solution: the impact of residual plasma in apheresis platelet concentrates', *Haematologica,* 104(1), pp. 207.

Maurer-Spurej, E. and Chipperfield, K. (2007) 'Past and future approaches to assess the quality of platelets for transfusion', *Transfusion medicine reviews,* 21(4), pp. 295-306.

Mazzeffi, M., Lund, L., Wallace, K., Herrera, A. V., Tanaka, K., Odonkor, P., Strauss, E., Rock, P. and Fiskum, G. (2016) 'Effect of cardiopulmonary bypass on platelet mitochondrial respiration and correlation with aggregation and bleeding: a pilot study', *Perfusion,* 31(6), pp. 508-515.

Melchinger, H., Jain, K., Tyagi, T. and Hwa, J. (2019) 'Role of Platelet Mitochondria: Life in a Nucleus-Free Zone', *Frontiers in Cardiovascular Medicine,* 6(153).

Metcalfe, P., Williamson, L. M., Reutelingsperger, C. P., Swann, I., Ouwehand, W. H. and Goodall, A. H. (1997) 'Activation during preparation of therapeutic platelets affects deterioration during storage: a comparative flow cytometric study of different production methods', *British journal of haematology,* 98(1), pp. 86-95.

Michelson, A. D., Cattaneo, M., Frelinger, A.L. & Newman, P.J. (2019) *Platelets.* London, UK: Elsevier.

Milford, E. M. and Reade, M. C. (2016) 'Comprehensive review of platelet storage methods for use in the treatment of active hemorrhage', *Transfusion,* 56(S2), pp. S140-S148.

Misselwitz, F., Leytin, V. and Repin, V. (1987) 'Effect of metabolic inhibitors on platelet attachment, spreading and aggregation on collagen-coated surfaces', *Thrombosis research,* 46(2), pp. 233-240.

Monroe, D. M., Hoffman, M. and Roberts, H. R. (2002) 'Platelets and Thrombin Generation', *Arteriosclerosis, Thrombosis, and Vascular Biology,* 22(9), pp. 1381-1389.

Moore, G., Knight, G. & Blann, A. (2016) *Haematology.* 2nd edn. Oxford: Oxford University Press. Reprint, 2.

Murphy, S. and Gardner, F. H. (1969) 'Effect of storage temperature on maintenance of platelet viability-deleterious effect of refrigerated storage', *N Engl J Med,* 280(20), pp. 1094-8.

Murphy, S., Rebulla, P., Bertolini, F., Holme, S., Moroff, G., Snyder, E. and Stromberg, R. (1994) 'In Vitro Assessment of the Quality of Stored Platelet Concentrates', *Transfusion Medicine Reviews,* 8(1), pp. 29-36.

Nair, P. M., Pandya, S. G., Dallo, S. F., Reddoch, K. M., Montgomery, R. K., Pidcoke, H. F., Cap, A. P. and Ramasubramanian, A. K. (2017) 'Platelets stored at 4°C contribute to superior clot properties compared to current standard-of-care through fibrin-crosslinking', *British Journal of Haematology,* 178(1), pp. 119-129.

Nash, J., Davies, A., Saunders, C., George, C., Williams, J. and James, P. (2023) 'Quantitative increases of extracellular vesicles in prolonged cold storage of platelets increases the potential to enhance fibrin clot formation', *Transfusion Medicine,* 33(6), pp. 467-477.

Nash, J., Saunders, C. V. and George, C. (2023) 'pH is unsuitable as a quality control marker in platelet concentrates stored in platelet additive solutions', *Vox Sanguinis,* 118, pp. 183-184.

Nasir, N. M., Sthaneshwar, P., Yunus, P. and Yap, S.-F. (2010) 'Comparing measured total carbon dioxide and calculated bicarbonate', *Malays J Pathol,* 32(1), pp. 21-26.

NasrEldin, E. (2017) 'Effect of cold storage on platelets quality stored in a small containers: Implications for pediatric transfusion', *Pediatric Hematology Oncology Journal,* 2(2), pp. 29-34.

Ng, M. S. Y., Tung, J.-P. and Fraser, J. F. (2018) 'Platelet Storage Lesions: What More Do We Know Now?', *Transfusion Medicine Reviews,* 32(3), pp. 144-154.

NIH, N. L. o. M. (2024) *National Centre for Biotechnology Information*. Available at: https://clinicaltrials.gov/search?term=cold%20stored%20platelets&page=2 (Accessed: 07/05/24.

Nolfi-Donegan, D., Braganza, A. and Shiva, S. (2020) 'Mitochondrial electron transport chain: Oxidative phosphorylation, oxidant production, and methods of measurement', *Redox Biology,* 37, pp. 101674.

Owens, M., Holme, S., Heaton, A., Sawyer, S. and Cardinali, S. (1992) 'Post-transfusion recovery of function of 5-day stored platelet concentrates', *British Journal of Haematology,* 80(4), pp. 539-544.

Paglia, G., Sigurjónsson, Ó. E., Rolfsson, Ó., Valgeirsdottir, S., Hansen, M. B., Brynjólfsson, S., Gudmundsson, S. and Palsson, B. O. (2014) 'Comprehensive metabolomic study of platelets reveals the expression of discrete metabolic phenotypes during storage', *Transfusion,* 54(11), pp. 2911-2923.

Palmer, D. S., Aye, M. T., Dumont, L., Dumont, D., McCombie, N., Giulivi, A., Rutherford, B., Trudel, E. and Hashemi-Tavoularis, S. (1998) 'Prevention of Cytokine Accumulation in Platelets Obtained with the COBE Spectra Apheresis System', *Vox Sanguinis,* 75(2), pp. 115-123.

Paulus, J., Deschamps, J., Prenant, M. and Casals, F. (1981) 'Kinetics of platelets, megakaryocytes, and their precursors: what to measure?', *Automation in Hematology: What to Measure and Why?*, pp. 111-124.

Perry, S. W., Norman, J. P., Barbieri, J., Brown, E. B. and Gelbard, H. A. (2011) 'Mitochondrial membrane potential probes and the proton gradient: a practical usage guide', *BioTechniques,* 50(2), pp. 98-115.

Pidcoke, H. F., Aden, J. K., Mora, A. G., Borgman, M. A., Spinella, P. C., Dubick, M. A., Blackbourne, L. H. and Cap, A. P. (2012) 'Ten-year analysis of transfusion in Operation Iraqi Freedom and Operation Enduring Freedom: increased plasma and platelet use correlates with improved survival', *Journal of Trauma and Acute Care Surgery,* 73(6), pp. S445-S452.

Pidcoke, H. F., Spinella, P. C., Ramasubramanian, A. K., Strandenes, G., Hervig, T., Ness, P. M. and Cap, A. P. (2014) 'Refrigerated platelets for the treatment of acute bleeding: a review of the literature and reexamination of current standards', *Shock,* 41, pp. 51-53.

Prestia, F. A., Galeano, P., Martino Adami, P. V., Do Carmo, S., Castaño, E. M., Cuello, A. C. and Morelli, L. (2019) 'Platelets Bioenergetics Screening Reflects the Impact of Brain Aβ Plaque Accumulation in a Rat Model of Alzheimer', *Neurochemical Research,* 44(6), pp. 1375-1386.

Protasoni, M. and Zeviani, M. (2021) 'Mitochondrial structure and bioenergetics in normal and disease conditions', *International journal of molecular sciences,* 22(2), pp. 586.

Quach, M. E., Chen, W. and Li, R. (2018) 'Mechanisms of platelet clearance and translation to improve platelet storage', *Blood, The Journal of the American Society of Hematology,* 131(14), pp. 1512-1521.

Ravi, S., Chacko, B., Kramer, P. A., Sawada, H., Johnson, M. S., Zhi, D., Marques, M. B. and Darley-Usmar, V. M. (2015a) 'Defining the effects of storage on platelet bioenergetics: The role of increased proton leak', *Biochimica et Biophysica Acta (BBA) - Molecular Basis of Disease,* 1852(11), pp. 2525-2534.

Ravi, S., Chacko, B., Sawada, H., Kramer, P. A., Johnson, M. S., Benavides, G. A., O'Donnell, V., Marques, M. B. and Darley-Usmar, V. M. (2015b) 'Metabolic plasticity in resting and thrombin activated platelets', *PloS one,* 10(4), pp. e0123597.

Reddoch-Cardenas, K. M., Bynum, J. A., Meledeo, M. A., Nair, P. M., Wu, X., Darlington, D. N., Ramasubramanian, A. K. and Cap, A. P. (2019a) 'Cold-stored platelets: A product with function optimized for hemorrhage control', *Transfus Apher Sci,* 58(1), pp. 16-22.

Reddoch-Cardenas, K. M., Peltier, G. C., Chance, T. C., Nair, P. M., Meledeo, M. A., Ramasubramanian, A. K., Cap, A. P. and Bynum, J. A. (2021) 'Cold storage of platelets in platelet additive solution maintains mitochondrial integrity by limiting initiation of apoptosis-mediated pathways', *Transfusion,* 61(1), pp. 178-190.

Reddoch-Cardenas, K. M., Sharma, U., Salgado, C. L., Montgomery, R. K., Cantu, C., Cingoz, N., Bryant, R., Darlington, D. N., Pidcoke, H. F., Kamucheka, R. M. and Cap, A. P. (2019b) 'An in vitro pilot study of apheresis platelets collected on Trima Accel system and stored in T-PAS+ solution at refrigeration temperature (1-6°C)', *Transfusion,* 59(5), pp. 1789-1798.

Reddoch, K. M., Montgomery, R. K., Rodriguez, A. C., Meledeo, M. A., Pidcoke, H. F., Ramasubramanian, A. K. and Cap, A. P. (2016) 'Endothelium-derived inhibitors efficiently attenuate the aggregation and adhesion responses of refrigerated platelets.', *Shock,* 45(2), pp. 220-7.

Reddoch, K. M., Pidcoke, H. F., Montgomery, R. K., Fedyk, C. G., Aden, J. K., Ramasubramanian, A. K. and Cap, A. P. (2014) 'Hemostatic function of apheresis platelets stored at 4°C and 22°C', *Shock (Augusta, Ga.),* 41 Suppl 1(0 1), pp. 54-61.

Reddy, E. C. and Rand, M. L. (2020) 'Procoagulant phosphatidylserine-exposing platelets in vitro and in vivo', *Frontiers in cardiovascular medicine,* 7, pp. 15.

Reddy, E. C., Wang, H., Christensen, H., McMillan-Ward, E., Israels, S. J., Bang, K. A. and Rand, M. L. (2018) 'Analysis of procoagulant phosphatidylserine-exposing platelets by imaging flow cytometry', *Research and Practice in Thrombosis and Haemostasis,* 2(4), pp. e12144.

Rinder, H. and Snyder, E. (1992) 'Activation of platelet concentrate during preparation and storage', *Blood cells,* 18(3), pp. 445-56; discussion 457.

Rinder, H. M., Snyder, E. L., Tracey, J. B., Dincecco, D., Wang, C., Baril, L., Rinder, C. S. and Smith, B. R. (2003) 'Reversibility of severe metabolic stress in stored platelets after in vitro plasma rescue or in vivo transfusion: restoration of secretory function and maintenance of platelet survival', *Transfusion,* 43(9), pp. 1230-7.

Rogatzki, M. J., Ferguson, B. S., Goodwin, M. L. and Gladden, L. B. (2015) 'Lactate is always the end product of glycolysis', *Frontiers in neuroscience,* 9, pp. 22-22.

Romero, N., Swain, P. M., Kam, Y., Rogers, G. and Dranka, B. P. (2018) 'Bioenergetic profiling of cancer cell lines: quantifying the impact of glycolysis on cell proliferation', *Cancer Research,* 78(13 Supplement), pp. 3487.

Sandgren, P., Hansson, M., Gulliksson, H. and Shanwell, A. (2007) 'Storage of buffy-coat-derived platelets in additive solutions at 4 °C and 22 °C: flow cytometry analysis of platelet glycoprotein expression', *Vox Sanguinis,* 93(1), pp. 27-36.

Sandgren, P., Shanwell, A. and Gulliksson, H. (2006) 'Storage of buffy coat–derived platelets in additive solutions: in vitro effects of storage at 4 C', *Transfusion,* 46(5), pp. 828-834.

Saunders, C. V. (2012) *Role of glucose, acetate and plasma in the maintenance of mitochondrial function, energy metabolism and cell integrity during platelet storage in additive solutions* PhD, Cardiff University.

Saunders, C. V., Pearce, N. B. and George, C. (2022) 'In vitro storage characteristics of neonatal platelet concentrates after addition of 20% PAS-E', *Vox Sanguinis,* 117, pp. 1171-1178.

Schlagenhauf, A., Kozma, N., Leschnik, B., Wagner, T. and Muntean, W. (2012) 'Thrombin receptor levels in platelet concentrates during storage and their impact on platelet functionality', *Transfusion,* 52(6), pp. 1253-1259.

Scorer, T., Sharma, U., Peltier, G., McIntosh, C., Reddoch-Cardenas, K. M., Mumford, A. D. and Cap, A. P. (2018) 'Ticagrelor Induced Platelet Dysfunction Can be Assessed

Under Shear Conditions and Correction By Platelets Is Influenced By Storage Temperature', *Blood,* 132(Supplement 1), pp. 526-526.

Scorer, T., Williams, A., Reddoch-Cardenas, K. and Mumford, A. (2019a) 'Manufacturing variables and hemostatic function of cold-stored platelets: a systematic review of the literature', *Transfusion,* 59(8), pp. 2722-2732.

Scorer, T. G., Reddoch-Cardenas, K. M., Thomas, K. A., Cap, A. P. and Spinella, P. C. (2019b) 'Therapeutic Utility of Cold-Stored Platelets or Cold-Stored Whole Blood for the Bleeding Hematology-Oncology Patient', *Hematol Oncol Clin North Am,* 33(5), pp. 873-885.

Scott, N., Harris, J. and Bolton, A. (1983) 'Effect of storage on platelet release and aggregation responses', *Vox sanguinis,* 45(5), pp. 359-366.

Segawa, K. and Nagata, S. (2015) 'An apoptotic ‘eat me’signal: phosphatidylserine exposure', *Trends in cell biology,* 25(11), pp. 639-650.

Shea, S. M., Reisz, J. A., Mihalko, E. P., Rahn, K. C., Rassam, R. M., Chitrakar, A., Gamboni, F., D’Alessandro, A., Spinella, P. C. and Thomas, K. A. (2023) 'Cold-stored platelet hemostatic capacity is maintained for three weeks of storage and associated with taurine metabolism', *Journal of Thrombosis and Haemostasis*.

Shea, S. M., Spinella, P. C. and Thomas, K. A. (2022) 'Cold-stored platelet function is not significantly altered by agitation or manual mixing', *Transfusion,* 62(9), pp. 1850-1859.

Shi, J., Shi, Y., Waehrens, L. N., Rasmussen, J. T., Heegaard, C. W. and Gilbert, G. E. (2006) 'Lactadherin detects early phosphatidylserine exposure on immortalized leukemia cells undergoing programmed cell death', *Cytometry Part A: the journal of the International Society for Analytical Cytology,* 69(12), pp. 1193-1201.

Shimizu, S., Matsuoka, Y., Shinohara, Y., Yoneda, Y. and Tsujimoto, Y. (2001) 'Essential role of voltage-dependent anion channel in various forms of apoptosis in mammalian cells', *The Journal of cell biology,* 152(2), pp. 237-250.

Six, K., Compernolle, V. and Feys, H. (2020) 'When platelets are left in the cold', *Annals of Blood,* 5.

Skripchenko, A., Kurtz, J., Moroff, G. and Wagner, S. J. (2008) 'Platelet products prepared by different methods of sedimentation undergo platelet activation differently during storage', *Transfusion,* 48(7), pp. 1469-1477.

Snyder, E. L., Koerner Jr, T. A., Kakaiya, R., Moore, P. and Kiraly, T. (1983) 'Effect of Mode of Agitation on Storage of Platelet Concentrates in PL-732 Containers for 5 Days 1', *Vox sanguinis,* 44(5), pp. 300-304.

Sperry, J. L., Guyette, F. X., Rosario-Rivera, B. L., Kutcher, M. E., Kornblith, L. Z., Cotton, B. A., Wilson, C. T., Inaba, K., Zadorozny, E. V., Vincent, L. E., Harner, A. M.,

Love, E. T., Doherty, J. E., Cuschieri, J., Kornblith, A. E., Fox, E. E., Bai, Y., Hoffman, M. K., Seger, C. P., Hudgins, J., Mallett-Smith, S., Neal, M. D., Leeper, C. M., Spinella, P. C., Yazer, M. H., Wisniewski, S. R. and group, t. C. S. P. f. H. S. s. (2024) 'Early Cold Stored Platelet Transfusion Following Severe Injury: A Randomized Clinical Trial', *Annals of Surgery,* 10, pp. 1097.

Stanworth, S. J., Dowling, K., Curry, N., Doughty, H., Hunt, B. J., Fraser, L., Narayan, S., Smith, J., Sullivan, I. and Green, L. (2022) 'Haematological management of major haemorrhage: a British Society for Haematology Guideline', *British Journal of Haematology,* 198(4), pp. 654-667.

Stolla, M., Bailey, S. L., Fang, L., Fitzpatrick, L., Gettinger, I., Pellham, E. and Christoffel, T. (2020) 'Effects of storage time prolongation on in vivo and in vitro characteristics of 4 C–stored platelets', *Transfusion,* 60(3), pp. 613-621.

Stolla, M., Vargas, A., Bailey, S., Fang, L., Pellham, E., Gettinger, I., Christoffel, T., Corson, J., Osborne, B. and Fitzpatrick, L. (2018) 'Cold-Stored Platelets to Reverse Dual Antiplatelet Therapy', *Blood,* 132(Supplement 1), pp. 525-525.

Strandenes, G., Kristoffersen, E., Bjerkvig, C., Fosse, T., Hervig, T., Haaverstad, R., Kvalheim, V., Cap, A., Lunde, T. and Braathen, H. 'Cold-stored apheresis platelets in treatment of postoperative bleeding in cardiothoracic surgery'. *Transfusion*, 1537-2995.

Strandenes, G., Sivertsen, J., Bjerkvig, C. K., Fosse, T. K., Cap, A. P., Del Junco, D. J., Kristoffersen, E. K., Haaverstad, R., Kvalheim, V., Braathen, H., Lunde, T. H. F., Hervig, T., Hufthammer, K. O., Spinella, P. C. and Apelseth, T. O. (2020) 'A Pilot Trial of Platelets Stored Cold versus at Room Temperature for Complex Cardiothoracic Surgery', *Anesthesiology,* 133(6), pp. 1173-1183.

Stubbs, J. R., Tran, S. A., Emery, R. L., Hammel, S. A., Haugen, A. L., Zielinski, M. D., Zietlow, S. P. and Jenkins, D. (2017) 'Cold platelets for trauma-associated bleeding: regulatory approval, accreditation approval, and practice implementation-just the "tip of the iceberg"', *Transfusion,* 57(12), pp. 2836-2844.

Sweeney, J. D., Blair, A. J., Cheves, T. A., Dottori, S. and Arduini, A. (2000) 'L-carnitine decreases glycolysis in liquid-stored platelets', *Transfusion,* 40(11), pp. 1313-9.

Tobian, A. A., Fuller, A. K., Uglik, K., Tisch, D. J., Borge, P. D., Benjamin, R. J., Ness, P. M. and King, K. E. (2014) 'The impact of platelet additive solution apheresis platelets on allergic transfusion reactions and corrected count increment (CME)', *Transfusion,* 54(6), pp. 1523-1529.

Tynngård, N. (2009) 'Preparation, storage and quality control of platelet concentrates', *Transfus Apher Sci,* 41(2), pp. 97-104.

Valeri, C. R. (1974) 'Hemostatic effectiveness of liquid-preserved and previously frozen human platelets', *N Engl J Med,* 290(7), pp. 353-8.

Valeri, C. R., Feingold, H. and Marchionni, L. D. (1974) 'The Relation Between Response to Hypotonic Stress and the 51Cr Recovery In Vivo of Preserved Platelets', *Transfusion,* 14(4), pp. 331-337.

van Hout, F. M. A., Bontekoe, I. J., de Laleijne, L. A. E., Kerkhoffs, J.-L., de Korte, D., Eikenboom, J., van der Bom, J. G. and van der Meer, P. F. (2017) 'Comparison of haemostatic function of PAS-C–platelets vs. plasma–platelets in reconstituted whole blood using impedance aggregometry and thromboelastography', *Vox Sanguinis,* 112(6), pp. 549-556.

Vassallo, R. R. and Murphy, S. (2006) 'A critical comparison of platelet preparation methods', *Current Opinion in Hematology,* 13(5).

Verhoeven, A. J., Verhaar, R., Gouwerok, E. G. W. and De Korte, D. (2005) 'The mitochondrial membrane potential in human platelets: a sensitive parameter for platelet quality', *Transfusion,* 45(1), pp. 82-89.

Vit, G., Klüter, H. and Wuchter, P. (2020) 'Platelet storage and functional integrity', *Journal of Laboratory Medicine,* 44(5), pp. 285-293.

Wagner, S. J., Myrup, A., Awatefe, H., Thompson-Montgomery, D., Hirayama, J. and Skripchenko, A. (2008) 'Maintenance of platelet in vitro properties during 7-day storage in M-sol with a 30-hour interruption of agitation', *Transfusion,* 48(12), pp. 2501-2607.

Wandall, H. H., Hoffmeister, K. M., Sørensen, A. L., Rumjantseva, V., Clausen, H., Hartwig, J. H. and Slichter, S. J. (2008) 'Galactosylation does not prevent the rapid clearance of long-term, 4 degrees C-stored platelets', *Blood,* 111(6), pp. 3249-56.

Wandt, H., Ehninger, G. and Gallmeier, W. M. (2001) 'New strategies for prophylactic platelet transfusion in patients with hematologic diseases', *Oncologist,* 6(5), pp. 446-50.

Wandt, H., Frank, M., Gröschel, W., Birkmann, J. and Gallmeier, W. (1995) 'Safety of the 10/nl trigger for prophylactic platelet transfusion in ASCT', *Bone Marrow Transplant,* 15(suppl 2), pp. 541a.

Wang, L., Wu, Q., Fan, Z., Xie, R., Wang, Z. and Lu, Y. (2017) 'Platelet mitochondrial dysfunction and the correlation with human diseases', *Biochemical Society Transactions,* 45(6), pp. 1213-1223.

White, J. G. and Krivit, W. (1967) 'An ultrastructural basis for the shape changes induced in platelets by chilling', *Blood,* 30(5), pp. 625-635.

Wilson-Nieuwenhuis, J., El-Mohtadi, M., Edwards, K., Whitehead, K. and Dempsey-Hibbert, N. (2021) 'Factors Involved in the onset of infection following bacterially contaminated platelet transfusions', *Platelets,* 32(7), pp. 909-918.

Wolberg, A. S. (2007) 'Thrombin generation and fibrin clot structure', *Blood Reviews,* 21(3), pp. 131-142.

Wood, B., Johnson, L., Hyland, R. A. and Marks, D. C. (2018) 'Maximising platelet availability by delaying cold storage', *Vox Sang,* 113, pp. 403-411.

Wood, B., Padula, M. P., Marks, D. C. and Johnson, L. (2016) 'Refrigerated storage of platelets initiates changes in platelet surface marker expression and localization of intracellular proteins', *Transfusion,* 56(10), pp. 2548-2559.

Xu, W., Cardenes, N., Corey, C., Erzurum, S. C. and Shiva, S. (2015) 'Platelets from asthmatic individuals show less reliance on glycolysis', *PloS one,* 10(7).

Yang, J., Yin, W., Zhang, Y., Sun, Y., Ma, T., Gu, S., Gao, Y., Zhang, X., Yuan, J. and Wang, W. (2018) 'Evaluation of the advantages of platelet concentrates stored at 4 C versus 22 C', *Transfusion,* 58(3), pp. 736-747.

Yun, S.-H., Sim, E.-H., Goh, R.-Y., Park, J.-I. and Han, J.-Y. (2016) 'Platelet Activation: The Mechanisms and Potential Biomarkers', *BioMed Research International,* 2016, pp. 1-5.

Zantek, N. D., Steiner, M. E., VanBuren, J. M., Lewis, R. J., Berry, N. S., Viele, K., Krachey, E., Dean, J. M., Nelson, S. and Spinella, P. C. (2023) 'Design and logistical considerations for the randomized adaptive non-inferiority storage-duration-ranging CHIlled Platelet Study', *Clinical Trials,* 20(1), pp. 36-46.

Zhao, H. and Devine, D. V. (2022) 'The missing pieces to the cold-stored platelet puzzle', *International Journal of Molecular Sciences,* 23(3), pp. 1100.

Zharikov, S. and Shiva, S. (2013) 'Platelet mitochondrial function: from regulation of thrombosis to biomarker of disease', *Biochemical Society Transactions,* 41(1), pp. 118-123.

Zhou, L. and Schmaier, A. H. (2005) 'Platelet Aggregation Testing in Platelet-Rich Plasma: Description of Procedures With the Aim to Develop Standards in the Field', *American Journal of Clinical Pathology,* 123(2), pp. 172-183.

Zucker, M. B. and Borrelli, J. (1954) 'Reversible alterations in platelet morphology produced by anticoagulants and by cold', *Blood,* 9(6), pp. 602-8.

Zwaal, R., Comfurius, P. and Bevers, E. (2005) 'Surface exposure of phosphatidylserine in pathological cells', *Cellular and Molecular Life Sciences CMLS,* 62, pp. 971-988.

Appendices

Appendix I

Donor study information sheet and consent form

We would like to invite you to help with our research

The Welsh Blood Service is undertaking research to establish if there are better ways to make and store platelets. We are asking if your next apheresis donation could be used for this research.

This would mean that your donation would not be available to be transfused to patients. But this is a one-off request.

What happens next?

Please attend your donation session as planned. On the day we will speak to you about this and answer any questions you have.

What if I don't want my donation to be used for research?

That's fine. Still come to your appointment where your donation will be taken and will be used for to make platelets for patients as normal.

Will anything be different?

If you are happy for your apheresis donation to be used we will ask you to sign a consent form. Your donation will be taken in the usual way.

This is a one-off request. Your next donation after this will be used to make platelets for patients.

Why are you doing this?

We are exploring ways to make platelets that can be made and stored in better ways. For example, lower than usual temperatures. Usually platelets are stored at 24°C.

If we were able to store platelets at lower temperatures it would allow platelets to be used in more settings, for example in emergency settings or outside of hospitals.

The Welsh Blood Service is a research active organisation and we are continuously looking for ways that we can improve transfusion.

Project ID: WBSRD0162 Version 1.0 09/06/2022

Gwasanaeth Gwaed Cymru
Welsh Blood Service

Consent Form for Donors

RD&I Project name: Bioenergetic Profiles of Platelets in Storage as an Indicator of Platelet Viability & Function)

If you are happy to take part in our research, please complete the following

		Please Initial in the box
1.	I have read and understood the project's **Information Sheet for Donors** (version 1.0, dated 09/06/2022).	
2.	I have been given the opportunity to ask questions about the study.	
3.	I voluntarily agree to take part.	
4.	I understand I can choose not to take part, or to withdraw at any time, without my care being affected.	

Donor

Donor Signature _____

Name in BLOCK LETTERS. _____

Date _____

Witnessed

Signature _____

Name in BLOCK LETTERS. _____

Date _____

Appendix II

Statistical analysis of RTP and CSP results during storage compared to the baseline results

The mean of the results for each time point for RTP and CSP were statistically compared to the mean results for the baseline. One-way ANOVAs were used except where there were missing values in the data set, in which case a mixed effects analysis was performed.

Storage Method	Platelet Yield ($x10^9$/unit)			
	D2	D8	D14	D21
RTP	0.9091	<0.0001	<0.0001	-
CSP	0.0247	<0.0001	<0.0001	<0.0001

Storage Method	Platelet Concentration ($x10^9$/L)			
	D2	D8	D14	D21
RTP	0.2669	0.2748	<0.0001	-
CSP	0.0215	0.9995	0.0003	<0.0001

Storage Method	Mean Platelet Volume (fL)			
	D2	D8	D14	D21
RTP	0.4879	0.5929	0.0233	-
CSP	0.9997	0.0430	0.0032	0.0065

Storage Method	CD62P % positive			
	D2	D8	D14	D21
RTP	<0.0001	<0.0001	<0.0001	-
CSP	<0.0001	<0.0001	<0.0001	<0.0001

Storage Method	CD62P MFI			
	D2	D8	D14	D21
RTP	0.4314	0.0004	<0.0001	-
CSP	0.0062	<0.0001	<0.0001	<0.0001

Storage Method	sCD62P			
	D2	D8	D14	D21
RTP	0.1263	<0.0001	<0.0001	-
CSP	0.9977	0.0219	0.0001	<0.0001

Storage Method	Annexin V Binding % Positive			
	D2	D8	D14	D21
RTP	0.0482	<0.0001	<0.0001	-
CSP	0.0058	<0.0001	<0.0001	<0.0001

Storage Method	Annexin V Binding MFI			
	D2	D8	D14	D21
RTP	0.9998	0.7864	0.0237	-
CSP	0.8296	0.6175	0.9751	0.0140

Storage Method	Lactadherin Binding (% Positive)			
	D2	D8	D14	D21
RTP	0.0537	0.0118	<0.0001	-
CSP	0.0237	0.1507	0.0066	<0.0001

Storage Method	HSR			
	D2	D8	D14	D21
RTP	0.0454	0.0400	0.0001	-
CSP	<0.0001	<0.0001	<0.0001	<0.0001

mixed effects analysis

Storage Method	ESC			
	D2	D8	D14	D21
RTP	0.0505	0.0007	<0.0001	-
CSP	<0.0001	<0.0001	<0.0001	<0.0001

mixed effects analysis

Storage Method	CAT ETP			
	D2	D8	D14	D21
RTP	0.9568	0.9060	0.6856	-
CSP	0.7128	0.1433	0.0418	0.1833

mixed effects analysis

Storage Method	CAT Peak			
	D2	D8	D14	D21
RTP	0.6085	0.1589	<0.0001	-
CSP	0.0813	0.0018	0.0001	0.0015

mixed effects analysis

Storage Method	CAT lag time			
	D2	D8	D14	D21
RTP	0.0162	0.0006	<0.0001	-
CSP	0.0002	<0.0001	<0.0001	<0.0001

mixed effects analysis

Storage Method	ADP (MAX %)			
	D2	D8	D14	D21
RTP	0.0342	0.0530	0.0517	-
CSP	0.9995	0.9942	0.9997	0.6228

Storage Method	Collagen (MAX %)			
	D2	D8	D14	D21
RTP	0.4682	0.0026	<0.001	-
CSP	0.9184	0.0009	<0.0001	<0.0001

Storage Method	TRAP-6 neat (MAX %)			
	D2	D8	D14	D21
RTP	0.6518	0.0296	<0.0001	-
CSP	0.0971	<0.0001	<0.0001	<0.0001

Storage Method	TRAP-6 1:2 (Max %)			
	D2	D8	D14	D21
RTP	0.9960	0.0342	<0.0001	-
CSP	0.0470	0.0027	0.0001	0.0002

Storage Method	Glucose (mmol/L)			
	D2	D8	D14	D21
RTP	<0.0001	<0.0001	<0.0001	-
CSP	<0.0001	<0.0001	<0.0001	<0.0001

Storage Method	Lactate (mmol/L)			
	D2	D8	D14	D21
RTP	<0.0001	<0.0001	<0.0001	-
CSP	<0.0001	<0.0001	<0.0001	<0.0001

Storage Method	pO2 (kPa) (37°C)			
	D2	D8	D14	D21
RTP	0.0058	0.8172	0.0071	-
CSP	<0.0001	<0.0001	<0.0001	<0.0001

Storage Method	pCO2 (kPa) (37°C)			
	D2	D8	D14	D21
RTP	0.0009	0.0005	<0.0001	-
CSP	0.0087	<0.0001	<0.0001	<0.0001

Storage Method	Bicarbonate mmol/L at 37°C			
	D2	D8	D14	D21
RTP	0.0310	0.0015	0.0084	-
CSP	<0.0001	<0.0001	<0.0001	<0.0001

Storage Method	pH (37°C)			
	D2	D8	D14	D21
RTP	0.1167	0.1478	0.1530	-
CSP	0.7630	0.0267	<0.0001	<0.0001

Storage Method	ATP µmol/10^{11}			
	D2	D8	D14	D21
RTP	0.4494	0.0005	<0.0001	-
CSP	0.0001	<0.0001	0.0005	<0.0001

Storage Method	TMRM (% Positive)			
	D2	D8	D14	D21
RTP	0.9998	0.9997	0.0641	-
CSP	0.9996	0.8873	0.2928	0.0082

Storage Method	JC-1 (% Positive)			
	D2	D8	D14	D21
RTP	0.8752	0.1178	0.0002	-
CSP	0.9604	0.8491	0.0002	<0.0001

Storage Method	basal respiration			
	D2	D8	D14	D21
RTP	0.6925	0.5297	0.0413	-
CSP	0.7639	0.8408	0.1038	0.0060

mixed effects analysis

Storage Method	Maximal respiration			
	D2	D8	D14	D21
RTP	>0.9999	0.9543	0.1749	-
CSP	0.7741	0.9999	0.3013	0.0141

Storage Method	Spare respiratory capacity			
	D2	D8	D14	D21
RTP	0.0632	0.8226	0.9692	-
CSP	0.9494	0.2396	0.9972	0.8692

mixed effects analysis

Storage Method	ATP coupled respiration			
	D2	D8	D14	D21
RTP	0.4980	0.5117	0.0238	-
CSP	0.9772	0.5730	0.0590	0.0124

mixed effects analysis

Storage Method	ATP PR			
	D2	D8	D14	D21
RTP	0.0499	0.0076	0.0001	-
CSP	0.6352	0.0166	0.0226	<0.0001

mixed effects analysis

Storage Method	MITO ATP			
	D2	D8	D14	D21
RTP	0.0719	0.0266	0.0004	-
SP	0.3433	0.0442	0.0079	0.0002

mixed effects analysis

Storage Method	GLYCO ATP			
	D2	D8	D14	D21
RTP	0.9947	0.4978	0.1418	-
CSP	0.9994	0.0850	0.8436	0.9937

mixed effects analysis

Storage Method	Proton Leak			
	D2	D8	D14	D21
RTP	0.9965	0.9992	>0.9999	-
CSP	0.3798	0.9978	0.9983	0.5154

mixed effects analysis

Storage Method	Non-MITO OCR			
	D2	D8	D14	D21
RTP	0.9329	0.9227	0.0663	-
CSP	>0.9999	0.7559	0.0698	0.1644

mixed effects analysis